UNCLASSIFIED

AD 295 868

Reproduced
by the

ARMED SERVICES TECHNICAL INFORMATION AGENCY
ARLINGTON HALL STATION
ARLINGTON 12, VIRGINIA

UNCLASSIFIED

Best
Available
Copy

NOTICE: When government or other drawings, specifications or other data are used for any purpose other than in connection with a definitely related government procurement operation, the U. S. Government thereby incurs no responsibility, nor any obligation whatsoever; and the fact that the Government may have formulated, furnished, or in any way supplied the said drawings, specifications, or other data is not to be regarded by implication or otherwise as in any manner licensing the holder or any other person or corporation, or conveying any rights or permission to manufacture, use or sell any patented invention that may in any way be related thereto.

295868

AID Report B-63-10

11 January 1963

CATALOGED BY ASTIA
AS AD No.

X-RAY AND OPTICAL SPECTRA

Annotated Bibliography of Soviet Literature

(Preliminary)

Work Assignment No. 43
Task 2

295 868

Aerospace Information Division
Library of Congress

AID Report B-63-10 11 January 1963

X-RAY AND OPTICAL SPECTRA

Annotated Bibliography of Soviet Literature

(Preliminary)

Work Assignment No. 43
Task 2

The publication of this report does not constitute approval by any U. S. Government organization of the inferences, findings, and conclusions contained herein. It is published solely for the exchange and stimulation of ideas.

Aerospace Information Division
Library of Congress

FOREWORD

The bibliography has been prepared in response to AID Work Assignment No. 43, Task 2 (Preliminary), and is based on Soviet open-source materials available at the Aerospace Information Division and the Library of Congress. Only information relevant to astrophysics is included. Titles of Soviet monographs are given in the transliterated form, followed by the English translation. Library of Congress call numbers are included at the end of an entry when the item is cataloged and available in the Library's collections.

Part One, on x-ray spectra, contains sections on x-ray spectroscopy and solar x-ray radiation. Part Two, on optical spectra, contains sections on oscillator strengths and related quantities, wave functions, and theoretical developments. Individual sections are further subdivided as appropriate. Arrangement of the 70 entries is chronological within each subdivision. The Appendix lists areas of intensive Soviet activity in x-ray research not covered in the present bibliography.

The treatment of individual sources has been kept flexible, varying from brief summaries of only a few lines in the case of works of marginal interest to full abstracts or extensive summaries of pertinent papers. In many cases, important theoretical calculations are reproduced step by step. Extensive use has also been made of tabulated material. In all, the bibliography contains 62 tables. To facilitate publication, the tables for Part Two are placed after the text and keyed to their original sources by numbers in brackets placed after each caption. In the data columns of many of the tables photoreproduced from the original sources, commas are used to designate decimal points.

TABLE OF CONTENTS

FOREWORD

INTRODUCTION

PART ONE. X-RAY SPECTRA.....1

1. X-Ray Spectroscopy.....1

Intensity calculations: methods and data.....1

Effects of external screening and satellite lines.....12

Fluorescence yields.....26

Reference works.....30

2. Solar X-Ray Radiation.....31

Major studies.....31

Studies of marginal interest.....59

PART TWO. OPTICAL SPECTRA.....61

1. Oscillator Strengths and Related Quantities.....61

Review paper.....61

Experimental values.....61

Theoretical values.....66

Experimental methods and criteria.....70

2. Wave Functions.....72

3. Theoretical Developments.....74

4. Tables for Part Two.....79

[illegible].....127

INTRODUCTION

In Part One, the following subjects are emphasized: absolute intensities, satellite lines, line widths, fluorescence yields, and oscillator strengths and related quantities. Particular attention is paid to theoretical developments and calculation results. The orientation of the report to Soviet x-ray research relevant to astrophysics precludes the inclusion of a great deal of Soviet material available on x-ray spectra. Many such research papers contain data useful to scientists, and for this reason the major fields of x-ray spectra not included in this report but given extensive coverage in the Soviet open literature are listed in the Appendix.

Although a considerable amount of material on x-ray spectra is available in Soviet periodicals and monographs, the number of papers published by Soviet scientists is many times smaller than the number of corresponding Western publications. Most of the Soviet x-ray research has been performed since World War II. Prior to 1930, no significant contributions were made by Soviet scientists in the field of x-ray spectroscopy. Even during the earlier part of the 1930's, precision instruments necessary to carry out experimental research were unavailable. Some of the necessary equipment was presented to the Soviet Union by British physicists in the middle of that decade. During World War II, research was conducted on a very limited scale. Compared to the West, the volume and the importance of the Soviet research prior to 1945 in all areas, except for x-ray spectral analysis, is negligible. Since 1945, however, the amount of research and the number of scientists so engaged have been increasing rapidly.

The greater part of the current research on x-rays is devoted to x-ray spectral analysis, applications to solid-state physics, and investigation and interpretation of the fine structures of x-ray absorption spectra of alloys, compounds, and solid solutions. Judging by the large number of Western references in Soviet papers, one can say that Western research has been widely disseminated and applied to current problems. As a result, Soviet x-ray specialists have been able to forge ahead in many areas within a relatively short time. This is especially true of developments of the last 10 years. In that time, significant contributions have been made in several areas: theories of the fine structure of absorption spectra and the temperature dependence of fine structure, determination of atomic and crystal structures, bonding forces, and methods of correcting x-ray spectra for various types of distortion. Excellent spectrographs and accessory equipment have been developed and used extensively in experimental research.

The extent of Soviet research in x-ray spectra can be exemplified by an analysis of the bibliography to one of the major Soviet works in the field: M. A. Blokhin's *Fizika rentgenovskikh luchey* (Physics of X-Rays), Moscow, 1957 [17]. A breakdown of the entries according to origin can serve to indicate the relative strength of Soviet and non-Soviet research. The table given below shows the number of Soviet and non-Soviet publications cited at the end of each chapter. From the table, one can conclude that the overall Soviet contribution prior to 1958 has been rather minor except in fine structure of x-ray spectra, generation and resolution of x-rays, and methods of measuring intensities of x-ray spectral lines.

Less than 10 of the Soviet references to periodical literature are dated prior to 1940, while the number of Western references for the same period exceeds 150. Even more illustrative, the tabulated data on energy levels of atoms, photon energies of the chief lines and absorption edges of the K and L series, relative line intensities, and line widths were compiled from 72 sources, all Western, published between 1936 and 1957.

The x-ray data directly pertinent to this report are also scarce. For example, only six articles dealing with fluorescence yields were found in the Soviet literature. Three of these gave experimental values of fluorescence yields measured by Soviet scientists; the other three dealt mainly with the Auger effect but contained fluorescence yield data and were therefore included. One of the latter [9] contains a comprehensive survey of theoretical and experimental developments in x-ray fluorescence yields based on 68 references, only four of which are Soviet. Of these four, one deals with nuclear decay, two with internal conversion, and only one provides experimental values of K and L fluorescence yields. The section on K fluorescence yields in the same article is based exclusively on literature published between 1957 and 1960. For developments prior to 1957, the author suggests two other review papers, both by Western scientists.

Part One also contains articles on solar x-ray emission and the application of solar x-ray emission data to the interpretation of some phenomena and processes in the earth's atmosphere. Articles concerning x-ray data recorded by Soviet rockets and satellites are not included. Since Soviet astrophysicists and astronomers generally make no distinction between solar x-ray emission and solar ultraviolet emission, but group them together under the terms "ultraviolet" or "shortwave" radiation, articles dealing with these topics are included if they contain significant data on x-ray emission. Papers dealing exclusively with solar ultraviolet emission are omitted. In the last two years, several significant papers on shortwave solar radiation have been published by G. S. Ivanov-Kholodnyy and G. M. Nikol'skiy. In [20], a method is developed for calculating the absolute line intensities of solar shortwave radiation independently of a solar model. This method was used to calculate the abso-

Breakdown of References According to Origin

Chapter	Title	Total references	Soviet	Non-Soviet
1	Systematics of x-ray spectra	6	3	3
2	Intensity of x-ray spectra	39	3	36
3	Shape and line widths of x-ray spectral lines	12	4	8
4	True absorption of x-rays	16	1	15
5	Optics of x-rays	19	4	15
6	Photoeffect and secondary spectra	18	6	12
7	Scattering of x-rays	24	5	19
8	Fine structure of emission spectra	96	26*	70
9	Fine structure of absorption spectra	94	48	46
10	Modern methods of investigation of matter by means of x-ray spectra	23	4	19

* Of the 26 Soviet references, 16 deal with the generation of x-rays, methods of measuring x-ray intensities, and resolution of x-rays according to wavelength by means of spectrographs.

lute intensities of 480 lines emitted by the sun in the ultraviolet and x-ray spectral regions [21]. In [24], 180 of the 225 solar emission lines in the region between 60 and 1100 Å recorded by rockets were identified on the basis of intensities calculated in [21].

Part Two, entitled "Optical Spectra", covers the optical and the ultraviolet spectral regions. It includes the following tabulated material: f-values, line strengths, transition probabilities, line intensities, and wave functions. Theoretical developments in this field are also given. This part of the report presents only papers published in the periodical literature between 1957 and 1962. Developments in the field prior to 1958 are summarized in an excellent review by V. N. Kolesnikov and L. V. Leskov [32].

Several significant theoretical contributions to the field of quantum mechanics have been made by Soviet scientists. In 1935, V. A. Fok extended the Hartree self-consistent-field method to include the effect of exchange. The Hartree-Fok method has become one of the basic methods of quantum mechanics and is often used in the calculation of transition probabilities, line strengths, and oscillator strengths.

Another significant achievement has been the development of the multiconfiguration approximation method by A. P. Yutsis in collaboration with other Soviet scientists during 1953-1956. Since Part Two of this report is confined to works published since 1957, earlier papers by Yutsis are not included. Over 45 articles by Yutsis in collaboration with his associates have been published since 1955 in the *Trudy, Seriya B,* of the Lithuanian Academy of Sciences. This figure does not include papers written solely by Yutsis' associates and published in the same periodical. A bibliography of the works of Yutsis and his associates to be published under separate cover is presently being planned.

According to Soviet scientists, D. S. Rozhdestvenskiy's anomalous dispersion method (hook method) for measuring oscillator strengths of resonance lines of metals, although less sensitive, is superior to other methods. It is especially useful for measuring oscillator strengths of strong absorption lines and is used almost exclusively for this purpose by the Soviets in preference to the total-absorption and emission methods. Although the relative oscillator strength values determined by the hook method are in general very precise, the results of the measurements give only the $N_i f_{ik}$ values (N_i is the concentration of atoms in state i, f_{ik} is the oscillator strength). Consequently, the determination of absolute oscillator strengths is hampered by the difficulty in obtaining reliable vapor pressure data. Since the other methods are similarly hampered, the best values of absolute oscillator strengths in most cases are calculated from relative oscillator strengths measured by the hook method.

PART ONE. X-RAY SPECTRA

1. X-Ray Spectroscopy

Intensity Calculations: Methods and Data

1. Narbutt, K. I. Structure of the zinc vapor K absorption spectrum of x-rays. IN: Akademiya nauk SSSR. Izvestiya. Seriya fizicheskaya, v. 15, no. 2, 1951, 231-238.
AS262.A62455, v. 15

Experimentally obtained spectra of zinc vapor are interpreted as being due to superposition of two processes: the transition of electrons from the K level into a continuum and transition of K electrons into one of the free optical levels (1s-np transitions). The latter results in the appearance of resonance absorption lines. The shape of the edge can be represented by the well known arc tangent curve. The intensity of the resonance lines, as shown by the author in an earlier paper, is

$$\tau_n = a\frac{\eta^6}{Z^4 n^3}, \tag{1}$$

where n is the main quantum line, η is the effective nuclear charge of the molecule in the np state, Z is the atomic number of the element, and a is a constant. In order to determine the shape of the resonance lines of absorption, the dispersion formula may be used:

$$\tau(\nu) = \frac{\Gamma_n}{2\pi}\cdot\frac{\tau_0}{(\nu-\nu_0)^2+\left(\frac{\Gamma_n}{2}\right)^2}, \tag{2}$$

where $\tau(\nu)$ is line intensity at frequency ν; $\Gamma_n = \Gamma_i + \Gamma_f$ (Γ_i and Γ_f are the initial and the final level widths); ν_0 is the frequency corresponding to the maximum in the line intensity; and τ_0 is the integral intensity

$$\tau_0 = \int_{-\infty}^{\infty} \tau(\nu)\, d\nu. \tag{3}$$

The dispersion formula may be transformed by substituting $\nu = \nu_0$

$$\tau(\nu_0) = \frac{\Gamma_n}{2\pi} \cdot \frac{\tau_0}{\left(\frac{\Gamma_n}{2}\right)^2} = \frac{2\tau_0}{\pi\Gamma_n}. \tag{4}$$

where $\tau(\nu_0)$ is the maximum intensity of the resonance absorption lines determined by (1), i.e.,

$$\frac{2\tau_0}{\pi\Gamma_n} = \tau_n, \tag{5}$$

from which

$$\tau_0 = \frac{\pi\tau_n\Gamma_n}{2}. \tag{6}$$

Substituting into (3) gives the final result for the line intensity at frequency

$$\tau(\nu) = \frac{\left(\frac{\Gamma_n}{2}\right)^2 \tau_n}{(\nu - \nu_0)^2 + \left(\frac{\Gamma_n}{2}\right)^2}. \tag{7}$$

The structure of an atom with atomic number Z, (in this case, zinc) with the K electron removed is similar to the structure of an atom with Z + 1 (in this case, gallium).

The K absorption edge of zinc was investigated in the range from 35 to 40 ev. Fig. 1 shows the position of resonance absorption lines and K absorption edges of zinc. The experimental curve consists of a superposition of two K absorption edges and two series of resonance absorption lines. The first main edge and the first series of resonance lines correspond to absorption of neutral atoms; the second main edge and the second series of resonance lines correspond to absorption by zinc ions. The width of the upper np levels of ions was found to be greater than the level width of the neutral atoms while the K levels were found to be equal in both cases.

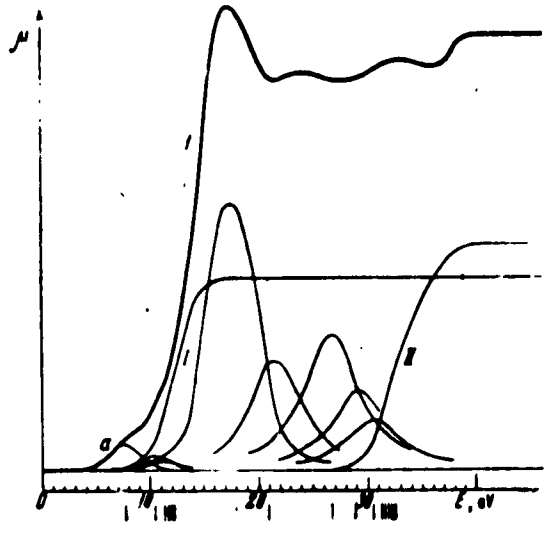

Fig. 1. Experimental curve (1) showing the dependence of the coefficient of absorption μ of zinc on the energy of the absorbed quantum. Fine lines show resonance absorption lines and K edges (I and II) of absorption, the sum of which gives the experimental curve. The position of gallium terms is shown under the scale.

A general method is given for the resolution of the experimental x-ray absorption curve of gases and metal vapors into the main absorption edge and a series of resonance absorption lines. It was shown that the four unknown quantities which must be determined can be obtained analytically. These are the widths of the resonance lines, the absolute intensity of one of these lines, the width of the K absorption edge, and the absolute height of the K absorption edges.

2. Blokhin, M. A., and V. P. Sachenko. Inner level widths and energy distribution of electronic state densities of the transition elements of the iron group. IN: Akademiya nauk SSSR. Izvestiya. Seriya fizicheskaya, v. 21, no. 10, 1957, 1343-1350. AS262.A62455, v. 21

The K level widths of 35 elements with atomic numbers ranging from 12 to 79 were calculated (Table 1). The L_{II} and L_{III} level widths were determined (Table 2) from the K level widths and available data on the widths of the $K_{\alpha_{1,2}}$ lines compiled exclusively from six American sources.

Table 1. K Level Widths

Element	Y, ev	Element	Y, ev	Element	Y, ev	Element	Y, ev
12 Mg	0,44	21 Sc	0,71	30 Zn	1,40	47 Ag	6,28
13 Al	0,48	22 Ti	0,74	31 Ga	1,53	50 Sn	7,98
14 Si	0,51	23 V	0,79	32 Ge	1,67	55 Cs	12,0
15 P	0,54	24 Cr	0,84	34 Se	1,98	60 Nd	17,7
16 S	0,57	25 Mn	0,92	36 Kr	2,37	65 Tb	26
17 Cl	0,60	26 Fe	1,00	38 Sr	2,82	70 Yb	36
18 Ar	0,63	27 Co	1,09	40 Zr	3,55	75 Re	48
19 K	0,65	28 Ni	1,19	42 Mo	4,10	79 Au	61
20 Ca	0,68	29 Cu	1,30	45 Rh	5,38		

Table 2. L_{II} and L_{III} Level Widths

Element	$Y_{L_{III}}$, ev	$Y_{L_{II}}$, ev	Element	$Y_{L_{III}}$, ev	$Y_{L_{II}}$, ev
22 Ti	0,64	1,16	32 Ge	1,06	1,27
23 V	0,79	1,42	38 Sr	1,68	1,78
24 Cr	1,12	1,59	40 Zr	1,85	2,05
25 Mn	1,54	2,04	41 Nb	2,09	1,69
26 Fe	1,65	2,00	42 Mo	1,76	2,08
27 Co	1,36	2,03	44 Ru	1,94	1,84
28 Ni	1,07	1,84	45 Rh	1,92	1,82
29 Cu	1,01	1,91	46 Pd	1,99	1,89
30 Zn	1,04	1,50	47 Ag	2,32	2,42
31 Ga	0,87	1,02			

The experimental values of $K_{\alpha_{1,2}}$ line widths were originally corrected by each author for distortions introduced by double-crystal spectrometers using different methods. To obtain uniform data, linear corrections were introduced to the experimental values of $K_{\alpha_{1,2}}$ line widths (Table 3). In view of the asymmetry of the $K_{\alpha_{1,2}}$ lines of the transition elements of the iron group, such a procedure is actually unjustified. In addition, since the L_{II} and L_{III} level widths are not equal to the difference between $K_{\alpha_{1,2}}$ line widths and the K level widths, the values of the L level widths obtained (Table 2) are only approximate.

Table 3. K_{α_1} and K_{α_2} Line Widths

Element	$\gamma_{K\alpha_1}$, ev	$\gamma_{K\alpha_2}$, ev	Element	$\gamma_{K\alpha_1}$, ev	$\gamma_{K\alpha_2}$, ev
22 Ti	1,38	1,90	32 Ge	2,73	2,94
23 V	1,58	2,21	38 Sr	4,5	4,6
24 Cr	1,96	2,43	40 Zr	5,2	5,4
25 Mn	2,46	2,96	41 Nb	5,8	5,4
26 Fe	2,65	3,00	42 Mo	5,86	6,18
27 Co	2,45	3,12	44 Ru	6,8	6,7
28 Ni	2,26	3,03	45 Rh	7,3	7,2
29 Cu	2,31	3,21	46 Pd	7,8	7,9
30 Zn	2,44	2,90	47 Ag	8,6	8,7
31 Ga	2,40	2,55			

The K level widths were calculated by interpolating all of the available experimental values of K level widths from any American sources. The following method was used:

The total probability for a change in state of an atom is equal to the sum of radiative transition probability P_p and radiationless transition probability $P_б$. Therefore, the level width γ is equal to

$$\gamma = A(P_p + P_б). \tag{1}$$

The value of the coefficient A is determined by the level shape and is equal to $6.58 \cdot 10^{-16}$ (if γ is in ev and P is the number of transitions per second) for the dispersion level

shape. The probabilities P_p P_ξ are

$$P_p = \sum_{|E_k|>|E_n|} P_{kn}, \tag{2}$$

$$P_\xi = \sum_{|E_k|>|E_{nm}|} P_{k,nm}, \tag{3}$$

where P_{kn} is the probability for radiative transition from level K into level N, and $P_{k,nm}$ is the probability of radiationless transition from level K into a state of double ionization nm.

In the case of single ionization

$$P_{kn}(Z) \sim Z^4. \tag{4}$$

Therefore, in this approximation

$$P_p(Z) \sim Z^4. \tag{5}$$

Accounting for the screening effect of electronic shells on probability P_{kn} leads to a slightly different expression for the dependence of P_{km} on Z. Calculation of transition probabilities

$$P_{K,\ L_{II,\ III}} \text{ and } P_{K,\ M_{II,\ III}}$$

in Slater's approximation for wave functions using formula

$$P_{kn} = \frac{32\pi e^2 \nu_{kn}^3}{3c^4\hbar}\left(\sum_{i=1}^{3} |X_{kn}^i|^2\right), \tag{6}$$

has shown that a good approximation for the dependence of P_{kn} on Z is given by the following formulas:

$$P_{K,L_{II,III}} = BZ^{4.55}, \qquad P_{K,M_{II,III}} = CZ^{4.00}. \tag{7}$$

The ratio X of these probabilities can also be determined from the experimental data of relative intensities of corresponding spectral lines given in two Western sources.

Comparison of the ratios determined from theoretical and experimental data indicates good agreement. Therefore, in the determination of $P_p(Z)$, the formula

$$P_{K,\ L_{II,\ III}} = BZ^{4.5\ 3}$$

was utilized. The remaining radiative transition probabilities were calculated from the experimental data on relative intensities of corresponding spectral lines. It was determined that Pp can be approximated by the following expression:

$$P_p = DZ^{4.7\ 1} \ . \qquad (8)$$

The total probability was found from the known experimental values of K x-ray fluorescence yield ω by means of the relationship:

$$\omega = \frac{P_p}{P_p + P_б} \ . \qquad (9)$$

Formulas (8) and (9) were used to calculate the total probability P(Z). Since the coefficient D in (8) is arbitrary, the curve for γ as a function of Z could be displaced with respect to the ordinate axis to obtain better correspondence with the experimental data (from seven American sources). Accordingly, D was determined to be 10^8 transitions per second. The values of γ listed in Table 1 were determined from Fig. 2, curve 2. The upper part of this curve beginning at Z = 30 may be approximated by

$$\gamma = Z^4 . \qquad (10)$$

For a smaller value of Z, this relationship does not hold.

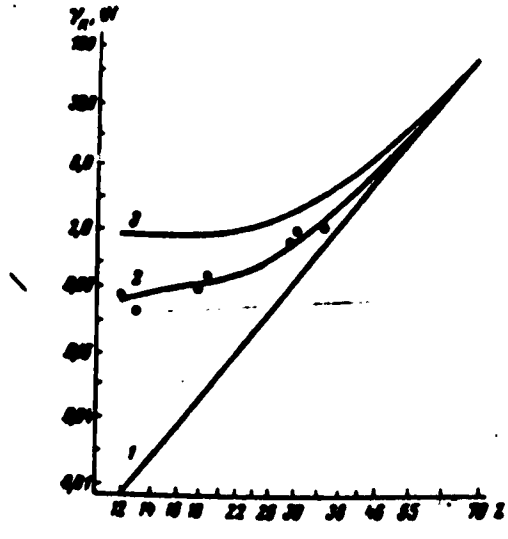

Fig. 2. Dependence of K level widths on the atomic number Z (logarithmic scale)

1 - dependence of radiative width on Z using formula 8; 2 - final dependence of γ_K (Z) on the basis of available experimental values of the fluorescence yield compiled from six Western sources; 3 - dependence of γ_K (Z), obtained from formula 5 on the assumption that $P_б$ = const (Z).

Probability $P_б$ was determined with the aid of formulas (8) and (9).

Other authors have noted that a dependence $\omega(Z)$ may be approximated by a formula in which $P_p(Z) \sim Z^4$ and $P_б(Z) = \text{const}\ (Z)$. However, experimental data on K level widths are in poor agreement with the results derived by this formula. Curve 3 in Fig. 2 was plotted on the assumption that $P_б(Z)^2 \sim Z^4$ and $P_б = \text{const}\ (Z)$ in such a way that the value of γ_K for $Z = 70$ corresponds to the experimental value. A significant deviation between the curve (1.7 ev) and the experimental data (0.6 ev) is obtained for light elements. If the curve is made to fit with the experimental data for light elements, then for $Z = 79$, γ should be equal to 40 ev in comparison to the experimental value of 62 ev. The curve $\gamma(Z)$ obtained by the authors is in better agreement with the actual dependence of $\gamma(Z)$.

3. Babushkin, F. A. Radiative transitions in a relativistic treatment. Optika i spektroskopiya, v. 13, no. 1, 1962, 141-143. QC350.068, v. 13

The relativistic theory of radiative transitions of Payne and Levinger is reviewed. The relativistic probability of electric multipole radiation of any order is obtained by using potentials corresponding to a photon in an electric-type state. The formulas for the potentials and the transformation of the corresponding matrix element are taken from Akhiyezer and Berestetskiy [*Kvantovaya elektrodinamika* (Quantum electrodynamics). Moskva, Fizmatgiz, 1959]. The radiation probability per unit time of photon with a moment L, projection of the moment M, and parity $(-1)^L$ is

$$W_{LM} = \frac{2(L+1)}{L(2L-1)[(2L-1)!!]^2}\,\omega^{2L+1}\left|\int \psi_2^*(r)\,e\sqrt{\frac{4\pi}{2L+1}}\,r^L Y^*_{LM}\psi_1(r)\,dr\right|^2 \qquad (1)$$

Use of Dirac's wave functions

$$\psi = \begin{pmatrix} -i/_2\chi^{\mu}_{-\varepsilon} \\ \varepsilon_2\chi^{\mu}_{\varepsilon} \end{pmatrix}. \qquad (2)$$

(where g and f are small and large components for the relativistic wave function) provides sufficient accuracy for the determination of transitions between lower levels 1s and 2p. The spinors χ are determined as follows:

$$\left.\begin{aligned} &\chi^{\mu}_{\varepsilon} = \sum_{\tau} c\left(l_{\varepsilon}\tfrac{1}{2}j;\ \mu-\tau,\tau\right)\chi^{\tau}_{1/2}Y^{\mu-\tau}_{l_{\varepsilon}}, \\ &\varepsilon = \pm\tfrac{1}{2};\ \chi^{1/2}_{1/2} = \begin{pmatrix}1\\0\end{pmatrix},\ \chi^{-1/2}_{1/2} = \begin{pmatrix}0\\1\end{pmatrix}. \end{aligned}\right\} \qquad (3)$$

Using these wave functions, the matrix element can be written as

$$\int \psi_2^*(r)\, r^L Y_{LM}^* \psi_1(r)\, dr = R_1(-\varkappa\psi \,|\, Y_{LM}^* \,|\, -\varkappa'\mu') + R_2(\varkappa\psi \,|\, Y_{LM}^* \,|\, \varkappa'\mu') = \tag{4}$$
$$= (\varkappa\psi \,|\, Y_{LM}^* \,|\, \varkappa'\mu') \cdot (R_1 + R_2),$$

where

$$R_1 = \int_0^\infty f_2 f_1' r^{L+2} dr; \quad R_2 = \int_0^\infty g_2 g_1' r^{L+2} dr \tag{5}$$

(prime quantities refer to the initial state). The spin angular part of the matrix element is

$$\sum_{\varkappa\mu} |(\varkappa\psi \,|\, Y_{LM}^* \,|\, \varkappa'\mu')|^2 = \frac{(2L+1)(2j+1)(2l'+1)}{4\pi} C^2(l'LI;\ 00)\, W^2\left(l'lIj;\ \tfrac{1}{2} L\right). \tag{6}$$

The final formula for the probability of electric multipole radiation for transitions between discrete states is of the form

$$W_L = \frac{2(L+1)}{L(2L+1)[(2L-1)!!]^2} \omega^{2L+1} e^2 (2j+1)(2l'+1) C^2(l'LI;\ 00) \times \tag{7}$$
$$\times W^2\left(l'lIj;\ \tfrac{1}{2} L\right) \cdot |R_1 + R_2|^2.$$

The Racah and the vector addition coefficients are used to obtain the usual selection rules

$$\Delta(l'LI) = \Delta(l'Lj), \text{ i.e. } |l'-l| \le L \le l'+l, \ |l'-j| \le L \le l'+j. \tag{8}$$

In addition, the sum of $l' + l + L$ must be even:

$$l' + l + L = 0 \pmod 2.$$

Neglecting the small components of the wave functions ($\alpha Z \ll 1$), a nonrelativistic expression is obtained for the probability of dipole transitions $n, l \to n-1, l-1$ (in usual units):

$$W = \frac{e^2\omega^3}{3\hbar c^3}\left(\frac{a_0}{Z}\right)^3 \frac{2^{l+2}(l+1)^{l+2}(n-1)^{n-l-2}}{(2n-1)^{n+l+2}} \left[\ldots\right]^4 \tag{9}$$

Using the standard formula for the mean oscillator strength,

$$f = \frac{mc^3}{2e^2\omega^2} W, \tag{10}$$

the following expression is obtained for electric dipole transitions (the detailed balance principle is used for reverse transitions):

$$fhfl \to n'l'f' = \frac{2m\omega}{3\hbar}(2f'+1)(2l'+1)\,C^2(l'1l;00)\cdot W^2\left((l'f'lj;\ \frac{1}{2}\,1\right)\cdot |R_1+R_2|^2. \tag{11}$$

The author notes that the formulas for oscillator strengths

$$f_{1s} \to np_{1/2}$$

and

$$f_{1s} \to np_{3/2}$$

derived by Payne and Levinger are probably incorrect, since for $\alpha Z \ll 1$ the small components disappear and both expressions are therefore equal to zero. For heavy elements, however, the results of calculations with Levinger's formulas correspond to the results derived by using formula (11). As an example, the oscillator strengths of $K_{\alpha 1}$, $K_{\alpha 2}$ lines of W^{74} are calculated and are compared with the relativistic values by Payne and Levinger for Pb^{82} and nonrelativistic values by Bethe (see Table 4).

The relative intensity of the $K_{\alpha 1}$ and $K_{\alpha 2}$ lines derived are

$$\frac{I_{\alpha_1}}{I_{\alpha_2}} = \left(\frac{\omega_{\alpha_1}}{\omega_{\alpha_2}}\right)^3 \frac{f_{\alpha_1}}{f_{\alpha_2}} = 1.87, \text{ i.e., } 100:\ 53.$$

Table 4. Oscillator Strengths

Transition	Bethe	Author	Payne Levinger
I $s_{1/2} \rightarrow 2p_{1/2}$	0.138	0.116	0.112
I $s_{1/2} \rightarrow 2p_{3/2}$	0.277	0.203	0.195
L shell	0.416	0.319	0.307

Effects of External Screening and Satellite Lines

4. Karal'nik, S. M. X-ray spectra and interatomic binding in alloys. IN: Akademiya nauk SSSR. Izvestiya. Seriya fizicheskaya, v. 20, no. 7, 1956, 815-819.
AS262.A62455, v. 20

This is the first of three articles published by Karal'nik on the effects of external screening. The shifting of the K-absorption limits of transition elements in alloys toward the shorter wavelengths is explained by the degree of external screening and the change in screening due to a change in the magnitude or the type of chemical binding in atoms under different conditions. The discussion in this paper is largely developmental, proceeding from the basic concepts of quantum mechanics. The mathematical apparatus is developed in a subsequent paper [6].

5. Karal'nyk [Karal'nik], S. M., and S. B. Nyzhnyk [Nizhnik]. On the origin of satellites in x-ray spectra. Ukrayins'kyy fizychnyy zhurnal, v. 2, no. 4, 1957, 333-337.
QC1.A4473, v. 2

A finite probability exists for electronic charge clouds to overlap. Accordingly, the effective charge of the nucleus is increased with respect to the inner electrons when the outer electrons are removed from the atom. According to the multiple-ionization theory, this type of ionization causes the formation of atoms in a state characterized by stable energy levels, which can be described with the aid of the effective value Z^*, where $Z < Z^* \ll Z + 1$. Transitions which cause the formation of the chief lines in the x-ray spectrum in singly ionized atoms cause the formation of shortwave satellites in multiply ionized atoms.

In order to determine satellite frequencies, the external screening must be evaluated. The change in the effective value of the atomic number with respect to inner electrons during additional ionization of the atom ΔZ_1 must be found and the value of Z^* ascribed to the frequency of the corresponding diagram line. Such an evaluation can be done only approximately. The following method is used:

The radial part of Bethe's hydrogenlike wave function for electrons in different shells is

$$R_{nl}(r) = \frac{1}{(2l+1)!}\sqrt{\frac{(n+l)!}{(n-l-1)!\,2n}}\left(\frac{2Z}{n}\right)^{\frac{3}{2}} \times \tag{1}$$
$$\times e^{-\frac{Zr}{n}}\left(\frac{2Zr}{n}\right)^{l} F\left[-(n-l-1);\ 2l+2;\ \frac{2Zr}{n}\right],$$

where F (α, β, χ) is a degenerate hypergeometric function.

Substitution of the dimensional quantities results in the following expression:

$$R_{nl} = \frac{1}{(2l+1)!}\sqrt{\frac{(n+l)!}{(n-l-1)!\,2n}}\left(\frac{2}{na_{nl}}\right)^{\frac{3}{2}} \times \tag{2}$$
$$\times e^{-\frac{r}{na_{nl}}}\left(\frac{2r}{na_{nl}}\right)^{l} F\left[-(n-l-1);\ 2l+2;\ \frac{2r}{na_{nl}}\right],$$

where $a_{nl} = a_б/Z^*$ is a quantity depending on the effective value of the nuclear charge for the corresponding electron in the atom. This value is determined from the expression analogous to that of Bethe for the radius of the Bohr orbit of the hydrogen atom:

$$\overline{r^2} = \frac{n^2}{2Z^2}a_б^2\left[5n^2+1-3l(l+1)\right]. \tag{3}$$

In this case,

$$\overline{r_{nl}^2} = \frac{n^2}{2}a_{nl}^2\left[5n^2+1-3l(l+1)\right]. \tag{3'}$$

Here r_{nl} is designated according to Slater as

$$r_{nl} = \frac{n^{*2}}{Z^*}a_б,$$

where n* and Z* are the values appropriate for n and l. In such a manner, r_{nl} values were calculated for Z = 26:

$$r_{4s} = 1.95\ \text{Å};\ r_{3d} = 0.77\ \text{Å};\ r_{3p} = 0.326\ \text{Å};$$

$$r_{3s} = 0.326\ \text{Å};\ r_{2p} = 0.098\ \text{Å};\ r_{2s} = 0.098\ \text{Å};$$

$$\text{and } r_{1s} = 0.021\ \text{Å}.$$

After substituting these values in (3), values of a_{nl} are determined. Then the following quantities are evaluated:

$$\int_0^{r_{ik}} r^2\ R_{nl}\ dr,$$

which is the probability that the nl electron is within a sphere of radius r_{ik}, and

$$\Delta Z_{nl/ik},$$

which is a part of the charge of the nl electron.

Table 5 lists the charge values for corresponding outer nl electrons inside the ik electron shells in the atom with Z = 26 (iron), i.e., $\Delta Z_{nl/ik}$.

Table 5. Charge Values of Outer Electrons in Corresponding Inner Atomic Shells of Iron

nl \ kl	1s	2s	3s	2p	3p
4s	0,001	0,003	0,036	0,003	0,036
3p	0,002	0,045	0,6[illegible]	0,0445	0,69
2s	0,045	0,63	0,9[illegible]	0,631	0,99
3p	0,00018	0,0[illegible]	0,504	0,0[illegible]	0,504
2p	0,0[illegible]	0,63	0,9[illegible]	0,63	0,999
3d	$1.5 \cdot 10^{-7}$	0,007	0,0[illegible]2	0,007	0,002

By starting with these values of $\Delta Z_{nl/1k}$, and extrapolating on the basis of Moseley's law, one can determine the frequencies and wavelengths of x-ray lines which correspond to diagram transitions for atoms with $Z^* = Z + Z_{nl/1k}$ -- i.e., the corresponding satellites.

For transitions of $K_{\alpha 1}$ lines in the atom with $Z = 26 + \Delta Z$, i.e., for K and L_{III} levels, the calculations can be made as follows:

The amount of energy of the K level for the atom with Z = 26 in Rydberg units (Ry) is

$$(\nu/R)_k = 523.77; \sqrt{(\nu/R)_k} = 22.886.$$

For the atom with Z = 27, it is

$$\sqrt{(\nu/R)_k} = 23.829.$$

An increase of Z by unity corresponds to an increase of

$$\sqrt{(\nu/R)_{k,27}} - \sqrt{(\nu/R)_{k,26}} = 0.943.$$

An increase of Z by $\Delta Z_{3Z/1s}$ corresponds to an increase of

$$0.943 \times 0.0325 = 0.031.$$

Thus

$$\sqrt{(\nu/R)_{k,26+0.03}} = 22.886 + 0.031 = 22.917.$$

And

$$(\nu/R)_{k,26+0.0325} = (22.917)^2 = 525.33.$$

Similar calculations for L_{III} are made, but only a small difference (0.001) from the $(J_{III})_{26}$ value is obtained. It should be noted, however, that the screening of 2p electrons by the 3s electrons is much greater than for K electrons, and in such cases the value $\Delta Z_{3s/2p} = 0.0445$ must be used for the 2p electrons.

But in this case as well, the change in screening of the 2p level due to removal of a 3s electron from the atom is insignificant, since the value of the energy of the 2p level for iron is less than the value of the energy of the K level

by an order of magnitude. Generally, the time that an outer electron spends within the inner electron orbits increases with increasing distance of the inner electrons from the nucleus, but the effect of screening on these electrons in a number of cases is nevertheless small in comparison with its effect on the K level. This is true because of the rapid decrease of the absolute value of the energy of the level during transition to the next main quantum number.

It should be pointed out that because of the rough approximation of $\Delta Z_{n\,l/1k}$ values obtained, extrapolation should not be carried out with the use of values of $\sqrt{\nu/R}$ but with values of ν/R, especially in view of the fact that extrapolation is done for two neighboring elements in the periodic table.

In such a manner, the frequency values for possible satellites are obtained: In the K_α group (assuming that the K_{α_1} line is the chief line with additional ionization of the 3s electron), we get 472.78 Rydberg units. (Experimental values are from 473.13 to 474.08.) In the K_β group of satellites we get 520.71 Rydberg units. (Experimental values are from 524.14 to 522.2.)

As mentioned above, it is also possible to explain the origin of longwave satellites by the method described. Their occurrence for example in the atoms of the iron-group elements is also apparently connected with multiple ionization (when the additional ionization is due to 3d electrons [or 3p electrons]; i.e., electrons which do not spend a finite period of time within the 1s shell, but whose external screening is more considerable at greater distances from the nucleus). Indeed, the removal of such an electron from the atom causes an increase in the effective value of Z for outer electrons, but the amount of energy of the K level remains unchanged, and the energy of the L levels is practically unchanged. The difference in energies of K and M_{III} levels in this case will be less than in the case of an absence of ionization of the type described. The calculation of K_β' for Fe gave the value 519.77 Rydberg units. (The experimental value is 518.95.)

The absence of longwave satellites in the K_α group can evidently be explained by the additional ionization in the 3d level, inasmuch as the K levels remain unchanged and the L levels remain practically unchanged.

It is also noted that such an approach can be helpful in understanding the changes observed in the position of satellite lines caused by a change in the chemical binding.

For example, it has previously been shown that the lateral shifting of longwaves of the $K\beta'$ satellite of chromium increases with the increase of its valence in compounds. The increase of the chromium valence means greater attraction, absorption from the 3d electron of chromium into the bond, and "transfer" of it to the other atoms taking part in the bond. As was shown above, one should observe an increase in the wavelength of the satellite positions on the longwave side of the chief $K\beta_1$ line.

6. Karal'nik, S. M. External screening and the fine structure of the x-ray spectra. IN: Akademiya nauk SSSR. Izvestiya. Seriya fizicheskaya, v. 21, no. 10, 1957, 1445-1451.
AS262.A62455, v. 21

Due to a finite probability of overlapping by an outer electron of the domain of inner electrons, the outer electron screens the interaction of the inner electrons of an atom with its nucleus. Since the interatomic binding depends on the outer electrons, the degree of screening varies with the changes in binding, causing the effective force exerted by the nucleus on the inner electrons to change. In turn, the details of x-ray spectral characteristics are affected. Karal'nik attempts to interpret the fine structure of x-rays with this new approach.

In the first part of the paper, he repeats step by step the mathematical procedure [detailed in entry 5 above] used to evaluate the charge values for outer electrons in an atom of iron. The values (Table 6) are slightly different from those in the earlier publication (Table 5).

Table 6. Charge Values of Outer Electrons in Inner Atomic Shells of Iron

Outer electrons	Inner electrons				
	1s	2s	3s	2p	3p
2s	0,0445	0,631	0,999	0,631	0,999
3s	0,0325	0,0445	0,69	0,0445	0,65
4s	0,001 (0,007)	0,003	0,036	0,003	0,036
2p	0,0055	0,63	0,999	0,63	0,999
3p	0,0002	0,088	0,594	0,088	0,594
3d	$1,5 \cdot 10^{-7}$	0,001			

Karal'nik notes that these values should be taken as roughly approximate, partly because they were derived in the approximation of hydrogenlike wave functions and partly because the radii of corresponding inner shells were originally derived for isolated atoms. But even more important, in complex atoms with many electrons the external screening must be different from screening in simple atoms. According to Karal'nik, better results can probably be obtained by the Thomas-Fermi method.

The remainder of the article is a qualitative analysis of screening by different electrons of an atom and of changes in screening caused by redistribution of electron density in solids as a result of changes in interatomic binding.

Karal'nik demonstrates that experimental data on the K limit shift of an element in a compound can be used to obtain approximate values of external screening. For a multivalent element of a compound displaying ionic binding the total shift of the K limit is due to removal of all the valence electrons. The shift per unit valence, expressed in energy units, divided by the difference in energy between the given element and its neighbor in the periodic table gives an idea of the magnitude of screening due to one electron. The authors conclude that there are good reasons to believe that the fine structure of x-ray spectra reflects the details of electronic distribution in atoms.

7. Gorak, Z. Origin of some satellites in x-ray spectra. IN: Akademiya nauk SSSR. Izvestiya. Seriya fizicheskaya, v. 24, no. 4, 1960, 422-423. AS262.A62455, v. 24

The origin of $K\alpha_1$ and $K\alpha_4$ lines in the spectrum of neon and neighboring elements ($Z \leq 14$) and the origin of $K\beta_1$ in the spectrum of Fe^{3+} are considered. To explain the origin of α_1 and α_4 lines, simultaneous excitation of vacancies in the 1s and 2p shells is assumed. The $K\alpha$ (1s → 2p) line is split into 3 lines as a result of electrostatic and exchange interactions with the additional 2p vacancy:

$$1s2p\,^1P - (2p)^2\,^1D, \quad (1)$$

$$1s2p\,^1P - (2p)^2\,^1S, \quad (2)$$

$$1s2p\,^3P - (2p)^2\,^3P. \quad (3)$$

Since both (1) and (2) originate from the same initial state in the case of neon, the energy intervals involved can be determined from the energy difference of final states $(2p)^2\,^1S$ and $(2p)^2\,^1D$, known from the optical spectra. In

addition, it is known from the atomic spectra theory that relative intensity $I_1/I_2 = 5$. Experiments have shown that these theoretical calculations hold true for the neon spectrum of two pairs of lines: α', α_4, and α'', α_3. In order to correlate these two pairs with (1) and (2), it is necessary to use the following theoretical relationships:

$$\left(\frac{\Delta\nu}{R}\right)_1 = \left(\frac{\nu}{R}\right)_1 - \frac{\nu}{R}(K_\alpha) = 0.12093\, Z + b_1; \tag{4}$$

$$\left(\frac{\Delta\nu}{R}\right)_2 = \left(\frac{\nu}{R}\right)_2 - \frac{\nu}{R}(K_\alpha) = 0.07194\, Z + b_2. \tag{5}$$

Numerical values for these expressions were obtained by the perturbation theory using hydrogenlike functions. Corrections due to the effect of 3sp electrons were introduced with the aid of a method by Slater. It was assumed that the multiplet structure due to interaction of incomplete 3sp shells with 2p shell vacancies could be neglected. The difference $b_1 - b_2$ (for $Z = 10$) was determined from optical terms. Fig. 3 shows lines

$$\left(\frac{\Delta\nu}{R}\right)_1 \text{ and } \left(\frac{\Delta\nu}{R}\right)_2$$

as a function of Z and the two possible positions for each. The positions identifying $\alpha_4 \equiv$ "1", $\alpha' \equiv$ "2" are preferable to those identifying $\alpha_3 \equiv$ "1", $\alpha'' \equiv$ "2", because these positions explain more adequately the experimental data. The line K_β' in the Fe^{3+} spectra originates analogously to lines α' and α_4. In this case, it is assumed that splitting of the K_β (1s-3p) line is specified by the interaction of the 3p vacancy with the incomplete $(3d)^5$ shell. Instead of K_β there are two lines:

$$1s(3d)^5\ {}^7S - 3p(3d)^5\ {}^7P; \text{ and}$$

$$1s(3d)^5\ {}^5S - 3p(3d)^5\ {}^5P.$$

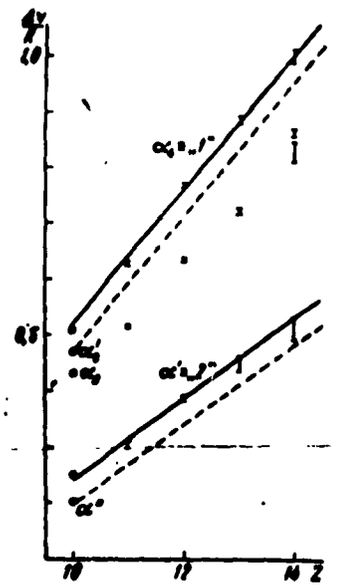

Fig. 3. Dependence of

$$\frac{\Delta\nu}{R}(Z) = \frac{\nu_{sat}}{R} - \frac{\nu}{R}(K_\alpha).$$

Scattering indicates the effect of chemical binding. Broken lines show the incorrect positions of α_3 = "1" and α'' = "2".

The order of magnitude of the energy interval and the relative intensity for these lines determined with the aid of Slater's wave functions agrees with those of K_β and K_β'. Therefore K_β and K_β' may be identified with $K_\beta \equiv$"1" and $K_\beta' \equiv$"2".

8. Shuvayev, A. T. On the interpretation of x-ray spectra. IN: Akademiya nauk SSSR. Izvestiya. Seriya fizicheskaya, v. 24, no. 4, 1960, 424-427. AS262.A62455, v. 24

The possibility is considered that shifting of the last spectral lines and K absorption limits of iron-group transition elements when chemical binding is changed can be explained as the result of K level shifting due to changes in external screening of this level by 4s valence electrons. Since the evaluation of such shifting of the K level using hydrogenlike functions is inadequate, the external screening constants are calculated for the transition elements of the iron group using wave functions determined by the self-consistent-field method. Contribution of one 4s electron to the 1s level screening constant is determined from the expression

$$\sigma_{4s}(r_{1s}) = \int_0^{r_{1s}} \psi_{4s}^2 r^2 dr, \qquad (1)$$

where ψ_{4s} is the wave function of the 4s level, and r is the radius corresponding to a maximum in the electronic density distribution of 1s electronic cloud. The results of calculations for Ca, Fe, and Zn atoms are shown in Table 7. The average external screening constants of 1s level by one 4s electron were determined for an iron atom from the following expression:

$$\sigma_{1s} = \int_0^{\infty} \psi_{1s}^2 \sigma_{4s}(r) r^2 dr. \qquad (2)$$

The values of ΔE listed in Table 7 are the amounts of shifting of the K level when the external screening constant is changed by σ_{4s}:

$$\Delta E = 13.6 \cdot 2(Z - \sigma)\sigma_{4s} \qquad (3)$$

where Z is the atomic number of the element, and $\sigma = 0.3$ is the internal screening constant for the K level.

Table 7. External Screening Constants for Ca, Fe, and Zn.

Element	$\sigma_{4s} \cdot 10^4$	ΔE, eV
Ca	2,0	0,11
Fe	2,4	0,17
	1,9(av)	0,10
Zn	1,9	0,15

Table 7 shows that shifting of the K level on the removal of one 4s electron is very small. In addition, removal of a valence electron causes a much smaller change in the external screening of the K level than the contribution of this electron to the screening (Table 8). In Table 8, N_{4p} is the number of 4p electrons in an atom or an ion; σ_{4p} is the value of external screening of the 1s level by 1p electron. Removal of one 4p electron from ssAs causes a change in screening of the 1s level by all 4p electrons ($\Sigma 4p$), which is two times smaller than screening by one 4p electron. This indicates that possible shifts of the K level are smaller than those given in Table 7. Therefore, a change of potential in the K shell region due to changes in external screening by valence electrons hardly affects the K level position.

Table 8. External Screening Constants for As, As^+, and As^{2+}.

Element	n_{4p}	$\sigma_{4p} \cdot 10^4$	$\Sigma_{4p} \cdot 10^4$
As	3	1,44	4,32
As^+	2	1,84	3,64
As^{2+}	1	2,26	2,26

The rest of the paper deals with the effect of a variation in internal screening on the position of the K_β spectral lines of the iron-group transition elements. For Z between 20 and 29, the dependence of the internal screening constant of 4s and 3p levels on Z from the data by Hartree shows that the electronic density between 4s and 3p levels increases significantly due to filling of the 3d shell. This affects the distance between these levels and also the magnitude of $\sigma_{4s,3p}$, which is determined from Moseley's law:

$$E_{4s} - E_{3p} = E_{4s,\,3p} = \left(\frac{1}{n_1^2} - \frac{1}{n_2^2}\right)(Z - \sigma_{4s,\,3p})^2, \tag{4}$$

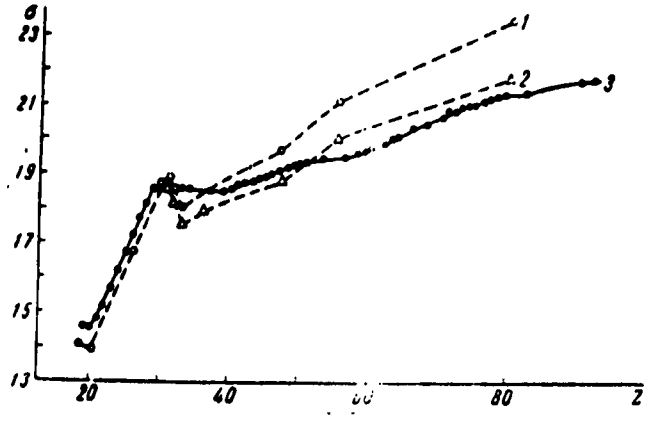

Fig. 4. Dependence on Z of 1) $\sigma_{4s,sp}$ and 2) $\sigma_{4p,sp}$ for free atoms and 3) for elements in the solid state.

Fig. 4 shows the dependence of $\sigma_{4s,sp}$ and $\sigma_{4p,sp}$ on Z for free atoms and elements in the solid state. It can be seen that $\sigma_{4s,sp}$ and $\sigma_{4p,sp}$ increase as the 3d, 4d, 4f, and 5d shells are filled but hardly change at all or increase only slightly in other cases. It was determined that shifting of the $K\beta_{5,2}$ line in atoms (Z = 20 to 29) of compounds with the same type of binding are determined mainly by the change in number of the d valence electrons. Removal of one d electron results in shifting of the $K\beta_{5,3}$ line in the shortwave direction by ~2 ev. Redistribution of valence electrons of the type s → d and s → p results in an analogous effect approximately equal to 1 ev.

9. Listengarten, M. A. The Auger effect. IN: Akademiya nauk SSSR. Izvestiya. Seriya fizicheskaya, v. 24, no. 9, 1960, 1041-1075. AS262.A62455, v. 24

This review is based on 116 references, only 15 of them Soviet, and includes the following topics: classification of Auger electrons, the energy of Auger electrons, conversion intensities of Auger electrons, K, L, and M fluorescence yields, and the Coster-Kronig effect.

A section on the K-fluorescence yields is a summary of data available in the literature from 1956 through 1959. Of the references [illegible] section, only three are Soviet: [illegible], another with conversion

electrons of Yb^{166} and Ti^{166} (K Auger yield = 4.5 ± 2.2%), and only the third with fluorescence yields. It is pointed out that data available prior to 1956 are summarized in two non-Soviet publications.

The experimental values of K fluorescence yields calculated by different authors and the values determined from the following formula are given in Table 9:

$$[\omega_K/(1-\omega_K)]^{1/4} = -A + BZ - CZ^3 \quad (C=\alpha A) \qquad (1)$$

A section on L and M fluorescence yields is based almost exclusively on non-Soviet sources (only one Soviet reference). Using the non-Soviet experimental data and making some additional assumptions, the author calculated the average L_I, L_{II}, L_{III} fluorescence yields for elements with Z = 54-56. For subshells L_I, L_{II}, and L_{III}, fluorescence yields are 0.05, 0.09, and 0.07, respectively.

On the basis of all of the available data, the fluorescence and the Coster-Kronig yield curves are plotted (Fig. 5) similarly to those of B.B. Kinsey, except that the latest experimental data for Z = 47, 54, and 56 are included and the curves extended up to Z = 47. The reference points are taken as Z = 55 and Z = 82; Auger widths are assumed to increase linearly from Z = 47 to Z = 82 and to increase even faster for Z > 82. Some other assumptions have also been made in order to obtain better results.

In Fig. 5, curve ω_1 is correct to within 10% for Z_s between 73 and 92 and to within 15 to 20% for other values of Z. The error is of the order of 20% for ω_2 and ω_3. These curves are believed to be more accurate than those obtained by H. Lay. Table 10 shows experimental data and results obtained from the curve of Fig. 5 and Lay's curve.

Table 9. K Fluorescence Yields

z	$\omega_{K_{exp}}$	ω_K **	ω_K †	z	$\omega_{K_{exp}}$	ω_K **	ω_K †
10	0,043±0,004	0,006	0,009	40	0,70 ±0,02	0,696	0,698
12	0,008±0,003	0,014	0,020	41	0,73 ±0,02	0,715	0,715
13	0,008±0,003	0,020	0,028	42	0,73 ±0,02	0,733	0,731
13	0,045±0,002			43	0,70 ±0,03	0,750	0,748
22	0,18 ±0,01	0,170	0,191	45	0,786±0,015	0,780	0,778
23	0,304±0,013	0,199	0,220	46	0,790±0,014	0,793	0,789
23	0,23 ±0,02*			47	0,821±0,015	0,805	0,800
24	0,219±0,012	0,229	0,250	48	0,827±0,014	0,817	0,811
25	0,308±0,015	0,261	0,280	49	0,87 ±0,03	0,828	0,821
26	0,308±0,015	0,293	0,311	50	0,836±0,015	0,838	0,830
27	0,31 ±0,01	0,327	0,343	50	0,846±0,012		
28	0,366±0,011	0,350	0,376	53	0,91 ±0,03	0,863	0,856
28	0,33 ±0,02			57	0,88 ±0,01	0,889	0,882
29	0,39 ±0,02	0,392	0,409	68	0,955±0,022*	0,932	0,925
29	0,410±0,012			70	0,936±0,010	0,937	0,930
29	0,42 ±0,02*			84	0,942±0,005	0,958	0,950
30	0,44 ±0,02	0,426	0,442	92	0,967±0,010	0,963	0,955
30	0,446±0,012			93	0,938±0,010	0,963	0,955
31	0,47 ±0,02*	0,456	0,471				
31	0,53 ±0,08						

* A value from a Soviet source.

** The values of constants used in equation (1) are taken from *Nuclear Spectroscopy Tables*, by A. Wapsta *et al.*, Amsterdam, 1959.

† The values of constants used in equation (1) are taken from Laberrique *et al.*, *J. Phys. et Radium*, v. 17, 1956.

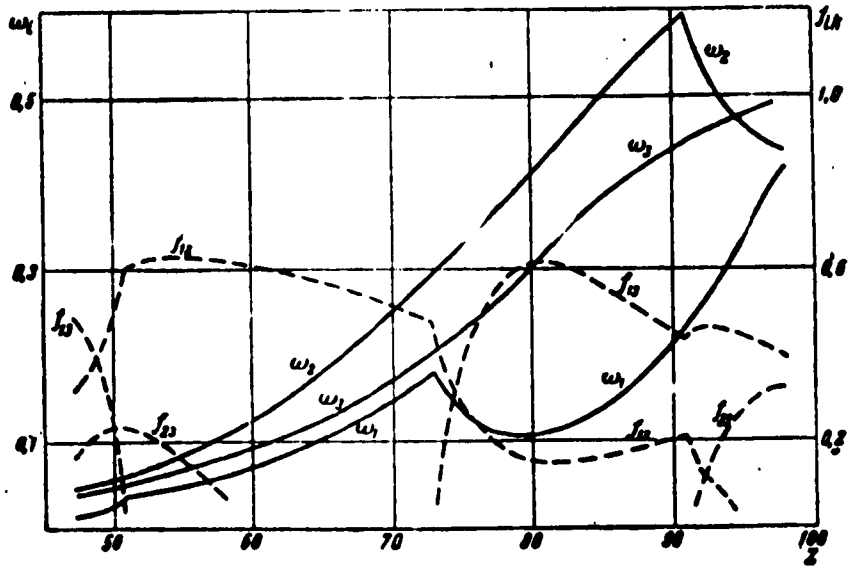

Fig. 5. Fluorescence yield ω_i (solid lines) and Coster-Kronig yield f_{ik} (broken lines) for L subshells (i, k = 1,2,3).

Table 10. Mean L Fluorescence yield $\bar{\omega}_L$

Z	$\bar{\omega}_L$ exp	$\bar{\omega}_L$ *	$\bar{\omega}_L$ **
23	0,0029±0,0002		—
29	0,0056±0,0008		—
31	0,0064±0,0008		—
47	0,029 ±0,003	0,047	0,095
54	0,10±0,01	0,08	0,14
63	0,17±0,02	0,155	0,19
72	0,17±0,02	0,23	0,26
80	0,34±0,04	0,35	0,38
80	0,37±0,04	0,35	0,38
81	0,50±0,02	0,39	0,39
81	0,39±0,08	0,39	0,39
81	0,32±0,02	0,39	0,39
82	0,39±0,02	0,39	0,40
81—83 (av)	0,48±0,02	0,39	0,40
83	0,51±0,03	0,38	0,41
	0,40±0,03	0,38	0,41
83	0,40±0,02	0,41	0,41
83	0,41±0,07	0,41	0,41
83	0,38±0,02	0,41	0,41
88	0,52±0,04	0,51	0,43

* According to the curve.
** According to Lay.

10. Konstantinov, A. A., T. Ye. Sazonova, and V. V. Perepelkin. Determination of L x-ray fluorescence yield of Ga^{71}, Cu^{65}, and V^{51}. IN: Akademiya nauk SSSR. Izvestiya. Seriya fizicheskaya, v. 24, no. 12, 1960, 1480-1483.
AS262.A62455, v. 24

A proportional 4π counter was used to record the L x-ray quantum yield of Ge^{71}, Zn^{65}, and Cr^{51} isotopes in the process of electron capture. The total number of L quanta was obtained by introducing experimentally obtained corrections due to absorption. These results and the data on the number of vacancies in the L shell due to electron capture were used to determine the L fluorescence yields for the daughter products given in Table 11. Two different values of fluorescence yield were obtained for Ga^{71} and V^{51} when two different sources of Ge^{71} and Cr^{51} were used.

Table 11. L Fluorescence Yields

Isotope	Yield
Ga^{71}	0.68
Ga^{71}	0.60
Cu^{65}	0.56
V^{51}	0.22
V^{51}	0.25

11. Konstantinov, A. A., I. A. Sokolova, and T. Ye. Sazonova. Determination of K x-ray fluorescence yields of V^{51}, Mn^{55}, Cu^{65}, and Ga^{71}. IN: Akademiya nauk SSSR. Izvestiya. Seriya fizicheskaya, v. 25, no. 2, 1961, 228-232.
AS262.A62455, v. 25

The total number of Auger electrons and the total K x-ray quantum yield formed as a result of disintegration of Cr^{51}, Fe^{55}, Zn^{65}, and Ge^{71} isotopes by electron capture were determined with the aid of a proportional π counter. From these data, the K x-ray fluorescence yields of the daughter products listed in Table 12 were determined.

Table 12. K x-Ray Fluorescence Yields

Element	Yield
V^{51}	0.23 $\pm$0.02
Mn^{55}	0.27 $\pm$0.02
Cu^{65}	0.42 $\pm$0.02
Ga^{71}	0.47 $\pm$0.02

12. Listengarten, M. A. Calculation of the probability of the Auger effect. IN: Akademiya nauk SSSR. Izvestiya. Seriya fizicheskaya, v. 25, no. 7, 1961, 792-797.
AS262.A62455, v. 25

A general relativistic formula for the Auger transition probability derived from the relativistic theory of retarded interaction between two electrons in jj coupling was used to calculate by means of an electronic computer the Auger K-LL transition probability for elements with atomic number 81. From this data, the K x-ray fluorescence yield for the elements with Z = 81 was determined to be $\omega_K = 0.962$.

13. Listengarten, M. A. Calculation of the probability of the Auger effect for heavy elements. IN: Akademiya nauk SSSR. Izvestiya. Seriya fizicheskaya, v. 26, no. 2, 1962, 182-190.
AS262.A62455, v. 26

A general relativistic formula for the probability of Auger transition is derived from the relativistic theory of retarded interaction between two electrons in jj coupling. This formula is used to calculate by means of an electronic computer the Auger K-LL transition probabilities for elements with atomic numbers Z between 65 and 92. The probabilities of Auger K-LL transitions obtained differ considerably from nonrelativistic calculations. To check the results, the K fluorescence yields were calculated (Table 13) for the elements with Z = 65, 81, and 92 using the probabilities of Auger K-LL transitions calculated by the author and data on the K level width available in other publications. Table 14 shows values of K fluorescence yield ω_K for elements with Z between 65 and 93 determined by interpolation using the K fluorescence yields of elements with Z = 65, 81 (from an earlier work), and 92 as anchor values.

Table 13. Fluorescence Yields

Z	ω_k
65	0.924
81	0.962
92	0.963

Table 14. K Fluorescence Yields Interpolated From the Anchor Values for Elements With Z = 65, 81, and 92

Z	ω_K	Z	ω_K
65	0.924	81	0.962
67	0.930	83	0.962
69	0.936	85	0.963
71	0.941	87	0.963
73	0.946	89	0.963
75	0.951	91	0.963
77	0.956	92	0.963
79	0.960	93	0.963

14. Rumsh, M. A., and V. N. Shchemelev. Determination of fluorescence yield by measuring the x-ray photoeffect in a massive cathode. Zhurnal eksperimental'noy i teoreticheskoy fiziki, v. 42, no. 3, 1962, 727-735. QC1.Z47, v. 42

Groups of photoelectrons from the x-ray photoelectric effect in a massive cathode are analyzed. It is shown that the contributions of different photoelectron groups change with variation of the x-ray wavelength. At the K edge, the contribution of one electron group to external emission vanishes, resulting in a jump of the quantum yield. It is also shown that the experimental jump of the quantum yield is related directly to the Auger yield and that the Auger yield and the fluorescence yield can be calculated from a measurement of the jump of the photoelectric quantum yield.

Table 15. L Fluorescence Yield

Element	Z	K jump of absorption	K jump of quantum yield	L fluorescence yield
Ti	22	9.2	5.9	0.22
V	23	9.1	5.75	0.24
Cr	24	8.9	5.55	0.26
Mn	25	8.8	5.36	0.28

The formulas derived are verified for Cr. The Auger yield according to photoemission data is shown to agree satisfactorily with the mean values of other authors. The photoelectric effect is used to determine the fluorescence yields of the elements shown in Table 15. It is pointed out that in determining the Auger yield the reliability of the method will increase with increasing values of the yield, i.e., with decreasing atomic number.

Reference Works

15. Vaynshteyn, E. Ye., and M. M. Kakhana, comps. Spravochnyye tablitsy po rentgenovskoy spektroskopii (Reference tables for x-ray spectroscopy). Moskva, Izd-vo AN SSSR, 1953. 270 p. QC453.V3

This is the first of a proposed two-volume reference work compiled from data available prior to 1952 for specialists in x-ray spectroscopy. [The second volume is unavailable at the Library of Congress and may never have been published.] The tabulated material includes the following: wavelengths of diagram and nondiagram emission lines and absorption edges of elements, their relative intensities (K and L series), and energies of x-ray levels for atoms of elements in Rydberg units. The tabulated material was obtained from Siegbahn, Cauchois, and Halubei, and scientific papers published during 1927-1952.

16. Borovskiy, I. B. Fizicheskiye osnovy rentgenospektral'nykh issledovaniy (Physical principles of x-ray spectral analysis). Moskva, Izd-vo Mosk.univ., 1956. 462 p. QC481.B74

This is an advanced-level textbook on the physics of x-rays and x-ray spectroscopy used at Moscow State University. Particular attention is paid to the dynamic theory of x-ray interference and the kinetic diffraction theory. Topics closely associated with solid-state physics, such as the fine structure of x-rays, are not covered. The value of this book is diminished by the fact that no bibliography is given. The chapter on the intensity of characteristic x-ray spectra contains a table of average experimental fluorrescense yield values (prior to 1955), which appears to have been taken from non-Soviet sources.

17. Blokhin, M. A. Fizika rentgenovskikh luchey (Physics of x-rays). 2d ed., rev., Moskva, Fizmatgiz, 1957. 518 p. QC481.B68 1957

This is the only known Soviet monograph dealing with the physics of x-rays published in the Soviet Union since 1936. The table of contents, a listing of the major tables, and a brief discussion of the sources listed in the bibliography have already appeared in the introduction to this report. This monograph can be used to trace Soviet (and Western) developments in the field of x-rays.

2. Solar X-Ray Radiation

Major Studies

18. Ivanov-Kholodnyy, G. S. Rocket observations of shortwave solar emission. IN: Akademiya nauk SSSR. Izvestiya. Seriya geofizicheskaya, no. 1,1959, 108-121.
QC801.A35 1959

The article is a survey of data published in scientific literature prior to December 1958 on ultraviolet and x-ray solar emission. Although it is primarily a summary of observation results, some conclusions and deductions are made. The paper is based on 79 sources, 68 of them non-Soviet. The paragraphs dealing with x-ray spectra are based almost exclusively on American sources. On the basis of available experimental data, the author states that x-ray emission from the solar corona, except in the region of 3 to 9 Å, can be represented by thermal radiation of a rarefied medium.

19. Kazachevskaya, T. V., and G. S. Ivanov-Kholodnyy. Continuous solar emission in the x-ray region. Astronomicheskiy zhurnal, v. 36, no. 6, 1959, 1022-1027. QB1.A47, v. 36

The average Gaunt factor for x-ray emission from the solar corona due to free-free transition is calculated for 17 different values of wavelengths from 1 to 10^{10} Å for temperatures of 10^6 and $2 \cdot 10^6$ °K. The values of the average Gaunt factor are then used to calculate the intensity of solar radiation, and the theoretical spectrum thus obtained is compared with obervational data. The temperature of the solar corona is also estimated.

On the basis of the data derived and available data on radio emission intensity, the authors conclude that the x-ray emission from the sun in the 10 to 100 Å region as recorded by rockets is mainly continuous. A later article [20] by Ivanov-Kholodnyy, however, admits that the intensity values in the spectral region of 100 to 500 Å calculated in this paper are approximately 20 times too high. Consequently, the x-ray solar radiation in the spectral region of 10 to 100 Å as recorded by rockets would be primarily linear.

20. Ivanov-Kholodnyy, G. S., and G. M. Nikol'skiy. Ultraviolet solar radiation and the transition layer between the chromosphere and corona. Astronomicheskiy zhurnal, v. 38, no. 1, 1961, 45-65. QB1.A47, v. 38

The authors hold that previous theoretical calculations of the absolute intensity of shortwave solar radiation do not agree with observational data because of the lack of plausible concepts of physical conditions in the transition region between the chromosphere and the corona. They develop a method to determine the absolute intensity of each shortwave spectral line emitted by the sun without recourse to a model of the solar transition region.

The initial data required for the determination of the absolute intensity of spectral lines are the intensities of some of the definitely identified shortwave solar lines. The intensity of radiation of an ion in a spectral line of the transition layer is determined from the following expression:

$$\Delta\varphi_i = \int_{h_1}^{h_2} n_e^2 T^{-1/2} dh, \tag{1}$$

where n_e is the electron concentration; T is the absolute temperature; and h is the height above the photosphere.

For ion emission lines in the whole temperature range of the transition region, $\Delta\varphi_i$ can be calculated using the ionization temperature T_i as a parameter:

$$\Delta\varphi(T_i) = \frac{2.3 \cdot 10^{12}/\lambda}{\varkappa f W'(T_i)}, \tag{2}$$

where $\varkappa$ is the amount of a given element in comparison to hydrogen; f is the oscillator strength, and $fW'T^{3/2}$ is the excitation probability of a line with a wavelength λ due to impact with an electron.

The expression for $\Delta\varphi_i$ was calculated on the assumption that excitation due to electron impacts is balanced out by spontaneous transitions. The dependence of $\Delta\varphi_i$ on T_i was obtained from the available absolute intensity data on 26 spectral lines in the region $\lambda \sim 1200$ Å. The graph of

$\Delta\varphi_1$ (T_1) makes it possible not to use a model of the transition region. Formula (2) for the resonance lines can be written as

$$\frac{I}{\chi f} = 4.3 \cdot 10^{-18} \frac{\Psi'(\lambda, T_i)}{\lambda} \Delta\varphi(T_i). \qquad (3)$$

Here, $I/\chi f$ is a function of parameters λ and T_1. The $\Delta\varphi_1$ in this formula contains all of the main characteristics of the radiation power of the transition layer.

In order to simplify intensity calculations, formula (2) can be represented nomographically. In the nomogram, log $I/\chi f$ is plotted as a function of log T_1, giving a family of curves for a range of values of λ.

The authors also construct a model of the transition region between the chromosphere and the corona for active and undisturbed regions. The model is in agreement with ionospheric data and the radio emission of the sun.

21. Ivanov-Kholodnyy, G. S., and G. M. Nikol'skiy. Prediction of solar line emission in the shortwave spectral region. Astonomicheskiy zhurnal, v. 38, no. 5, 1961, 828-843.
QB1.A47, v. 38

A method developed earlier by Ivanov-Kholodnyy and Nikol'skiy [20] is used to calculate the absolute intensities of 480 of the stronger shortwave lines in the ultraviolet and x-ray spectral regions of the sun (Table 16). Since the highest degree of ionization of elements in hot coronal condensations is unknown, all of the emission lines of ions due to allowed transitions of all isoelectronic series were considered. The possible maximum temperature was taken to be approximately equal to $3 \cdot 10^6$ °K.

The column designations in Table 16 require some explanation: In the second column, the word series denotes the isoelectronic sequence. In the third column, T_1 is the ionization temperature characterizing the maximum ion concentration. It is determined from the curve showing the variation of ion concentration with electronic temperature by a method developed in [20]. Symbol χ_1 is the ionization potential. In the fifth column, the wavelengths of shortwave lines were calculated from tables of atomic energy levels by C. E. Moore. Terms not given in those tables were obtained by extrapolating along isoelectronic sequences, and the corresponding wavelengths are given in parentheses.

Lines belonging to the same multiplet are enclosed by braces. In some cases, only the wavelengths of boundary lines of a multiplet are given. In such cases, the strongest line is given first, and the value of I in the table is the sum of component intensities.

The seventh column lists the known oscillator strength values. When the f-values are unknown, they are assumed to be equal to 1 for resonance excitations of ions and between 0.5 and 0.1 for excitation of higher levels. These f-values are given in parentheses.

In reference to the last column, if several transitions are possible from the same excited level, the line intensity due to transitions into the ground state (3 → 1) is

$$I_{31} = I \frac{A_{31}}{\Sigma A}.$$

For the transition (3 → 2),

$$I_{32} = I \frac{A_{32} \lambda_{31}}{\Sigma A \, \lambda_{32}} .$$

Here, A is the spontaneous transition probability.

[Table 16 follows.]

Table 16. Absolute Intensities of Solar Emission Lines

No	No series	Ion χ_i eV	Transition	λ, A	I/f, erg/cm² sec	f	I, erg/cm² sec	A/Σ A
	HI							
1		H I	$1s^2S - 2p^2P^\circ$	1215.7		0.416		
2		13.60	$-3p^2P^\circ$	1025.7	2	0.08	0.14	0.9
3		3.84	$-4p^2P^\circ$	972.5	1.5	0.03	0.04	0.9
4			$-5p^2P^\circ$	949.7	1	0.015	0.015	0.8
5			$-6p^2P^\circ$	937.8	1	0.008	0.008	0.8
6		He II	$1s^2S - 2p^2P^\circ$	303.8	0.5	0.4	0.18	0.9
7		54.4	$-3p^2P^\circ$	256.3	0.05	0.08	0.004	0.9
8		4.75	$-4p^2P^\circ$	243.0	0.02	0.03	$5\cdot10^{-4}$	0.8
9			$2p^2P^\circ - 3d^2D$	1640.4	0.05	0.08	$5\cdot10^{-4}$	0.1
10		C VI	$1s^2S - 2p^2P^\circ$	33.8	0.2	0.4	<0.08	
11		489.8 (6.3)	$2p^2P^\circ - 3d^2D$	182.5	0.2	0.08	<0.002	0.1
12		N VII 666.8 (6.4)	$1s^2S - 2p^2P^\circ$	24.8	0.01	0.4	<0.004	
13		O VIII	$1s^2S - 2p^2P^\circ$	19.0	0.5	0.4	<0.2	
14		871 (6.5)	$2p^2P^\circ - 3d^2D$	102.6	0.5	0.08	<0.005	
	LiI							
15		C IV	$2s^2S - 2p^2P^\circ$	1548.2	1.5	0.28	0.3	
16		64.48		1550.8			0.15	
17		5.00	$-3p^2P^\circ$	312.4	0.1	(0.3)	0.03	
18			$2p^2P^\circ - 3s^2S$	419.5	0.2	(0.3)	0.05	
19			$-3d^2D$	384.2	0.02	(0.3)	0.006	
20		N V	$2s^2S - 2p^2P^\circ$	1238.8	0.07	0.23	0.010	
21		97.86		1242.8			0.005	
		5.25						
22		O VI	$2s^2S - 2p^2P^\circ$	1031.9	5	0.20	0.06	
23		138.08		1037.6			0.03	
24		5.42	$-3p^2P^\circ$	150.1	0.06	0.24	0.015	
25			$-4p^2P^\circ$	115.8	0.03	(0.3)	0.005	0.5
26			$2p^2P^\circ - 3s^2S$	184.1	0.1	(0.3)	0.03	
27			$-3d^2D$	172.9	0.08	(0.3)	0.02	
28			$-4s^2S$	132.3	0.03	(0.3)	0.005	0.5
29		Ne VIII	$2s^2S - 2p^2P^\circ$	(770.5)	1	(0.15)	0.09	
30		239.0		(780.3)			0.06	
31		5.82	$-3p^2P^\circ$	(87)	0.06	(0.2)	0.01	
32		Na IX	$2s^2S - 2p^2P^\circ$	(682)	0.05	(0.15)	0.005	
33		299.8		(695)			0.002	
		5.97						
34		Mg X	$2s^2S - 2p^2P^\circ$	(609.9)	0.5	(0.15)	0.05	
35		367.4		(624.9)			0.025	
36		6.08	$-3p^2P^\circ$	58.0	0.03	(0.2)	0.006	
37		Al XI	$2s^2S - 2p^2P^\circ$	(550)	0.05	(0.13)	0.004	
38		441.9		(569)			0.002	
		6.2						
39		Si XII	$2s^2S - 2p^2P^\circ$	(499.3)	0.7	(0.12)	0.06	
40		523.2		(521.1)			0.03	
41		6.23	$-3p^2P^\circ$	(41)	0.03	(0.2)	0.006	
42		S XIV	$2s^2S - 2p^2P^\circ$	(421)	0.3	(0.1)	<0.02	
43		706.4 (636)		(446)			<0.01	
	NaI							
44		Mg II	$3s^2S - 3p^2P^\circ$	2795.5	30	0:9	20	
45		15.03		2802.7			9	
46		4.05	$-4p^2P^\circ$	1239.8	0.06	(0.5)	0.02	
47				1240.4			0.01	
48			$-5p^2P^\circ$	1026.0	0.015	(0.3)	0.003	
49			$3p^2P^\circ - 5s^2S$	1026.1			0.002	
50				1757.6		(0.2)	0.005	
51		Al III	$3s^2S - 3p^2P^\circ$	1854.7	0.025		0.03	
52		28.44		1862.8	0.06	(0.8)	0.02	
		4.40						

Table 16 (Cont.)

№№	Series	Ion x_i, $\lg T_i$	Transition	λ, A	I/f, erg/cm²·sec	f	I, erg/cm²·sec	A/EA
53		Si IV	$3s^2S - 3p^2P^\circ$	1393.7	0.1	(0.7)	0.05	
54		45 13		1402.7			0.02	
55		4.75	$-4p^2P$	457.8	0.002	(0.5)	0.001	
56				458.1				
57			$3p^2P^\circ - 3d^2D$	2128.0—	0.02	(0.5)	0.005	0.5
				—1123.0				
58			$-4s^2S$	815.1	0.004	(0.5)	0.001	0.5
59				818.1				
60		S VI	$3s^2S - 3p^2P^\circ$	933.4	0.05	(0.7)	0.02	
61		88.03		944.5			0.01	
62		5.18	$3p^2P^\circ - 3d^2D$	706.5—	0.01	(0.5)	0.002	0.5
				—712.7				
63		Cl VII	$3s^2S - 3p^2P^\circ$	800.7	0.002	(0.6)	0.001	
64		96.75		813.0				
		5.2						
65		A VIII	$3s^2S - 3p^2P^\circ$	700.4	0.01	(0.6)	0.004	
66		143.5		714.0			0.002	
		5.45						
67		K IX	$3s^2S - 3p^2P^\circ$	621.4	0.002	(0.6)	0.001	
68		175.9		636.3				
		5.59						
69		Ca X	$3s^2S - 3p^2P^\circ$	557.7	0.01	(0.6)	0.004—	
70		211.3		574.0			0.002	
		5.68						
71		Ti XII	$3s^2S - 3p^2P^\circ$	460.9	0.005	(0.5)	0.002	
72		291.5		480.1			0.001	
		5.93						
73		Cr XIV	$3s^2S - 3p^2P^\circ$	390.1	0.007	(0.5)	0.003	
74		384.2		412.5			0.001	
		6.12						
75		Mn XV	$3s^2S - 3p^2P^\circ$	361.5	0.008	(0.5)	0.003	
76		435		385.4			0.001	
		6.22						
77		Fe XVI	$3s^2S - 3p^2P^\circ$	336.2	1.8	(0.5)	<0.5	
78		489		361.7			<0.3	
79		(6.4)	$-4p^2P^\circ$	50.3—	0.3	(0.5)	<0.15	
				—50.5				
80			$3p^2P^\circ - 4s^2S$	637.2	0.3	(0.3)	<0.1	
81			$-3d^2D$	(250)			<0.01	
82				(262)	1	(0.1)	<0.05	
83				(264)			<0.04	
84		Ni XVIII	$3s^2S - 3p^2P^\circ$	293.3	0.1	(0.5)	<0.03	
85		607		322.0			0.02	
		(6.43)						
	KI							
86		Fe VIII	$3d^2D - 4f^2F^\circ$	130.9	0.02	(0.5)	0.01	
87		151	$-4p^2P^\circ$	196.0—	0.06	(0.5)	0.01	
		5.59		—195.5			0.02	
88			$4p^2P^\circ - 5s^2S$	370.5	0.02	(0.3)	0.004	
89				365.9			0.002	
	BI							
90		C II	$2p^2P^\circ - 3s^2S$	858.6	0.03	(0.2)	0.004	
91		24.38		858.1			0.002	
92		4.25	$-2p^{22}D$	1335.7	0.5	(0.6)	0.2	
93				1334.5			0.1	
94			$-2p^{22}S$	1036.3	0.1	(0.5)	0.05	
95			$-2p^{22}P$	903.6	0.05	(0.2)	0.01	
96			$-3d^2D$	687.4	$2\cdot10^{-3}$	(0.2)	$4\cdot10^{-4}$	
97			$2p^{24}P^\circ - 2p^{24}S^\circ$	1010.7	$6\cdot10^{-3}$	(0.1)	$6\cdot10^{-4}$	

Table 16 (Cont.)

№ №	Series	Ion χ_i $\lg T_i$	Transition	λ, Å	I/f, erg/cm²sec	I	I, erg/cm²sec	$\frac{A}{\Sigma A}$
98		N III 47.43 4.7	$2p^2P^\circ - 2p^{23}D$	980.8—991.6	0.02	(0.5)	0.01	
99			$-2p^{23}S$	764.4	0.008	(0.5)	0.004	
100			$-2p^{23}P$	687	0.004	(0.2)	$8\cdot10^{-4}$	
101			$-3d^2D$	374.2	$2\cdot10^{-4}$	(0.2)	$4\cdot10^{-5}$	
102		O IV 77.39 5.05	$2p^3P^\circ - 3s^2S$	279.9 279.6	0.05	(0.2)	0.01	
103			$-2p^{23}D$	790.2 787.7	1.5	(0.5)	0.5 0.2	
104			$-2p^{23}S$	609.8 608.4	0.8	(0.5)	0.3 0.1	
105			$-2p^{23}P$	554.1	0.6	(0.2)	0.1	
106			$-3d^2D$	238.6	0.02	(0.2)	0.004	
107			$2p^{23}D - 2p^{23}D^\circ$	779.8	0.2	(0.1)	0.002	0.2
108			$-3d^2F^\circ$	260.4	0.01	(0.2)	0.001	0.5
109			$2p^{24}P - 2p^{24}S^\circ$	625.1	0.3	(0.1)	0.03	
110		Ne VI 151.9 5.52	$2p^3P^\circ - 3s^2S$	138.6	0.03	(0.2)	0.006	
111			$-2p^{23}S$	432.4 430.0	0.5	(0.5)	0.015 0.008	
112			$-2p^{23}D$	562.8 558.6	0.8	(0.5)	0.02 0.015	
113			$-2p^{23}P$	399.8—403.3	0.4	(0.2)	0.08	
114			$2p^{23}D - 3p^2P^\circ$	171.2 171.1	0.02	(0.2)	0.002 0.001	
115		Na VII 208.4 5.7	$2p^{22}P^\circ - 3s^2S$	381.3	0.015	(0.5)	0.008	
116			$-2p^{23}D$	491.9—486.7	0.02	(0.5)	0.01	
117		Mg VIII 266.0 5.82	$2p^2P^\circ - 2p^{23}S$	339.0 335.3	0.25	(0.5)	0.08 0.04	
118			$-2p^{23}D$	436.7—430.5	0.3	(0.5)	0.15	
119			$-3s^2S$	82.6 83.2	0.02	(0.2)	0.002 0.001	
120			$-2p^{23}P$	311.8—317.0	0.25	(0.2)	0.05	
121			$2p^{24}P - 2p^{24}S^\circ$	352.4	0.[illegible]	(0.1)	0.015	
122			$2p^{23}P - 2p^{23}D^\circ$	680.3	0.1	(0.1)	0.003	0.3
123			$-2p^{23}P^\circ$	490.8	0.1	(0.1)	0.003	0.3
124			$2p^{23}S - 2p^{23}D$	597.7—597.2	0.1	(0.1)	0.003	0.3
125			$-2p^{23}P^\circ$	442.2	0.1	(0.1)	0.003	0.3
126			$2p^{23}D - 2p^{23}P^\circ$	342.2	0.1	(0.1)	0.003	0.3
127		Al IX 330.1 6.00	$2p^2P^\circ - 2p^{23}S$	305.1	0.04	(0.5)	0.02	
128			$-2p^{23}D$	392.4—385.0	0.05	(0.5)	0.025	
129		Si X 401.3 6.05	$2p^2P^\circ - 2p^{23}S$	277.3 272.1	0.3	(0.5)	0.1 0.05	
130			$-2p^{23}D$	356.1 347.5	0.4	(0.5)	0.15 0.07	
131			$-2p^{23}P$	258.4	0.3	(0.2)	0.06	
132			$-3d^2D$	50.5 50.7	0.02	(0.5)	0.006 0.003	
133			$2p^{23}P - 2p^{23}D^\circ$	555.0	0.2	(0.1)	0.006	0.3
134			$-2p^{23}P^\circ$	392.0—399.3	0.2	(0.1)	0.006	0.3
135			$2p^{23}D - 2p^{23}P^\circ$	280.0	0.2	(0.1)	0.006	0.3
136			$-2p^{23}D^\circ$	349.0	0.2	(0.1)	0.006	0.3
137			$2p^{23}S - 2p^{23}P^\circ$	360.8	0.2	(0.1)	0.006	0.3
138			$2p^{24}P - 2p^{24}S^\circ$	287.2	0.2	(0.1)	0.02	
139			$-3s^{24}P$	54.5	0.015	(0.1)	0.002	
140		P XI 479.4 6.2	$2p^2P^\circ - 2p^{23}D$	325.2 315.3	0.01	(0.5)	0.003 0.002	
141								
142								
143								
144								
145								
146								
147								
148								
149								
150								
151								
152								

Table 16 (Cont.)

№№	Series	Ion χ_i, eV	Transition	λ, Å	I_λ erg/cm² sec	f	$I_{\lambda\rho}$ erg/cm³ sec	$\frac{A}{\Sigma A}$
153			$-2p^{22}S$	254.0— —247.9	0.01	(0.5)	0.005	
154			$-2p^{22}P$	240— —232	0.008	(0.5)	0.004	
155			$-3s^2S$	46.1	$5\cdot10^{-4}$	(0.2)	$1\cdot10^{-4}$	
156		S XII	$2p^3P^\circ - 2p^{22}D$	(290)— —(302)	0.3	(0.5)	< 0.15	
157		564.6	$-2p^{22}S$	231.5	0.2	(0.5)	< 0.1	
158		(6.3)	$-3s^6S$	(38)	0.02	(0.5)	< 0.01	
159			$2p^{34}P - 2p^{34}S^\circ$	(239)			< 0.01	
160	AII	Si II	$3p^2P^\circ - 4s^2S$					
161		16.34		1533.4 1526.7	0.1 0.1	(0.2) (0.2)	0.015 0.008	
162		4.0	$-3p^{22}D$	1817.1	1	(0.5)	0.3	
163				1808.2			0.15	
164		S IV	$3p^2P^\circ - 3p^{22}S$	816.0	0.01	(0.5)	0.03	
165		47.29		809.7			0.002	
166		4.67	$-3p^{22}D$	1062.7— —1073.3	0.03	(0.5)	0.015	
167		A VI	$3p^2P^\circ - 3p^{22}S$	596.7	0.006	(0.5)	0.002	
168		91.41		589.0			0.001	
169		5.15	$-3p^{22}P$	545— —555	0.002	(0.2)	$5\cdot10^{-4}$	
170			$-3p^{22}D$	457— —461	0.001	(0.5)	$5\cdot10^{-4}$	
171		Ca VIII	$3p^2P^\circ - 3p^{22}D$	596.9	0.015	(0.5)	0.004	
172		148.1		582.8			0.002	
173		5.47	$-3p^{22}S$	471.1	0.007	(0.5)	0.002	
174				461.7			0.001	
175		Fe XIV	$3p^2P^\circ - 3p^{22}D$	(356)	1.2	(0.5)	0.4	
176		390		(342)			0.2	
		6.20						
177			$-3p^{22}P$	(266)	1	(0.2)	0.15	
178				(264)			0.05	
179			$-3p^{22}S$	(285)	1	(0.5)	0.3	
180				(276)			0.2	
181			$-3d^2D$	(223)	0.8	(0.5)	0.3	
182				(208)			0.1	
183			$-4s^2S$	59.0	0.2	(0.5)	0.05	
184				59.6			0.05	
185		Ni XVI	$3p^2P^\circ - 3p^{22}D$	(312)	0.06	(0.5)	< 0.02	
186		(480)		(300)			< 0.01	
187		(6.3)	$-3p^{22}S$	(250)	0.06	(0.5)	< 0.02	
188				(242)			< 0.01	
189			$-3p^{22}P$	(236)	0.05	(0.2)	< 0.006	
190				(233)			< 0.003	
191			$-3d^2D$	(199)	0.04	(0.5)	< 0.015	
192				(190)			< 0.005	
	ScI							
193		Fe VI 102	$s^4F - s^4G^\circ$	296.7— —293.5	0.025	(1)	0.025	
194		5.25	$-s^4F^\circ$	295.0— —293.0	0.025	(0.3)	0.01	
	He I							
195		He I	$1s^{21}S - 2p^1P^\circ$	584.4	2	0.36	0.7	
196		24.58	$-3p^1P^\circ$	537.0	0.6	0.07	0.04	
197		4.25	$-4p^1P^\circ$	522.2	0.3	0.03	0.01	
198		C V 392 6.14	$1s^{21}S - 2p^1P^\circ$	40.3	0.08	0.36	0.03	

Table 16 (Cont.)

№ №	Series	Ion x_i $\lg T_i$	Transition	λ, Å	I/f erg/cm² sec	f	I erg/cm² sec	$\frac{A}{A\Sigma}$
199		N VI 551.9 (6.35)	$1s^2 {}^1S - 2p\,{}^1P^\circ$	28.8	0.01	0.36	<0.003	
200		O VII	$1s^2 {}^1S - 2p\,{}^1P^\circ$	21.6	0.4	0.36	<0.15	
201		739.1	$- 3p\,{}^1P^\circ$	18.6	0.2	0.07	<0.015	
202		(6.4)	$2p\,{}^1P^\circ - 3s\,{}^1S$	(138.3)	0.2	0.05	<0.002	0.2
203			$2s\,{}^3S - 2p\,{}^3P^\circ$	1642.3	0.4	(0.1)	<0.001	0.01
	Bel							
204		C III	$2s^2 {}^1S - 2p\,{}^1P^\circ$	977.0	0.6	1	0.6	
205		47.86	$- 2p\,{}^3P^\circ$	1908.6— —1911.5	2	(0.1)	[0.2]	
206		4.68	$2p\,{}^3P^\circ - 3s\,{}^3S$	538.3	0.005	(0.2)	0.001	
207			$- 4d\,{}^3D$	371.7	$4\cdot10^{-4}$	(0.1)	$4\cdot10^{-5}$	
208			$- 2p^2\,{}^3P$	1176.0	0.1	0.1	0.01	
209			$2p\,{}^1P^\circ - 2p^2\,{}^1D$	2297.6	0.1	(0.2)	0.005	0.4
210			$- 2p^2\,{}^1S$	547.9	0.025	(0.1)	0.001	0.2
211			$- 3s\,{}^1S$	690.9	0.004	(0.1)	10^{-4}	0.2
212		N IV	$2s^2 {}^1S - 2p\,{}^1P^\circ$	765.1	0.02	0.5	0.01	
213		77.45 5.05	$- 2p\,{}^3P^\circ$	1490— —1488	0.08	(0.1)	[0.008]	
214			$2p\,{}^3P^\circ - 2p^2\,{}^3P$	922.0— —923.6	0.03	(0.2)	0.006	
215			$2p\,{}^1P^\circ - 2p\,{}^1D$	1717.5	0.03	(0.2)	0.006	
216		O V	$2s^2 {}^1S - 2p\,{}^1P^\circ$	629.7	1.5	0.2	0.3	
217		113.9	$- 2p\,{}^3P^\circ$	1217.7	5	(0.2)	[0.5]	
218		5.26		1216.9				
219			$- 3p\,{}^1P^\circ$	172.2	0.02	(0.1)	0.002	
220			$2p\,{}^3P^\circ - 2p^2\,{}^3P$	758.7— —761.9	0.9	(0.1)	0.09	
221			$2p\,{}^1P^\circ - 2p^2\,{}^1D$	1371.3	0.7	(0.1)	0.07	
222			$- 2p^2\,{}^1S$	774.5	0.5	(0.1)	0.05	
223		Ne VII	$2s^2 {}^1S - 2p\,{}^1P^\circ$	(464)	0.4	(0.2)	0.08	
224		207.3 5.51	$- 2p\,{}^3P^\circ$	(892)	1	(0.1)	[0.1]	
225		Na VIII	$2s^2 {}^1S - 2p\,{}^1P^\circ$	411.2	0.02	(0.2)	0.004	
226		264.1 5.86	$- 2p\,{}^3P^\circ$	778.9— —793.3	0.05	(0.1)	[0.005]	
227		Mg IX	$2s^2 {}^1S - 2p\,{}^1P^\circ$	368.2	0.4	(0.2)	0.08	
228		327.9 5.90	$- 2p\,{}^3P^\circ$	710.3— —692.4	0.6	(0.1)	0.06	
229		Al X	$2s^2 {}^1S - 2p\,{}^1P^\circ$	332.9	0.04	(0.2)	0.008	
230		398.5 6.1	$2p\,{}^3P^\circ - 2p^2\,{}^3P$	401.2	0.03	(0.3)	0.005	
231		Si XI	$2s^2 {}^1S - 2p\,{}^1P^\circ$	303.6	0.4	(0.15)	0.06	
232		476.0 6.14	$- 2p\,{}^3P^\circ$	565.1— —591.2	0.6	(0.1)	[0.06]	
233			$2p\,{}^3P^\circ - 2p^2\,{}^3P$	365.4	0.3	(0.3)	0.06	
234		P XII	$2s^2 {}^1S - 2p\,{}^1P^\circ$	278.7	0.01	(0.2)	<0.002	
235		560.3 (6.3)	$2p\,{}^3P^\circ - 2p^2\,{}^3P$	335.6	0.008	(0.3)	<0.002	
236		S XIII	$2s^2 {}^1S - 2p\,{}^1P^\circ$	(257.5)	0.15	(0.3)	<0.05	
237		651.7 (6.33)	$2p\,{}^3P^\circ - 2p^2\,{}^3P$	(311)	0.1	(0.3)	<0.02	
	MgI							
238		Al II	$3s^2 {}^1S - 3p\,{}^1P^\circ$	1670.9	0.03	(1.5)	0.05	
239		18.82 4.10	$- 3p\,{}^3P^\circ$	2669.2	1	(0.1)	[0.1]	
240		Si III	$3s^2 {}^1S - 3p\,{}^1P^\circ$	1206.5	0.06	(1.1)	0.06	
241		33.46 4.40	$- 3p\,{}^1P^\circ$	1895.5	1	(0.1)	[0.1]	
242		S V	$3s^2 {}^1S - 3p\,{}^1P^\circ$					
243		72.5 5.00	$- 3p\,{}^3P^\circ$	786.5	0.025	(0.7)	0.02	
				1188.7— —1203.8	0.05	(0.1)	[0.005]	

Table 16 (Cont.)

№ №	Series	Ion χ_i $\lg T_i$	Transition	λ, Å	I/f, erg/cm²·sec	f	I, erg/cm²·sec	$\frac{A}{\Sigma A}$
244		A VII	$3s^{21}S - 3p^1P^\circ$	585.8	0.007	(0.6)	0.004	
245		124	$3p^3P^\circ - 3d^3D$	475.6	0.002	(0.5)	$5\cdot10^{-4}$	
246		5.35		479.4			$2\cdot10^{-4}$	
247		Ca IX	$3s^{21}S - 3p^1P^\circ$	466.2	0.01	(0.6)	0.006	
248		188.2	$-3p^3P^\circ$	678.6—701.1	0.02	(0.1)	[0.002]	
		5.63						
249		Fe XV	$3s^{21}S - 3p^1P^\circ$	(298)	1	(0.5)	<0.5	
250		457	$-4p^1P^\circ$	52.9	0.2	(0.75)	<0.1	
251		(6.33)	$-3p^3P^\circ$	391.2—424.2	1.5	(0.1)	$<$[0.15]	
252			$3p^3P^\circ - 3d^3D$	231.5	0.8	(0.3)	<0.1	
	Ca I							
253		Fe VII	$a^3F - z^3F^\circ$	231.7—232.2	0.02	(0.3)	0.006	
		128						
254		5.38	$a^3P - z^3P^\circ$	239.9	0.02	(0.3)	0.06	
255			$a^1D - z^1D^\circ$	245.2	0.02	(0.1)	0.002	
256			$-y^1P^\circ$	152.9	0.006	(0.1)	$6\cdot10^{-4}$	
257			$a^1G - z^1F^\circ$	243.4	0.02	(0.1)	0.002	
	CI							
258		CI	$2p^{23}P - 3s^3P^\circ$	1656—1657	3	1	3	
		11.26						
259		3.85	$-2p^{23}D$	1560—1561	1	(1)	1	
260			$-2p^{23}P^\circ$	1328.8	0.2	(0.1)	0.02	
261			$-4s^3P^\circ$	1279.7	0.15	(0.1)	0.01	
262			$-3d^3D^\circ$	1277.6	0.15	(0.5)	0.07	
263			$-5d^3D^\circ$	1158.1	0.1	(0.5)	0.05	
264			$2p^{21}D - 3s^1P^\circ$	1930.9	2	0.1	0.1	0.5
265			$2p^{21}S - 3s^1P^\circ$	2479.3	2	0.1	0.1	0.5
266		N II	$2p^{23}P - 2p^{23}D$	1085.7—1084.0	0.01	(1)	0.01	
		29.61						
267		4.40	$-2p^{23}P^\circ$	916.0	0.01	(0.1)	0.001	
268			$-2p^{23}S^\circ$	644.8	$5\cdot10^{-4}$	(0.3)	10^{-4}	
269			$2p^{21}D - 2p^{21}D^\circ$	776.0	0.003	(0.1)	$3\cdot10^{-4}$	
270			$-3s^1P^\circ$	746.9	$5\cdot10^{-4}$	(0.1)	$2\cdot10^{-4}$	0.5
271			$2p^{21}S - 3s^1P^\circ$	858.5	$5\cdot10^{-4}$	(0.1)	$2\cdot10^{-4}$	0.5
272		O III	$2p^{23}P - 2p^{23}P^\circ$	703.9—702.3	0.6	(0.1)	0.06	
		54.93						
273		4.80	$-2p^{23}D^\circ$	835.3—832.9	1	(0.3)	0.3	
274			$-3s^3P^\circ$	374.1	0.03	1	0.03	
275			$2p^{21}D - 2p^{21}D^\circ$	599.6	0.26	(0.1)	0.01	0.5
276			$-2p^{21}P^\circ$	525.8	0.1	(0.1)	0.005	0.5
277			$2p^{23}D^\circ - 2p^{43}P$	610.9—609.7	0.03	(0.3)	0.01	
278			$2p^{21}S - 2p^{21}P^\circ$	597.8	0.1	(0.1)	0.005	0.5
279			$-3s^1P^\circ$	434.9	0.025	0.8	0.02	
280			$-3d^1P^\circ$	345.3	0.006	(0.1)	$6\cdot10^{-4}$	
281		Ne V	$2p^{23}P - 2p^{23}P^\circ$	483.0—480.4	0.4	(0.3)	0.1	
		126.4						
282		5.37	$-2p^{23}D^\circ$	572.3—568.4	0.5	(1)	0.5	
283			$-2p^{23}S^\circ$	358.0	0.1	(1)	0.1	
284			$2p^{21}D - 2p^{21}D^\circ$	416.2	0.25	(0.1)	0.02	
285			$-2p^{21}P^\circ$	365.4	0.1	(0.1)	0.01	
286			$-3s^1P^\circ$	173.9	0.01	(0.1)	$5\cdot10^{-4}$	0.5
287			$2p^{21}S - 3s^1P^\circ$	151.3	0.01	(0.1)	$5\cdot10^{-4}$	0.5
288			$-2p^{21}P^\circ$	416.8	0.1	(0.1)	0.01	
289		Na VI	$2p^{23}P - 2p^{23}P^\circ$	414.3	0.01	(0.1)	0.001	
290		172.4	$-2p^{23}D^\circ$	494.3	0.015	(0.5)	0.005	
291		5.58		491.4			0.003	
292			$-2p^{23}S^\circ$	313.7—311.9	0.01	(1)	0.01	

Table 16 (Cont.)

№№	Series	Ion x_i $\lg T_i$	Transition	λ, Å	I/r_3 erg/cm³ sec	I	I_{2p} erg/cm³ sec	$\frac{A}{A\Sigma}$
293			$2p^{21}D - 2p^{21}D^{\circ}$	361.2	0.01	(0.1)	0.001	
294			$- 2p^{21}P^{\circ}$	317.6	0.006	(0.1)	$6\cdot10^{-4}$	
295		Mg VII	$2p^{23}P - 2p^{23}P^{\circ}$	367.8—	0.2	(0.3)	0.06	
		225.3		—363.7				
296		5.75	$- 2p^{23}D^{\circ}$	434.9—	0.25	(1)	0.25	
				—429.2				
297			$- 2p^{23}S^{\circ}$	278.4	0.2	(1)	0.2	
298			$2p^{21}D - 2p^{21}D^{\circ}$	319.0	0.2	(0.1)	0.01	0.5
299			$- 2p^{21}P^{\circ}$	280.7	0.1	(0.1)	0.005	0.5
300			$- 3s^{1}P^{\circ}$	98.0	0.02	(0.1)	0.001	0.5
301			$2p^{21}S - 3s^{1}P^{\circ}$	102.3	0.02	(0.1)	0.001	0.5
302		Al VIII	$2p^{23}P - 3s^{3}P^{\circ}$	328.2—	0.02	(0.3)	0.006	
		285.1		—323.5				
303		5.92	$- 2p^{23}D^{\circ}$	388.0—	0.02	(1)	0.02	
				—381.1				
304			$2p^{21}D - 3s^{1}P^{\circ}$	251.3	0.015	(0.1)	0.001	0.5
305			$2p^{21}S - 3s^{1}P^{\circ}$	287.0	0.015	(0.1)	0.001	0.5
306		Si IX	$2p^{23}P - 2p^{23}P^{\circ}$	296.2—	0.2	(0.3)	0.06	
		351.8		—290.6				
307		6.08	$- 2p^{23}D^{\circ}$	—342.2	0.4	(1)	0.4	
				350.0—				
308			$- 2p^{23}S^{\circ}$	223.7—	0.2	(1)	0.2	
				—227.0				
309			$2p^{21}D - 2p^{21}P^{\circ}$	227.3	0.15	(0.1)	0.01	0.5
310			$2p^{21}S - 2p^{21}P^{\circ}$	259.7	0.15	(0.1)	0.01	0.5
311		S XI	$2p^{23}P - 2p^{23}D^{\circ}$	—(282)	0.2	(1)	0.2	
				(293)—				
312		506.4	$- 2p^{23}P^{\circ}$	(253)	0.2	(0.3)	0.06	
313		6.25	$- 2p^{23}S^{\circ}$	(191)	0.15	(0.1)	0.1	
314		Ca XV	$2p^{23}P - 2p^{23}D^{\circ}$	(228)—	0.1	(1)	<0.1	
				—(210)				
315		898.3	$- 2p^{23}P^{\circ}$	(185)	0.08	(0.3)	<0.02	
316		(6.5)	$- 2p^{23}S^{\circ}$	(144)	0.05	(1)	<0.05	
	SiI							
317		S III	$3p^{23}P - 3p^{23}P^{\circ}$	1012.6	0.02	(0.3)	0.006	
318		34.7	$- 3p^{23}D^{\circ}$	1190.21			0.003	
319		4.48		1194.04			0.006	
320				1194.43			0.002	
321				1200.95	0.025	(1)	0.012	
322				1201.70			0.002	
323				1202.1			$2\cdot10^{-4}$	
324			$- 3p^{23}S^{\circ}$	728.7	0.002	(1)	0.002	
325			$3p^{21}D - 3p^{21}P^{\circ}$	796.7	0.001	(0.1)	10^{-4}	0.5
326			$3p^{21}S - 3p^{21}P^{\circ}$	911.8	0.001	(0.1)	10^{-4}	0.5
327		A V	$3p^{23}P - 3p^{23}D^{\circ}$	822.2	0.006	(1)	0.003	
328				836.0			0.003	
329		75.0	$- 3p^{23}P^{\circ}$	716.4	0.004	(0.3)	0.001	
330		5.03	$- 3p^{23}S^{\circ}$	527.7	0.002	(1)	0.002	
331		Ca VII	$3p^{23}P - 3p^{23}D^{\circ}$	624.4—	0.01	(1)	0.01	
				—610.5				
332		128.0	$- 3p^{23}P^{\circ}$	551.5	0.008	(0.3)	0.002	
333		5.39	$- 3p^{23}S^{\circ}$	414.7	0.005	(1)	0.005	
334		Fe XIII	$3p^{23}P - 3p^{23}D^{\circ}$	(360)—	1.2	(1)	1.2	
				—(386)				
335		355	$- 3p^{23}P^{\circ}$	(330)	1	(0.3)	0.3	
336		6.18	$- 3d^{23}P^{\circ}$	(210)	0.6	(0.3)	0.2	
337			$- 3p^{23}S^{\circ}$	(250)	0.7	(1)	0.7	
338			$- 4s^{3}P^{\circ}$	(75)	0.15	(0.3)	0.05	
339		Ni XV	$3p^{23}P - 3p^{23}D^{\circ}$	(316)—	0.07	(1)	<0.07	
				—(346)				
340		455	$- 3p^{23}P^{\circ}$	(290)	0.06	(0.3)	<0.02	
341		6.3	$- 3d^{3}P^{\circ}$	(182)	0.04	(0.3)	<0.01	
342			$- 3p^{23}S^{\circ}$	(220)	0.05	(1)	<0.05	
343			$- 4s^{3}P^{\circ}$	(58)	0.008	(0.3)	<0.002	

Table 16 (Cont.)

№ №	Series	Ion z_i $\lg T_i$	Transition	λ, Å	I/I_λ, erg/cm²·sec	f	I_λ, erg/cm²·sec	$\frac{A}{A\Sigma}$
	NI							
344		N I 14.54	$2p^{34}S^\circ - 3s^4P$	1199.5— —1200.7	0.005	(1)	0.005	
345		3.91	$- 2p^{44}P$	1135.0— —1134.1	0.003	(1)	0.003	
346			$- 4s^4P$	964.0— —965.1	$3\cdot10^{-5}$	(0.1)	$2\cdot10^{-6}$	0.5
347			$2p^{32}D^\circ - 3d^2P$	1171.1	$5\cdot10^{-5}$	(0.1)	$\sim 10^{-6}$	0.2
348			$- 3s^2P$	1492.5	0.003	(0.1)	$2\cdot10^{-4}$	0.5
349			$2p^{32}P^\circ - 3s^2P$	1742.7	0.003	(0.1)	$2\cdot10^{-4}$	0.5
350		O II	$2p^{34}S^\circ - 2p^{44}P$	834.5			0.15	
351		35.15		833.3	0.3	(1)	0.1	
352		4.50		832.8			0.05	
353			$- 3s^4P$	539.1	0.02	(1)	0.02	
354			$- 3d^4P$	430.2	0.002	(1)	$4\cdot10^{-4}$	0.2
355			$2p^{32}D^\circ - 2p^{42}P$	538.3	0.004	(0.3)	$3\cdot10^{-4}$	0.25
356			$2p^{32}P^\circ - 2p^{42}D$	796.8	0.03	(0.3)	0.005	0.5
357		No IV	$2p^{34}S^\circ - 2p^{44}P$	543.9			0.12	
358		97 16		542.0	0.25	(1)	0.08	
359		5.20		541.1			0.04	
360			$2p^{32}D^\circ - 2p^{42}D$	470.0	0.1	(0.1)	0.005	0.5
361			$2p^{32}P^\circ - 2p^{42}D$	521.3	0.1	(0.1)	0.005	0.5
362		Na V	$2p^{34}S^\circ - 3p^{44}P$	463.2— —459.9	0.008	(1)	0.008	
363		138.6	$2p^{32}D^\circ - 2p^{42}D$	400.7	0.005	(0.1)	$2\cdot10^{-4}$	0.5
364		5.43	$2p^{32}P^\circ - 2p^{42}D$	445.2	0.005	(0.1)	$2\cdot10^{-4}$	0.5
365		Mg VI	$2p^{34}S^\circ - 3p^{44}P$	111.7— —112	0.01	(1)	0.01	
366		186.9	$- 2p^{44}P$	403.3			0.13	
367		5.63		400.7	0.25	(1)	0.08	
368				399.3			0.04	
369			$2p^{32}P^\circ - 2p^{42}D$	388.0	0.1	(0.1)	0.005	0.5
370			$- 2p^{42}S$	314.5	0.1	(0.1)	0.01	
371			$2p^{32}D^\circ - 2p^{42}D$	349.1	0.1	(0.1)	0.001	0.5
372		Al VII	$2p^{34}S^\circ - 2p^{44}P$	356.9			0.01	
373		241.9		353.8	0.02	(1)	0.005	
374		5.82		352.2			0.003	
375			$- 3s^4P$	86.9— —87.2	0.002	(1)	0.002	
376			$2p^{32}D^\circ - 2p^{44}P$	309.0	0.01	(0.1)	$5\cdot10^{-4}$	0.5
377		Si VIII	$2p^{34}S^\circ - 2p^{44}P$	319.8			0.15	
378		303.9		316.2	0.3	(1)	0.1	
379		5.96		314.3			0.05	
380			$- 3s^4P$	69.6— —69.9	0.02	(1)	0.02	
381			$2p^{32}D^\circ - 2p^{42}D$	276.8— —277.1	0.2	(0.1)	0.01	0.5
382			$- 2p^{42}S$	229.8— —230.2	0.15	(0.1)	0.008	0.5
383			$- 2p^{42}P$	214.8— —216.9	0.15	(0.1)	0.008	0.5
384			$2p^{32}P^\circ - 2p^{42}S$	251	0.15	(0.1)	0.008	0.5
385		S X	$2p^{34}S^\circ - 2p^{44}P$	(264) — —(258)	0.15	(1)	0.15	
386		448.6 6.20	$- 3s^4P$	47.6— —47.8	0.01	(1)	0.01	
387		A XII	$2p^{34}S^\circ - 2p^{44}P$	(226) — —(220)	0.04	(1)	<0.04	
388		621.1 (6.4)	$- 3s^4P$	(33)	0.005	(1)	<0.005	
389		Ca XIV	$2p^{34}S^\circ - 2p^{44}P$	(197) — —(191)	0.06	(1)	<0.06	
390		821.2 (6.5)	$- 3s^4P$	(22)	0.002	(1)	<0.002	

Table 16 (Cont.)

№	Series	Ion z_i $\lg T_i$	Transition	λ, Å	I/f_j erg/cm² sec	f	I_{ik} erg/cm² sec	$\frac{A}{\Delta E}$
	PI							
391		S II 23.4	$3p^{34}S^{\circ} - 3p^{44}P$	1259.5—1250.1	0.01	(1)	0.01	
392		4.23	$- 4s^{4}P$	906.9—912.7	0.002	(1)	0.002	
393		A IV 59.8	$3p^{34}S^{\circ} - 3p^{44}P$	850.6—840.0	0.004	(1)	0.004	
394		4.88	$3p^{33}D^{\circ} - 3p^{43}P$	683.3—689.0	0.002	(0.1)	$2\cdot10^{-4}$	
395		Ca VI 109	$3p^{34}S^{\circ} - 3p^{44}P$	629.6—641.9	0.008	(1)	0.008	
396		5.28	$3p^{33}D^{\circ} - 3p^{43}P$	510	0.003	(0.1)	3.10^{-4}	
397			$3p^{33}P^{\circ} - (^{3}D)$	766.6	0.006	(0.1)	6.10^{-4}	
398			$- 3p^{43}D$	674.3	0.005	(0.1)	5.10^{-4}	
399		Fe XII	$3p^{34}S^{\circ} - 3p^{44}P$	(369)—(356)	0.6	(1)	0.6	
400		325	$- 4s^{4}P$	(80)	0.06	(1)	0.06	
401		6.00	$- 3d^{4}D$	(238)	0.4	(0.5)	0.2	
402			$- 3d^{4}P$	(209)	0.4	(0.5)	0.2	
403			$3p^{33}D^{\circ} - 3p^{43}P$	(283)	0.6	(0.1)	0.04	0.7
404			$3p^{33}P^{\circ} - 3p^{43}P$	(326)	0.6	(0.1)	0.02	0.3
405		Ni XIV	$3p^{34}S^{\circ} - 3p^{44}P$	(323)—(311)	0.06	(1)	0.06	
406		422 6.18	$- 4s^{4}P$	(63)	0.006	(1)	0.006	
	VI							
407		Fe IV 57.1 4.78	$3d^{34}S - 4p^{6}P^{\circ}$	526.6—525.7	0.01	(1)	0.01	
408		Ni VI 136 5.42	$3d^{34}S - 4p^{6}P^{\circ}$	260.4—260.7	0.002	(1)	0.002	
	OI							
409		O I 13.61	$2p^{43}P - 3s^{3}S^{\circ}$	1302.1—1306.2	0.6	(1)	0.6	
410		3.85	$- 3s^{5}S^{\circ}$	1355	1	(0.1)	[0.1]	
411			$- 4s^{3}S^{\circ}$	1040.9—1039.2	0.02	(0.5)	0.01	
412			$- 4d^{3}D^{\circ}$	1025.7	0.02	(0.5)	0.01	
413		Ne III 64.43	$2p^{43}P - 2p^{53}P^{\circ}$	489.5—487.3	0.04	(0.3)	0.01	
414		4.90	$- 3s^{3}S^{\circ}$	313.0	0.005	(1)	0.005	
415			$2p^{61}S - 2p^{51}P^{\circ}$	427.8	0.015	(0.1)	0.001	0.5
416			$2p^{61}D - 2p^{51}P^{\circ}$	379.3	0.015	(0.1)	0.001	0.5
417		Na IV 98.9	$2p^{43}P - 2p^{53}P^{\circ}$	411.3—408.7	0.003	(0.3)	0.001	
		5.20						
418		Mg V 141.2	$2p^{43}P - 2p^{53}P^{\circ}$	353.1—350.0	0.006	(0.3)	0.002	
		4.95						
419		Al VI 190.4	$2p^{43}P - 2p^{53}P^{\circ}$	309.6—306.0	0.01	(0.3)	0.003	
420		5.66	$2p^{61}D - 2p^{51}P^{\circ}$	243.8	0.006	(0.1)	$3\cdot10^{-4}$	0.5
421			$2p^{61}S - 2p^{51}P^{\circ}$	275.4	0.006	(0.1)	$3\cdot10^{-4}$	0.5
422		Si VII 246.4	$2p^{43}P - 2p^{53}P^{\circ}$	275.4			0.06	
423		5.82		278.4			0.02	
424				276.8			0.015	
425				275.7	0.15	(1)	0.015	
426				274.1			0.015	
427				272.7			0.02	
428			$2p^{61}S - 2p^{51}P^{\circ}$	246.1	0.06	(0.1)	0.003	0.5
429			$2p^{61}D - 2p^{51}P^{\circ}$	217.8	0.06	(0.1)	0.003	0.5

Table 16 (Cont.)

№№	Series	Ion x_i $\lg I_i$	Transition	λ, Å	I/I', erg/cm² sec		I, erg/cm² sec	$\frac{A}{A\Sigma}$
430		S IX	$2p^{43}P - 2p^{33}P^{\circ}$	(222) — —(228)	0.1	(0.3)	0.03	
431		379.0	$- 3s^{3}S^{\circ}$	56.1	0.015	(1)	0.015	
432		6.1	$2p^{41}D - 2p^{31}P^{\circ}$	(555)	0.2	(0.1)	0.01	0.5
433			$2p^{41}S - 2p^{31}P^{\circ}$	(488)	0.2	(0.1)	0.01	0.5
434		A XI	$2p^{43}P - 2p^{33}P^{\circ}$	(188) — —(195)	0.03	(0.3)	<0.01	
435		539.5 (6.3)	$- 3s^{3}S^{\circ}$	(39.7)	0.004	(1)	<0.004	
436		Ca XIII	$2p^{43}P - 2p^{33}P^{\circ}$	(162) — —(171)	0.05	(0.3)	<0.02	
437		728.8 (6.4)	$- 3s^{3}S^{\circ}$	(29.6)	0.005	(1)	<0.005	
	SI							
438		S I	$3p^{43}P - 4s^{3}S^{\circ}$	1807.3			0.55	
439		10.36		1820.3	1	(1)	0.33	
440		(3.7)		1826.2			0.11	
441			$- 3s^{3}D^{\circ}$	1474.0	0.1	(1)	0.05	
442				1483.0			0.025	
443		A III	$3p^{43}P - 3p^{33}P^{\circ}$	887.4			$4\cdot10^{-4}$	
444		40.9		879.6	0,002	(0.3)	$1\cdot10^{-4}$	
445		4.59		878.7			$2\cdot10^{-4}$	
446		Ca V 84.4 5.08	$3p^{43}P - 3p^{33}P^{\circ}$	637.9— —656.8	0.005	(0.3)	0.002	
447		Fe XI 290.3 5.89	$3p^{43}P - 3p^{3}P^{\circ}$	(350) — —(376)	0.5	(0.3)	0.15	
448			$- 4s^{3}S^{\circ}$	(89.3)	0.05	(1)	0.05	
449		Ni XIII	$3p^{43}P - 3p^{33}P^{\circ}$	(304) — —(332)	0.06	(0.3)	0.02	
450		(380) (6.1)	$- 4s^{3}S^{\circ}$	(69)	0.006	(1)	0.006	
	NeI							
451		Si V 166.7 5.55	$2p^{61}S - 3s^{1}P^{\circ}$	117.9	0.01	(1)	0.01	
452		S VII 281 5.92	$2p^{61}S - 3s^{1}P^{\circ}$	72.0	0.003	(1)	0.003	
453		A IX 422.6 6.16	$2p^{61}S - 3s^{1}P^{\circ}$	48.7	0.006	(1)	0.006	
454		Ca XI 592.5 (6.4)	$2p^{61}S - 3s^{1}P^{\circ}$	35.2	0.005	(1)	0.005	
	AI							
455		Fe IX 234.6 5.73	$3p^{61}S - 4s^{1}P^{\circ}$	103.6	0.03	(1)	0.03	
456		Ni XI 318 5.95	$3p^{61}S - 4s^{1}P^{\circ}$	(78.1)	0.003	(1)	0.003	
	FI							
457		Mg IV	$2p^{53}P^{\circ} - 2p^{63}S$	321.0— —323.3	0.02	(1)	0.02	
458		109.3 5.25	$- 3s^{3}P$	180.6	0.002	(0.3)	$6\cdot10^{-4}$	
459		Al V 153.8 5.51	$2p^{53}P^{\circ} - 2p^{63}S$	278.7— —281.4	0.005	(1)	0.005	
460		Si VI	$2p^{53}P^{\circ} - 2p^{63}S$	240.0— —249.1	0.08	(1)	0.08	

Table 16 (Cont.)

[illegible]	Series	Ion x_i $\lg T_i$	Transition	λ, A	I/f, erg/cm²·sec	I	I, erg/cm²·sec	$\frac{A}{A\Sigma}$
461		205.1	$-3s^2P$	100.0	0.01	(0.3)	0.003	
462		5.70	$-5d'^2P$	65	0.002	(0.1)		
....			.....	....			0.02	
			$-3d^2P$	85	0.004	(0.3)		
463		S VIII	$2p^{52}P^\circ - 2p^{62}S$	198.6	0.08	(1)	0.05	
464		328.8		202.6			0.03	
465		6.00	$-3s^2P$	63.3	0.006	(0.3)	0.002	
466			$-3s'^2D$	61.6	0.006	(1)	0.006	
467			$-3s'^2S$	59.2	0.005	(1)	0.005	
468			$-3d^2P$	54.3	0.003	(0.3)	0.001	
469			$-3d^2D$	54.2	0.003	(1)	0.003	
470			$-3d'^2P$	53.0	0.003	(0.3)	0.001	
471			$-d'^2D$	52.9	0.005	(0.3)		
			.....	....			0.03	
			$-4d'^2S$	44.5	0.003	(0.1)		
472		A X	$2p^{52}P^\circ - 3s^2P$	(43.8)	0.003	(0.3)	$<$0.001	
473		480	$-2p^{62}S$	(166)	0.02	(1)	$<$0.02	
474		(6.25)	$-3d^2P$	50	0.003	(0.3)		
			.....	...			$<$0.02	
			$-5d^2P$	45	0.002	(0.1)		
475		Cd XII	$2p^{52}P^\circ - 3s^2P$	32.3	0.003	(0.3)	$<$0.001	
476		655	$-2p^{62}S$	(141)	0.03	(1)	$<$0.03	
477		(6.3)	$-3d^2P$	42	0.004	(0.3)		
			.....	....			$<$0.01	
			$-5d^2P$	34	0.002	(0.1)		
	Cl							
478		Fe X	$3p^{52}P^\circ - 3d^2D$	(347.0)	0.5	(1)	0.5	
479		262	$-4s^2P$	96.1	0.06	(0.3)	0.02	
480		5.86	$-4s^{12}D$	97	0.05	(0.3)		
			.....	....			0.05	
			$-5d$	94	0.05	(0.1)		
481		Ni XII	$3p^{52}P^\circ - 3d^2D$	(299)	0.03	(1)	0.03	
482		350	$-4s^2P$	(84.8)	0.006	(0.3)	0.002	
		6.08						

22. Nikol'skiy, G. M. Shortwave solar radiation. Review. Geomagnetizm i aeronomiya, v. 2, no. 1, 1962, 3-37.

The first part of the article deals with experimental observations of shortwave solar radiation and includes a summary of data (for the shortwave region only) on absolute intensities, energy distribution in the solar spectrum, and identification of solar emission lines. The identification of shortwave solar lines is based on the results of theoretical intensity calculations by G. S. Ivanov-Kholodnyy and Nikol'skiy [21] (given in greater detail in [24]) and experimental data by T. Violett and W. A. Rense and H. E. Hinteregger. A method of calculating the absolute intensities of shortwave solar radiation developed in [20] is summarized.

On the basis of all available data, it is concluded that solar radiation intensity at the earth in the spectral region $\lambda \leq 1100$ Å is equal to 15 ergs/cm^2·sec. Nikol'skiy's analysis shows a need for reevaluating previous calculations of shortwave solar radiation by Western scientists. The present theory explaining the ionization of the D layer is in agreement with the theoretical and experimental data.

The structure of the solar atmosphere is also reviewed and an analysis given of the physical conditions of the solar atmosphere which determine the shortwave radiation. The distribution of temperature and electron density in the solar atmosphere based on shortwave-radiation observations is determined, and in connection with this determination the shortwave line radiation process is reviewed. The method used here is identical to the one for calculating absolute intensities proposed in [20]. The transparency of the solar atmosphere to hard-line radiation is reviewed.

Finally, the latest Western developments in continuous x-ray solar emission in the spectral region $\lambda < 10$ to 20 Å are summarized.

23. Ivanov-Kholodnyy, G. S. Intensity of shortwave solar radiation and rate of ionization and recombination processes in the ionosphere. Review. Geomagnetizm i aeronomiya, v. 2, no. 3, 1962, 377-406.

This review is very similar to the one published by G. M. Nikol'skiy [22] except that the main emphasis here is placed on ionization and recombination processes taking place in the ionosphere rather than shortwave solar radiation. The review consists of three parts, dealing with 1) total energy and the spectrum of ionizing solar radiation,

2) ionic composition of the atmosphere, and 3) corpuscular streams in the ionosphere.

The following topics are discussed in the first part: determination of the total flux of shortwave solar radiations at $\lambda \leq 1100$ Å on the basis of ionospheric data; calculation of S from astrophysical data; rocket data on shortwave solar radiation and its interpretation; and variation of radiation intensity in the active solar regions.

The second part summarizes the available data on the following subjects: the abundance of molecular ions in the ionosphere; laboratory investigations of dissociative recombination processes; effective recombination coefficients in the ionosphere; confirmation of the dissociative recombination processes in the ionosphere; experimental data on the effective coefficient of recombination in the ionosphere; and the intensity of solar energy in the upper atmosphere.

Ivanov-Kholodnyy concludes that the latest data point up the inadequacy of present concepts on the rate of recombination and ionization processes in the ionosphere. Processes of ionization and recombination are much more intense than presently believed, and new concepts of principal physical and chemical processes in the ionosphere will have to be developed. In addition, new interpretations are required of such phenomena as the general state of the ionosphere, the diurnal and annual variation of ionospheric parameters, and diffusion.

24. Ivanov-Kholodnyy, G. S., and G. M. Nikol'skiy. Identification of solar emission lines in the shortwave spectral region $\lambda \leq 1100$ Å. Geomagnetizm i aeronomiya, v. 2, no. 3, 1962, 425-442.

One hundred eighty of 225 solar emission lines in the region between 60 and 1100 Å recorded by satellites are identified from the tabulated line intensities of 500 lines calculated earlier by the authors [21]. An analysis of the earlier calculations is presented.

The spectral energy distribution of shortwave solar radiation is given in Fig. 6. The total energy of line radiation for $\lambda \leq 1100$ Å was found to be not less than 15 erg/cm^2·sec at the earth. The relative nitrogen content on the sun was shown to be $[N]/[H] = 3 \cdot 10^{-5}$.

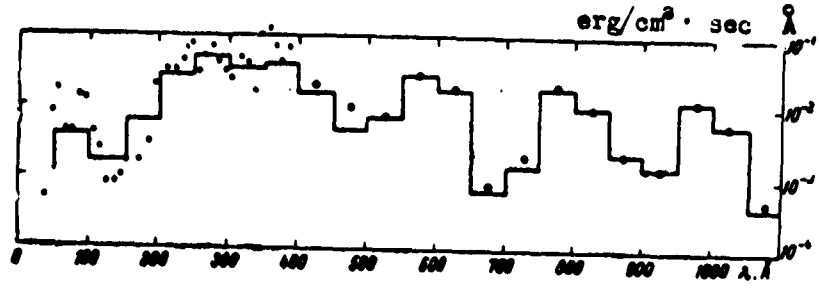

Fig. 6. Spectral Energy Distribution of Shortwave Solar Radiation (λ = 30 to 1100 Å)

The possible emission lines determined in [21] are listed in Table 17 in the order of increasing λ, together with their intensities measured at the earth and the number assigned to the lines in that work. In some cases, the wavelengths of multiplet components are calculated. Also in this table, theoretical data are compared with available experimental data, and the lines recorded by satellites are compared with their theoretical values. In the identification column, the plus sign indicates positive identification, the minus sign no identification, and the plus sign with question mark doubtful identification (i.e., the wavelengths do correspond, but the theoretical values of intensities are below the observed intensities by more than one order of magnitude).

[Table 17 follows]

Table 17. Absolute Intensities of Solar Lines and Their Identification

№ п. п.	No. in [21]	λ	Ion	I, erg/cm²·sec	Experimental data λ *	I *	λ **	I **	Identification
1	201	18,6	OVII	<0,015					
2	13	19,0	OVIII	<0,2					
3	200	21,6	OVII	<0,15					
4	390	(22)	CaXIV	<0,002					
5	12	24,8	NVII	<0,004					
6	199	28,8	NVI	<0,003					
7	437	(29,6)	CaXIII	<0,005					
8	475	32,3	CaXII	<0,001					
9	388	(33)	AXII	<0,005					
10	10	33,8	CVI	<0,08					
11	477	~35	CaXII	<0,005					
12	454	35,2	CaXI	0,005					
13	158	(38)	SXII	<0,01					
14	435	(39,7)	AXI	<0,004					
15	198	40,3	CV	0,03					
16	41	(41)	SiXII	0,006					
17	477	~41	CaXII	<0,005					
18	472	(43,8)	AX	<0,001					
19	471	45—50	SVIII	0,02					
20	474	45—50	AX	<0,02					
21	386	~47,7	SX	0,01					
22	453	48,7	AIX	0,006					
23	474	(45—50)	AX	<0,02					
24	79	50,5	FeXVI	<0,15					
25	143	50,6	SiX	0,01					
26	250	52,9	FeXV	<0,1					
27	471	~53	SVIII	0,01					
28	470	53,0	SVIII	0,001					
29	469	54,2	SVIII	0,003					
30	468	54,3	SVIII	0,001					
31	150	54,5	SiX	0,002					
32	431	56,1	SIX	0,015					
33	36	58,0	MgX	0,006					
34	343	(58)	NiXV	<0,002					
35	183	59,0	FeXIV	0,05					
36	467	59,2	SVIII	0,005					
37	184	59,6	FeXIV	0,05			} 62	0,01	+
38	466	61,6	SVIII	0,006					
39	406	(63)	NiXIV	0,006					
40	465	63,3	SVIII	0,002					
41	462	65—69	SiVI	0,003			66	0,01	+
42	450	(69)	NiXIII	0,006			} 69	0,015	+
43	380	~69,8	SiVIII	0,02					
44	452	72,0	SVII	0,003					
45	482	72—77	SiVI	0,007			74	0,015	+
46	338	(75)	FeXIII	0,05					
47	456	(78,1)	NiXI	0,003					
48	400	(80)	FeXII	0,06	83,9	30	83	0,02	+
49	482	80—83	SiVI	0,01					
50	126	82,6	MgVIII	0,002					
51	127	83,2	MgVIII	0,001					
52	482	(84,8)	NiXII	0,002					
53	375	~87,0	AlVII	0,002					
54	31	(87)	NeVIII	0,01					
55	448	(89,3)	FeXI	0,05					?
56	480	94—96	FeX	0,03					
57	479	96,1	FeX:	0,02			} 93	0,015	+
58	480	96—97	FeX	0,02					
59	300	98,0	MgVII	0,001					
60	461	100,0	SiVI	0,003					
61	301	102,3	MgVII	0,001					
62	14	102,6	OVIII	0,005					
63	455	103,6	FeIX	0,03	103,7	25			+
64	—				109,8	20			—
65	365	~111,9	MgVI	0,01	111,5	5	111	0,005	+

* Data by T. Violett and W. A. Rense, *Astrophysical journal*, v. 30, 1959, p. 954. Designation i is the visual estimate of intensity.

** Data by H. E. Hinteregger, *Astrophysical journal*, v. 132, 1960, p. 801; *Proceedings* of the 11th International Space Science Symposium, Florence, 1961. Intensity I was evaluated from the curves given in these sources.

Table 17 (Cont.)

№	No. in [21]	λ	Ion	I, erg/cm² · sec	Experimental data λ*	I*	λ**	I**	Identification
66	—				113,6	20			—
67	25	115,8	OVI	0,005	115,8	5			+
68	451	117,9	SiV	0,01	118,9	10	120	0,005	+
69	86	130,9	FeVIII	0,01			} 132	0,004	+
70	28	132,3	OVI	0,005					
71	113	138,6	NeVI	0,006	138,5	15	138	0,004	+
72	202	(138,3)	OVII	<0,002					
73	476	(143)	CaXII	<0,02					
74	316	(144)	CaXV	<0,05					
75	476	(149)	CaXII	<0,01					
76	24	150,1	OVI	0,015	150,0	10	149	0,003	+
77	436	(162)	CaXIII	<0,02					
78	473	(166)	AX	<0,015			166	0,01	+ ?
79	473	(171)	AX	<0,007	169,9	15	169	0,03	
80	120	171,1	NeVI	0,002	171,1	5			+ ?
81	119	171,2	NeVI	0,001	171,9	5			—
82	219	172,2	OV	0,002	172,7	5			—
83	27	172,9	OVI	0,02	174,8	30	174	0,045	+
84	458	180,6	MgIV	$6 \cdot 10^{-4}$			180	0,055	—
85	11	182,5	CVI	<0,002					
86	341	(182)	NiXV	<0,01					
87	26	184,1	OVI	0,03	184,7	5	187	0,055	+
88	315	(185)	CaXV	<0,02					
89	434	(188,7)	AXI	<0,01					
90	192	(190)	NiXVI	<0,005					
91	313	(191)	SXI	0,15					
92	389	(191)	CaXIV	<0,01			} 192	0,10	+
93	389	(193)	CaXIV	<0,02					
94	87	~195,7	FeVIII	0,03			194	0,05	+
95	389	(197)	CaXIV	<0,03					
96	463	198,6	SVIII	0,05			198	0,03	+
97	191	(199)	NiXVI	<0,015					
98	464	202,6	SVIII	0,03			201	0,08	+
99	182	(208)	FeXIV	0,1	205,9	10	204	0,07	+
100	402	(209)	FeXII	0,2	} 206,7	5	209	0,07	+
101	336	(210)	FeXIII	0,2					
102	383	~215,8	SiVIII	0,008					
103	429	217,8	SiVII	0,003					
104	342	(220)	NiXV	<0,05			} 218	0,055	+
105	387	(220—222)	AXII	<0,02					
106	181	(223)	FeXIV	0,3			} 222	0,035	+
107	308	223,7	SiIX	0,1					
108	430	(224)	SIX	0,03					
109	308	225,0	SiIX	0,07					
110	314	(225)	CaXV	<0,1					
111	387	(226)	AXII	<0,02			226	} 0,045	+
112	308	227,0	SiIX	0,02					
113	308	227,3	SiIX	0,01					
114	382	~230,0	SiVIII	0,008	229,1	10			+ ?
115	157	231,5	SXII	0,1	} 231,0	20	232	0,02	+
116	252	(231)	FeXV	0,1					
117	253	~231,9	FeVII	0,006					
118	154	232	PXI	0,0005					
119	190	(233)	NiXVI	<0,003					
120	154	234,8	PXI	0,001	234,6	5			—
121	189	(236)	NiXVI	<0,006					
122	154	237,0	PXI	0,002	237,1	10			—
123	109	238,6	OIV	0,004					
124	401	(238)	FeXII	0,2	} 238,5	5	238±1	0,025	+
125	159	(239)	SiXII	<0,01					
126	254	239,9	FeVII	0,06					
127	154	240	PXI	0,0006					
128	188	(242)	NiXVI	<0,01					

Table 17 (Cont.)

No. in table	No. in [21]	λ	Ion	I, erg/cm²·sec	Experimental Data λ*	I*	λ**	I**	Identification
129	8	243,0	HeII	$5\cdot10^{-4}$	243,3	10	243	0,025	+ ?
130	257	243,4	FeVII	0,002					
131	255	245,2	FeVII	0,002					
132	460	246,0	SiVI	0,05					?
133	428	246,1	SiVII	0,003					
134	153	247,9	PXI	0,003					
135	460	249,1	SiVI	0,025					
136	337	(250)	FeXIII	0,7			249	0,025	+
137	187	250	NiXVI	0,02					
138	81	(250)	FeXVI	0,01					
139	384	251	SiVIII	0,008					
140	304	251,3	AlVIII	0,001					
141	312	(253)	SXI	0,06			252	0,003	+
142	153	254,0	PXI	0,002					
143	7	256,3	HeII	0,004					
144	236	(257,5)	SXIII	<0,05	257,1	20	257:	0,003	+
145	385	(258)	SX	0,03					
146	141	258,4	SiX	0,06					
147	310	259,7	SiIX	0,01					
148	385	(260)	SX	0,05	260,0	5	259	0,01	+
149	111	260,4	OIV	0,001					
150	408	~260,5	NiVI	0,002	261,2	15			+ ?
151	82	(262)	FeXVI	<0,05					
152	83	(264)	FeXVI	<0,04					
153	178	(264)	FeXIV	0,05			264	0,003	+
154	385	(265)	SX	0,08	266,4	10	266	0,008	+
155	177	(266)	FeXIV	0,15					
156	138	272,1	SiX	0,05	272,3	5	273	0,005	+
157	427	272,7	SiVII	0,02					
158	426	274,1	SiVII	0,015					
159	422	275,4	SiVII	0,06	276,8	5	276	0,009	+
160	424	276,2	SiVII	0,015					
161	180	(276)	FeXIV	0,2					
162	425	276,8	SiVII	0,015					
163	381	~276,9	SiVIII	0,01					
164	137	277,3	SiX	0,1			278,5	0,006	+
165	297	278,4	MgVII	0,2					
166	423	278,4	SiVII	0,02					
167	234	278,7	PXII	<0,002					
168	459	278,7	AlV	0,003					
169	103	~279,8	OIV	0,01	280	5			+
170	146	280,0	SiX	0,006					
171	299	280,7	MgVII	0,005					
172	459	281,4	AlV	0,002					
173	403	(283)	FeXII	0,04	281,4	5	282	0,002	+
174	179	(285)	FeXIV	0,3			285	0,035	+
175	305	287,0	AlVIII	0,001					
176	149	287,2	SiX	0,02					
177	156	(290)	SXII	<0,05	289,1	10	289	0,002	+
178	340	(290)	NiXV	<0,02					
179	306	290,6	SiIX	0,007					
180	306	292,8	SiIX	0,015					
181	311	(293)	SXI	0,2			292	0,003	+
182	84	293,3	NiXVIII	<0,03					
183	194	~294	FeVI	0,01					
184	193	~296	FeVI	0,025			296	0,002	+
185	306	296,2	SiIX	0,04					
186	249	(298)	FeXV	<0,5	298,2	10	299	0,002	+
187	481	(299)	NiXII	0,02					
188	186	(300)	NiXVI	<0,01					
189	156	(302)	SXII	<0,1					
190	231	303,6	SiXI	0,06	303,8	30	303	0,13	+
191	6	303,8	HeII	0,18					
192	449	(304)	NiXIII	0,003					

Table 17 (Cont.)

№ n.n.	No. in [21]	λ	Ion	I, erg/cm²·sec	Experimental Data λ*	I*	λ**	I**	Identification
193	135	305,1	AlIX	0,02			305:	0,01	+
194	419	~308	AlVI	0,003			308	0,001	+
195	405	(311)	NiXIV	0,01	310,1	10	311	0,002	+
196	237	(311)	SXIII	<0,02					
197	128	311,8	MgVIII	0,005					
198	292	311,9—313,7	NaVI	0,01					
199	449	(312)	NiXIII	0,01					
200	185	(312)	NiXVI	<0,02			313	0,005	+
201	17	312,4	CIV	0,03					
202	414	313,0	NeIII	0,005					
203	128	313,7	MgVIII	0,01					
204	379	314,3	SiVIII	0,05					
205	370	314,5	MgVI	0,01					
206	128	315,0	MgVIII	0,03					
207	405	(315)	NiXIV	0,02					
208	152	315,3	PXI	0,002			316±1	0,002	+
209	339	(316)	NiXV	<0,01					
210	378	316,2	SiVIII	0,1					
211	128	317,0	MgVIII	0,005					
212	449	(317)	NiXIII	0,002					
213	298	319,0	MgXII	0,01			319	0,002	+
214	377	319,8	SiVIII	0,15			321	0,005	+
215	457	321,0	MgIV	0,015					
216	481	(322)	NiXII	0,01					
217	85	322,0	NiXVIII	<0,02					
218	457	323,3	MgIV	0,007					
219	405	(323)	NiXIV	0,03					
220	449	(323)	NiXIII	0,004					
221	302	323,5	AlVIII	0,001					
222	151	325,2	PXI	0,003					
223	302	325,3	AlVIII	0,002					
224	404	(326)	FeXII	0,02			326	0,003	+
225	302	328,2	AlVIII	0,004					
226	335	(330)	FeXIII	0,3					?
227	449	(332)	NiXIII	0,003					
228	229	332,9	AlX	0,008					
229	339	(333)	NiXV	<0,025					
230	124	335,3	MgVIII	0,04					
231	235	335,6	PXII	<0,002					
232	77	336,2	FeXVI	<0,5	338,0	10	335	0,027	+
233	123	339,0	MgVIII	0,08			339	0,004	+
234	307	342,0	SiIX	0,04					
235	134	342,2	MgVIII	0,003					
236	176	(342)	FeXIV	0,2	342,6	5	343	0,005	+
237	307	345,0	SiIX	0,15					
238	280	345,3	OIII	$6 \cdot 10^{-4}$	344,7	20	347	0,01	+
239	339	(346)	NiXV	<0,04					
240	478	(347,0)	FeX	0,35					
241	140	347,5	SiX	0,07					
242	371	349,1	MgVI	0,001					
243	147	349,0	SiX	0,006					
244	307	~349,8	SiIX	0,2			349	0,003	+
245	447	(350)	FeXI	0,02					
246	374	352,2	AlVII	0,003					
247	129	352,4	MgVIII	0,015	352,9	5	352	0,006	+
248	418	~352,7	MgV	0,002					
249	373	353,8	AlVII	0,005					
250	399	(356)	FeXII	0,1					
251	175	(356)	FeXIV	0,4	354,9	30	354	0,006	+
252	139	356,1	SiX	0,15					
253	372	356,9	AlVII	0,01					

Table 17 (Cont.)

No. in [21]	λ	Ion	I, erg/cm²·sec	Experimental Data λ *	I *	λ **	I **	Identification
447	(358)	FeXI	0,06					
283	358,0	NeV	0,1					
399	(360)	FeXII	0,2			359	0,017	+
334	(360)	FeXIII	0,15					
447	(360)	FeXI	0,015					
148	360,8	SiX	0,006					
293	361,2	NaVI	0,001					
75	361,5	MnXV	0,003					
78	361,7	FeXVI	<0,3			363	0,005	+
295	364—368	MgVII	0,06					
233	365,4	SiXI	[0,06]					
285	365,4	NeV	0,01					
89	365,9	FeVIII	0,002					
[10]	(367)	FeX	0,15					
447	(367)	FeXI	0,01					
295	367,8	MgVII	0,03			368±1	0,02	+
227	368,2	MgIX	0,08					
399	(369)	FeXII	0,3					
447	(369)	FeXI	0,015					
88	370,5	FeVIII	0,004					
334	(373)	FeXIII	0,4	372,2	10			+
274	374,1	OIII	0,03	373,6	15	375	0,002	+
447	(376)	FeXI	0,02	379,0	25	378	0,004	+
416	379,3	NeIII	0,001					
303	381,1	AlVIII	0,002					
121	381,3	NaVII	0,008					
303	383,7	AlVIII	0,007			383	0,002	+
19	384,2	CIV	0,006					
136	385,0	AlIX	0,01					
76	385,4	MnXV	0,001			387,5	0,004	+
334	(386)	FeXIII	0,65					
303	~387,8	AlVIII	0,01					
369	388,0	MgVI	0,005					
73	390,1	CrXIV	0,003					
251	391,2	FeXV	[<0,08]					
145	~392,4	SiX	0,002			391±1	0,003	+
136	392,4	AlIX	0,015					
145	~398,9	SiX	0,004					
368	399,3	MgVI	0,04					
118	399,8	NeVI	0,01					
367	400,7	MgVI	0,08					
118	401,1	NeVI	0,02					
230	401,2	AlX	0,005					
118	401,9	NeVI	0,04			404±1	0,004	+
366	403,3	MgVI	0,13					
118	403,3	NeVI	0,01					
417	~409	NaIV	0,001					
225	411,2	NaVIII	0,004					
74	412,5	CrXIV	0,001					
251	414,1	FeXV	[<0,05]					
289	414,3	NaVI	0,001					
333	414,7	CaVII	0,005					
284	416,2	NeV	0,02			416	0,003	+
288	416,8	NeV	0,01					
18	419,5	CIV	0,05	419,4	10	418	0,006	+
42	(421)	SXIV	<0,02			420	0,002	+ ?
251	424,1	FeXV	[<0,02]					
415	427,8	NeIII	0,001					
296	429,2	MgVII	0,03			429	0,002	+
115	430,0	NeVI	0,008					
354	430,2	OII	$4\cdot10^{-4}$					
125	430,5	MgVIII	0,05	430,7	10	432	0,002	+
296	431,3	MgVII	0,08					
114	432,4	NeVI	0,015					

Table 17 (Cont.)

№ п.п.	№ in [21]	λ	Ion	I, erg/cm²·sec	Experimental Data λ *	I *	λ **	I **	Identification
318	296	434,9	MgVII	0,14					
319	279	434,9	OIII	0,02	435,1	25	437	0,005	+
320	125	436,7	MgVIIII	0,1					
321	133	442,2	MgVIII	0,003			441	0,003	+ ?
322	—						445	0,004	—
323	43	(446)	SXIV	<0,01	448,0	15	449	0,003	+ ?
324	55	457,8	SiIV	0,001			456	0,003	+ ?
325	56	458,1	SiIV	$3\cdot10^{-4}$					
326	362	459,9	NaV	0,001					
327	71	460,9	TiXII	0,002					
328	362	461,0	NaV	0,003					
329	174	461,7	CaXIII	0,001					
330	362	463,3	NaV	0,004			463	0,003	+ ?
331	223	(464)	NeVII	0,08	463,8	10	467	0,006	+
332	247	466,2	CaIX	0,006					
333	360	470,0	NeIV	0,005					
334	173	471,1	CaVIII	0,002					
335	—						473±1	0,002	—
336	—				477,4	15			—
337	72	480,1	TiXII	0,001					
338	281	480,4	NeV	0,015					
339	281	481,4	NeV	0,025					
340	281	483,0	NeV	0,08	483,7	10	484±1	0,005	+
341	122	486,7	NaVII	0,003					
342	433	(488)	SIX	0,01					
343	413	488,1	NeIII	0,001					
344	413	489,5	NeIII	0,005					
345	131	490,8	MgVIII	0,003					
346	413	491,0	NeIII	0,001					
347	291	491,4	NaVI	0,003					
348	122	491,9	NaVII	0,006					
349	290	494,3	NaVI	0,005	495,0	5	494	0,005	+?
350	39	(499,3)	SiXII	0,06	498,3	5	500±1	0,005	+
351	—				503,9	15	503	0,004	
352	—						507	0,003	—
353	—						514±1	0,004	—
354	40	(521,1)	SiXII	0,03					
355	361	521,3	NeIV	0,005			521	0,01	+
356	197	522,2	HeI	0,01					
357	276	525,8	OIII	0,005	525,8	15			+
358	407	525,7—526,6	FeIV	0,01			529±1	0,004	+ ?
359	330	527,7	AV	0,002					
360	—				535,3	5			—
361	196	537,0	HeI	0,04	536,5	5	537	0,002	+
362	206	538,3	CIII	0,001	538,8	5			+ ?
363	355	538,3	OII	$3\cdot10^{-4}$					
364	353	539,1	OII	0,02	539,2	5			+
365	359	541,1	NeIV	0,04			540±1	0,006	+
366	358	542,0	NeIV	0,08					
367	357	543,9	NeIV	0,12			545	0,003	+
368	210	547,9	CIII	0,001					
369	37	(550)	AlXI	0,004			551	0,005	+ ?
370	332	551,5	CaVII	0,002					
371	108	554,1	OIV	0,1	553,7	10	555	0,011	+
372	432	(555)	SIX	0,01					
373	144	555,0	SiX	0,006					
374	69	557,7	CaX	0,004					
375	117	558,6	NeVI	0,015			560	0,002	+
376	116	562,8	NeVI	0,02			565	0,003	+
377	232	565,1	SiXI	[0,03]					
378	282	568,4	NeV	0,06			569	0,02	+
379	38	(569)	AlXI	0,002					
380	282	569,9	NeV	0,17					
381	282	572,1	NeV	0,04					

Table 17 (Cont.)

№ n. n.	No. in [21]	λ	Ion	I, erg/cm² sec	Experimental Data λ*	I*	λ**	I**	Identification
382	282	572,3	NeV	0,23	572,9	5			+
383	70	574,0	CaX	0,002					
384					576,6	10	578±1	0,004	—
385	—				578,5	10			—
386	—				580,6	10			—
387	172	582,8	CaVIII	0,002	581,5	10	581	0,004	+ ?
388	232	582,9	SiIX	[0,02]					
389	195	584,4	HeI	0,7	584,7	10	585	0,03	+
390	244	585,8	AVII	0,004					
391	168	589,0	AVI	0,001	589,9	5			+ ?
392	232	591,2	SiXI	[0,007]	593,6	5	592	0,003	+
393	167	596,7	AVI	0,002					
394	171	596,9	CaVIII	0,004					
395	132	~597,5	MgVIII	0,003					
396	278	597,8	OIII	0,005	597,9	5	599	0,003	+ ?
397	275	599,6	OIII	0,01	599,2	5			+
398	—				602,9	5			—
					607,6	50	606	0,05	
399	107	608,4	OIV	0,1	608,5	5	608:	0,006	+
400	106	609,8	OIV	0,3	609,8	5			+
401	34	(609,9)	MgX	0,05					
402	277	610,0	OIII	0,003					
403	277	610,8	OIII	0,005					
404	—				611,4	5			—
405					614,9	20			—
406	—				617,2	25	617	0,002	
407	67	621,4	KIX	0,001			622	0,01	+ ?
408	331	624,4	CaVII	0,001					
409	35	(624,9)	MgX	0,025	625,1	5	625	0,008	+
410	112	625,1	OIV	0,03					
411	216	629,7	OV	0,3	630,3	20	629	0,02	+
412	395	629,6	CaVI	0,004					
413	331	630,6	CaVII	0,003					
414	395	633,8	CaVI	0,003	635,5	10	634	0,002	+ ?
415	68	636,3	KIX	$3\cdot10^{-4}$					
416	80	637,2	FeXVI	<0,1			638	0,003	+
417	331	639,2	CaVII	0,005					
418	331	640,5	CaVII	0,001					
419	395	641,9	CaVI	0,001					
420	268	644,8	NII	10^{-4}					
421	446	646,6	CaV	0,001	644,9	20			+ ?
422	97	651,3	CII	10^{-4}	651,5	10	653	0,001	—
423	[11]	658,7	AXIII				661	0,003	+
424	—						670±1	0,01	
425	248	678,6	CaIX	[0,001]			676	0,003	+ ?
426	130	680,3	MgVIII	0,003					
427	32	(682)	NaIX	0,005			682±1	0,004	+ ?
428	100	687	NIII	0,001	687,3	15	689	0,004	+ ?
429	228	692,4	MgIX	[0,03]					
430	248	693,8	CaIX	[0,001]	694,5	25	695±1	0,005	+
431	33	(695)	NaIX	0,002					
432	65	700,4	AVIII	0,004			700	0,004	+ ?
433	272	702,3—703,9	OIII	0,06	703,3	20	704	0,01	+
434	228	704,5	MgIX	[0,02]					
435	62	706,5	SVI	0,002	707,9	20			+ ?
436	228	710,3	MgIX	[0,01]			710±1	0,005	+ ?
437	62	712,7	SVI	0,001					
438	66	714,0	AVIII	0,002					
439	329	716,4	AV	0,001					
440	—						720	0,01	
441	324	728,7	SIII	0,002			729	0,007	
442	—				737,1	15	738	0,01	
443	—						745	0,004	
444	—				754,8	10	752±1	0,004	—

Table 17 (Cont.)

No.	No. in [21]	λ	Ion	erg/cm² · sec	Experimental Data λ *	I *	λ **	I **	Identification
445	220	758,7—759,5	OV	0,02					
446	220	760,2—760,4	OV	0,045			762±1	0,005	+
447	220	761,2—761,9	OV	0,02					
448	99	764,4	NIII	0,004					
449	212	765,1	NIV	0,01	764,5	10	767	0,007	+
450	29	770,5	NeVIII	0,09			771	0,01	+
451	222	774,5	OV	0,05					
452	269	776,0	NII	$3 \cdot 10^{-4}$					
453	226	778,9	NaVIII	[0,003]					
454	110	779,8	OIV	0,002					
455	30	780,3	NeVIII	0,06	779,4	5	781	0,007	+
456	242	786,5	SV	0,02					
457	105	787,7	OIV	0,2			786:	0,004	+
458	226	788,6	NaVIII	[0,002]					
459	104	790,2	OIV	0,5	791,2	5	790	0,014	+
460	226	793,3	NaVIII	[0,001]			793	0,005	+ ?
461	356	796,8	OII	0,005					
462	63	800,7	ClVII	0,001			802	0,002	+ ?
463	165	809,7	SIV	0,002	809,4	5	808	0,002	+ ?
464	—				810,9	5	812	0,002	—
465	58	815,1	SiIV	0,001					
466	164	816,0	SIV	0,003					
467	—				819,3	5	818	0,005	—
468	328	822,2	AV	0,001	822,5	5	821	0,003	+ ?
469	—				823,0	5			—
470	—				825,6	5	824	0,004	—
471	328	827,2	AV	0,002					
472	—				829,9	10	829	0,004	—
473	352	832,8	OII	0,05					
474	273	832,9	OIII	0,03					
475	351	833,3	OII	0,1	834,0	5			+
476	273	833,7	OIII	0,1					
477	350	834,5	OII	0,15					
478	327	834,9	AV	0,003	835,2	5	835±1	0,015	+
479	273	~835,2	OIII	0,15					
480	327	836,0	AV	0,001	836,7	5			+ ?
481	393	840,0	AIV	0,001					
482	393	843,8	AIV	0,002			846	0,003	+ ?
483	393	850,6	AIV	0,002	852,6	10	852	0,01	+
484	—				855,4	30			
485	91	858,1	CII	0,002	858,2	10	858±1	0,003	+ ?
486	90	858,6	CII	0,004	859,4	20			+ ?
487	—						868	0,003	—
488	—						871	0,005	—
489	—						877	0,01	—
490	—						880	0,01	—
491	—						887	0,003	—
492	224	(892)	NeVII	[0,1]			893±1	0,005	+
493	95	903,6	CII	0,01	902,9	5	901	0,003	+
494	392	906,9	SII	0,001	905,5	5			+ ?
495	392	911,0	SII	0,001	911,4	100	912	0,04	
496	—				913,0	10			+ ?
497	—				914,2	50	914	0,013	—
498	267	916,0	NII	0,001	916,0	10	917	0,005	+ ?
499	214	~922,2	NIV	0,002			921	0,008	+ ?
500	214	~923,3	NIV	0,004			925	0,006	+ ?
501	60	933,4	SIV	0,02	932,2	10	932±1	0,008	+
502	5	937,8	HI	0,008			937	0,007	+
503	—				940,9	10			—
504	61	944,5	SVI	0,01	943,	10	942±1	0,004	+
505	4	949,7	HI	0,015			949±1	0,008	+
506	—				960,5	10	961±1	0,003	—
507	—				961,4	10			—

Table 17 (Cont.)

№	Main [21]	λ	Ion	I, erg/cm²·sec	Experimental Data λ *	I *	λ **	I **	Identification
508	346	~964,5	NI	2,10⁻⁴	964,5	10			+ ?
509	—				970,1	10			—
510	3	972,5	HI	0,04	972,9	10	972	0,02	+
511	204	977,0	CIII	0,6	977,0	30	978	0,08	+
512	—						986	0,006	—
513	96	989,8—991,6	NIII	0,01	990,0	15	992±1	0,007	+
514	—						996	0,013	
515	—						1006	0,014	
516	97	1010,7	CII	6·10⁻⁴	1009,8	10	1009	0,004	+
517	317	1012,6	SIII	0,006	1013,3	15	1013	0,002	+
518	—				1018,1	10	} 1018±1	0,004	—
519	—				1019,7	10			—
520	—				1022,0	10			—
521	2	1025,7	HI	0,14	1025,7	60	1024	0,04	+
522	412	1025,7	OI	0,01					
523	48	1026,0	MgII	0,003					
524	49	1026,1	MgII	0,002					
525	—				1028,7	10			—
526	—				1030,3	15			—
527	22	1031,9	OVI	0,06	1032,2	30	1029±1	0,03	+
528	94	1036,3	CII	0,05	} 1038,2	40	1035	0,02	+
529	23	1037,6	OVI	0,03					
530	411	1039,2—1040,9	OI	0,01	1040,9	5	1040	0,007	+
531	[11]	1048,9	SiVII		1048,9	5	1049	0,004	+
532	—				1051,4	10			—
533	[11]	1058,7	AlVIII		1058,7	10	1055±2	0,007	+
534	166	1062,7	SIV	0,005	1065,3	15	1063	0,007	+ ?
535	166	1073,3	SIV	0,01			1073	0,004	+
536	—						1080	0,013	
537	266	1084,0—1084,6	NII	0,005	} 1085,1	10	1083	0,013	+
538	266	1085,5—1085,7	NII	0,005					
539	—						1091±1	0,01	—
540	—						1100	0,01	—

25. Ivanov-Kholodnyy, G. S. Ionization of the upper atmosphere by shortwave solar radiation. Geomagnetizm i aeronomiya, v. 2, no. 4, 1962, 674-687.

The latest available data on shortwave solar radiation in the spectral region between 0 and 1000 Å, effective ionization cross sections, and photoionization are used to calculate the rate of ion formation (q) at altitudes between 100 and 800 km for different times of the day.

Analysis of data on q shows that maximum ion formation occurs in the F1 region during the day and in the F2 region during the evening and in the morning. During the day, q changes by two orders of magnitude in the F1 region but changes very little in the F2 region and higher. The graph of q as a function of height displays a characteristic peak at 120 km.

During the day q was found to vary in proportion to $(\cos Z_{\odot})^m$, where $Z_{\odot}$ is the zenith distance of the sun. The values of m for the E, F1, and F2 regions contradict the simple-layer theory but agree with the experimental data. During the day m changes in the region between the F1 and F2 layers. Since the density of the atmosphere at altitudes > 200 km increases in the daytime, q increases at altitudes of about 250 km and decreases at altitudes between 150 and 250 km. In addition, the gradients of q and n_l (electron concentration) decrease above the maximum of the F2 layer. Due to asymmetry of diurnal variation in particle concentration, asymmetry is observed in variations of q and n_l. This leads to incorrect effective values for the recombination coefficient, if the latter is calculated by the method developed in 1959 by V. Appleton.

Values of q and experimental data on n_l and concentration of molecular ions obtained by rockets and satellites are used to calculate the effective recombination coefficients.

Studies of Marginal Interest

26. Shklovskiy, I. S. Ultraviolet radiation of the solar corona and the chromosphere and ionization of the earth's atmosphere. IN: Akademiya nauk SSSR. Krymskaya astrofizicheskaya observatoriya. Izvestiya, v. 4, 1949, 80-113.
QB1.A17642, v. 4

Although most of the article deals with ultraviolet solar radiation, some calculations are given for x-ray radiation. The absorption of hard radiation in the ionosphere is investigated on the basis of x-ray and optical data, and it is shown that only radiation with a wavelength $\lambda < 75$ Å can reach the E layer. This type of radiation may be responsible for ionization of the E layer. It is pointed out that the Dellinger effect may be caused by hard radiation ($\lambda \sim 1$ Å) formed during solar eruptions.

27. Shklovskiy, I. S. A new theory of solar eruptions and the resultant ionospheric disturbances in the D layer. IN: Akademiya nauk SSSR. Doklady, v. 64, no. 1, 1949, 37-39.
AS262.A3663, v. 64

The Dellinger effect is explained on the basis of ionization of the D layer by hard solar radiation ($\lambda \sim 1$ Å) which increases considerably during solar flare eruptions. The total number of photons passing an area of one square centimeter of the earth's atmosphere during the period of disturbance (~ 15 min) was estimated as 10^{10} photons (or 0.2 erg/cm^2·sec at the earth).

28. Mandel'shtam, S. L. Review of research on shortwave ultraviolet solar radiation. Uspekhi fizicheskikh nauk, v. 46, no. 2, 1952, 145-178.
QC1.U8, v. 46

The review contains some data on x-ray emission derived from investigations conducted with V-2-type rockets. The references cited consist of 28 Western and three Soviet sources.

29. Mandel'shtam, S. L., and A. I. Yefremov. Investigation of shortwave ultraviolet solar radiation. Uspekhi fizicheskikh nauk, v. 63, no. 1, 1957, 163-180. QC1.U8, v. 63

This article is a review of experimental and theoretical research on shortwave solar radiation, including x-ray emission, conducted between 1952 and 1957. Of the 24 references cited, only three are Soviet. The section on coronal radiation is based almost exclusively on American data. Experiments to be carried out in the Soviet Union involving x-ray radiation measurements by means of artifical satellites are discussed.

30. Shklovskiy, I. S. Ultraviolet and soft x-ray solar radiation. Uspekhi fizicheskikh nauk, v. 75, no. 2, 1961, 351-388. QC1.U8, v. 75

Both theoretical developments and experimental research are summarized in this review. The following topics are included: ultraviolet coronal radiation, rocket and artificial satellite observations of ultraviolet and soft x-ray solar radiation, and the effect of hard solar radiation on the ionization of the earth's atmosphere. The article is based on 42 Western and 10 Soviet sources.

31. Shklovskiy, I. S. Fizika solnechnoy korony (Physics of the solar corona). 2d ed., rev. and enl., Moskva, Fizmatgiz 1962. 516 p.

This is the second, thoroughly revised, edition of an excellent monograph on the physics of the solar corona orginally published in 1951. The chapter on ultraviolet solar radiation and its effect on the earth's atmosphere also provides a summary of work on solar x-ray emission available prior to 1961 in which both experimental data and theoretical results are discussed. In this chapter, one of the works of Ivanov-Kholodnyy and Nikol'skiy [20] is analyzed and the theory developed therein found to be sound.

The monograph contains numerous original theories developed by the author, who is considered one of the foremost Soviet astrophysicists, including his theory of ionization in the solar corona, which he first worked out in the 1940's.

The text acknowledges all of the important contributions to the field, listed in an extensive bibliography (274 entries).

PART TWO. OPTICAL SPECTRA

1. Oscillator Strengths and Related Quantities

Review Paper

32. Kolesnikov, V. N., and L. V. Leskov. Optical transition probability for atoms and diatomic molecules. Uspekhi fizicheskikh nauk, v. 65, no. 1, 1958, 3-38.
QC1.V8, v. 65

This is an exhaustive review of optical transitions in atoms and simple diatomic molecules. It is based on material published up to and including the early part of 1958. Of the 370 references, approximately 22% are Soviet. Four tables [not presented in this report] summarize the data available in this field. The first lists theoretical papers dealing with the calculation of transition probabilities, oscillator strengths, line strengths, and transition integrals. Elements, transitions, or configurations for which calculations were carried out are included along with their sources. The second lists experimental papers dealing with the determination of transition probabilities and oscillator strengths and includes elements, number of lines investigated and the spectral region, the method used, and the sources. The sources in which absolute values were determined are pointed out. The third and fourth tables give similar data for diatomic molecules.

Experimental Values

33. Ostrovskiy, Yu. I. Relative f-values for chief lines of diffuse and sharp series of Al I. Optika i spektroskopiya, v. 2, no. 5, 1957, 673. QC350.068, v. 2

The relative oscillator strengths for the four strongest lines of Al I were measured by the anomalous dispersion method. The results of the measurements are given in Table 18.

34. Ostrovskiy, Yu. I., and N. P. Penkin. Absolute values of oscillator strengths for the lines of chromium, manganese, and copper. Optika i spektroskopiya, v. 3, no. 3, 1957, 193-201. QC350.068, v. 3

The absolute values of oscillator strengths were determined by the anomalous dispersion method for resonance lines of chromium, manganese, and copper. The relative oscillator strengths were also measured for other spectral lines of these elements. On the basis of these data and the results of earlier f-value measurements, the absolute values of oscillator strengths were obtained for 34 lines of chromium (Table 19), 10 lines of manganese (Table 20), and the following lines of copper:

$$f_{(3247)} = 0.7,\ f_{(3274)} = 0.38,\ f_{(5106)} = 0.011.$$

35. Ostrovskiy, Yu. I., and N. P. Penkin. Relative f-values for spectral lines of scandium. Optika i spektroskopiya, v. 3, no. 4, 1957, 391-393. QC350.068, v. 3

Relative oscillator strengths of Sc I spectral lines were determined by the anomalous dispersion method. The results of measurements are given in Table 21.

36. Ostrovskiy, Yu. I., and N. P. Penkin. Measurement of absolute values of oscillator strengths in the spectral lines of Ga I and In I. Optika i spektroskopiya, v. 4, no. 6, 1958, 719-724. QC350.068, v. 4

Absolute oscillator strengths of the five strongest lines in the spectrum of Ga I ($4^2P^o_{3/2} - 5^2S_{1/2}$ and $4^2P^o_{3/2,\,1/2} - 4^2D_{3/2,\,5/2}$) were determined (Table 22) from data obtained by the anomalous dispersion method and pressure values by Speiser and Johnston. Absolute oscillator strengths for the five strongest spectral lines of In I were also calculated (Table 23) from data obtained by the authors and pressure measurements by Anderson.

37. Nagibina, I. M. Calculation of relative oscillator strengths in an arc discharge from the width of the spectral lines. IN: Akademiya nauk SSSR. Izvestiya. Seriya fizicheskaya, v. 22, no. 6, 1958, 681-682. AS262.A62455, v. 22

The method of Cowan and Dicke was used to calculate the relative oscillator strengths given in Table 24.

38. Ostrovskiy, Yu. I., N. P. Penkin, and L. N. Shabanova. Measurement of oscillator strengths in spectra of atoms. IN: Akademiya nauk SSSR. Izvestiya. Seriya fizicheskaya, v. 22, no. 6, 1958, 725-729. AS262.A62455, v. 22

The absolute values of oscillator strengths for resonance lines of Al I, Mg I, Ca I, and Ba I were determined. Better results are given in a later paper [46].

39. Gurvich, L. V. Absolute transition probabilities of the Tl atom. Optika i spektroskopiya, v. 5, no. 2, 1958, 205-207. QC350.068, v. 5

Absolute oscillator strengths of thallium spectral lines (λ = 3776 Å and 5350 Å) calculated or measured by six different authors are given. The experimental data obtained by G. S. Kvater (USSR) in 1941 are considered the most reliable, but in view of the inaccurate vapor pressure data used in the determination of absolute oscillator strengths, the latter were recalculated using a new method based on the calculation of the vapor pressure of the metal from the thermodynamical potential and the temperature variation of enthalpy in the gaseous and solid states. The absolute f-values of thallium were determined to be

$$f_{(3776)} = 0.125 \pm 0.004 \text{ and } f_{(5350)} = 0.135 \pm 0.004.$$

From these data and the results of earlier measurements, the absolute value of $f_{(2768)}$ was calculated as 0.272.

40. Ostrovskiy, Yu. I., and N. P. Penkin. Relative f-values for spectral lines of vanadium and cobalt. Optika i spektroskopiya, v. 5, no. 4, 1958, 345-353. QC350.068, v. 5

Relative oscillator strengths for 79 lines of V I (3000 to 4900 Å) and 82 lines of Co I (2900 to 4200 Å) were measured by the anomalous dispersion method. The results of the measurements are given in Tables 25 and 26.

41. Penkin, N. P., and T. P. Red'ko. Relative oscillator strengths of some lines of Zn I and Cd I. Optika i spektroskopiya, v. 9, no. 5, 1960, 680-682. QC350.068, v. 9

The relative oscillator strengths of 30 Zn I and Cd I lines with lower energy levels $^3P_{0,1,2}$ were measured. The results of the measurements are given in Tables 27 and 28.

42. Ostrovskiy, Yu. I., and N. P. Penkin. The f-number measurements for the spectral lines of barium. Optika i spektroskopiya, v. 9, no. 6, 1960, 703-706.
QC350.068, v. 9

The relative oscillator strengths of 65 lines of Ba I between 3889 Å and 7911 Å were measured by the anomalous dispersion method. The results of the measurements are given in Table 29. Since the absolute f-value for the $6^1S_0 - 6^1P_1^0$ transition at $\lambda = 5535.484$ Å is known [1.6, according to Wessel; 1.8, according to the authors], the absolute f-values for the 65 lines given in the table can easily be calculated.

43. Khokhlov, M. Z. Oscillator strengths for p^2-ps transitions in lead, tin, germanium, silicon, and carbon. Part I: Lead and tin. IN: Akademiya nauk SSSR. Krymskaya astrofizicheskaya observatoriya. Izvestiya, v. 25, 1961, 249-267.
QB1.A17642, v. 25

The absolute f-values for p^2-ps transitions in lead (Table 30) and tin (Table 31) are determined. Conversion to the absolute f-values was made from data of H. D. Engler and C. W. Allen. Three of the f-values given in Table 30 were determined earlier by Khokhlov, but apparently with a lesser degree of accuracy.

44. Ostrovskiy, Yu. I., and N. P. Penkin. Measurement of absolute values of oscillator strengths for the resonance lines of calcium, strontium, and barium ions. Optika i spektroskopiya, v. 10, no. 1, 1961, 8-14. QC350.068, v. 10

The absolute values of oscillator strengths for resonance doublet lines of Ca II, Sr II, and Ba II were determined. These values were later recalculated [46] on the basis of more accurate measurements of absolute oscillator strengths of Ca I, Sr I, and Ba I resonance lines.

45. Ostrovskiy, Yu. I., and N. P. Penkin. Oscillator strengths of calcium spectral lines. Optika i spektroskopiya, v. 10, no. 4, 1961, 429-435.

The relative oscillator strengths of 34 lines of Ca I between 2275 Å and 6572 Å were measured by the anomalous dispersion method. The results of the measurements are given in Table 32.

46. Ostrovskiy, Yu. I., and N. P. Penkin. Measurement of the absolute values of oscillator strengths in atomic spectra. Part II. Optika i spektroskopiya, v. 11, no. 5, 1961, 565-576. QC350.068, v. 11

The absolute oscillator strengths of resonance lines $^1P_1 - {}^1S_0$ of calcium, strontium, and barium are calculated (Table 33). The results obtained are more accurate than those obtained earlier by the same authors [38]. The absolute values of oscillator strengths of Ca II, Sr II, and Ba II resonance lines obtained earlier [44] were recalculated. The values obtained are listed in Table 34.

47. Penkin, N. P., and L. N. Shabanova. Oscillator strengths of the spectral lines of magnesium, strontium, and barium. Optika i spektroskopiya, v. 12, no. 1, 1962, 3-11. QC350.068, v. 12

The anomalous dispersion method was used to measure the relative oscillator strengths of 13 lines in the principal series of strontium and barium. The absolute oscillator strengths were determined from experimental data and absolute f-values for resonance lines ($^1S_0 - {}^1P^o_1$) of these elements determined earlier by Ostrovskiy and Penkin. The relative and absolute f-values of strontium and barium obtained are given in Table 35. Relative oscillator strengths for the $ns^2 - (n-1)dmp$ transitions of barium arising in simultaneous excitation of two electrons were measured and the absolute f-values calculated (Table 36). The f-values for the $^3P^o_{0,1,2} - {}^3S_1$ and $^3P^o_{0,1,2} - {}^3D_{1,2,3}$ transitions in Mg I and Sr I were also measured. The data obtained are listed in Tables 37 and 38.

48. Ostrovskiy, Yu. I., and N. P. Penkin. Measurement of the absolute values of oscillator strengths in atomic spectra. Part III. Optika i spektroskopiya, v. 12, no. 6, 1962, 669-670. QC350.068, v. 12

The absolute value of the oscillator strength in the resonance doublet of K I ($4^2S_{1/2} - 4^2P^o_{1/2, 3/2}$; λ = 7664.907 Å and 7698.979 Å) was determined to be equal to 1.03 ± 0.03.

49. Boyarchuk, M. Ye., and A. A. Boyarchuk. Oscillator strengths determined on the basis of stellar spectra study. IN: Akademiya nauk SSSR. Krymskaya astrofizicheskaya observatoriya. Izvestiya, v. 22, 1960, 234-256.
QB1.A17642, v. 22

If a growth curve is constructed from stellar spectrograms using only the lines for which laboratory f-values are known, then the log η values which are proportional to oscillator strengths can be determined for all lines from the equivalent line widths. The authors use this method, developed by K. O. Wright, and available log η data from five non-Soviet scientists to determine relative oscillator strengths (log g f λ) for 1184 lines of 21 different atoms and ions (Table 39).

A comparison of the relative oscillator strengths obtained by the authors with the available experimental values shows that the former are a little less precise. The main source of error is believed to be due to blending. The factors for the conversion of relative oscillator strengths to absolute values (Table 40) are determined from the known experimental and theoretical absolute oscillator strength values for all of the ions and atoms for which relative f-values were determined with the exception of Y II, Zr II, and La II ions.

50. Khokhlov, M. Z. Oscillator strengths for p^2-ps transitions in Ci, Si I, Ge I, Sn I, and Pb I. Part II. IN: Akademiya nauk SSSR. Krymskaya astrofizicheskaya observatoriya. Izvestiya, v. 26, 1961, 52-62. QB1.A17642, v. 26

The line strengths for the p^2-ps transitions in C I, Si I, Ge I, Sn I, and Pb I were computed in intermediate coupling by means of quantum mechanics (Table 41). Spin-orbit interaction was taken into account, but configuration interaction was neglected. The coupling parameters of the configurations were selected to obtain the best agreement between experimental and computed values of the level energies.

51. Nikitin, A. A. Study of the Raman spectrum of N III in the envelopes of stars and nebulae. Part V:* Determination of approximate values of the transition probabilities and coefficient of absorption for energy levels of N II with $1s^2 2s^2 nl$ and $1s^2 2s2p(^{1,3}p)nl$ configurations. IN: Leningrad. Leningradskiy universitet. Vestnik, no. 13. Seriya matematiki, mekhaniki i astronomii, no. 3, 1962. 113-137.

The wave functions determined in [60] are used to calculate approximate values of transition probabilities and coefficients of absorption for some N III energy levels. The oscillator strengths and transition probabilities for transition between levels of $1s^2 2s^2 nl$ configurations were determined from the following formulas:

$$f(nl^2L \to n'l'^2L') = \frac{\max(ll')}{3(2l+1)} \cdot \frac{\nu_{nn'}}{R_y} \rho^2,$$
$$\rho^2 = \left| \int_0^\infty P(nl|r) P(n'l'|r) r\,dr \right|^2, \qquad (1)$$

where nl^2L is the lower level; $n'l'^2L'$, the upper level; and max (ll'), the highest value of the l level in the transition. The other symbols are standard. The probability of spontaneous transition from level n' to level n is

$$A_{n'n} = \frac{2.68 \cdot 10^8}{\omega_{n'}} i^3 S, \qquad i = \frac{\nu_{nn'}}{R_y},$$
$$S = \div S_{LL'} = \frac{\rho^2_{nn'}}{4l^2 - 1} S_{LL'}, \qquad (2)$$

where $\omega_n = (2s + 1)(2L + 1)$ is the statistical weight of the upper term, and $S_{LL'}$ is the multiplet strength which for one electron spectrum is proportional to the statistical weight.

The results of calculations for transitions between some of the levels of $1s^2 2s^2 nl$ configurations are given in Table 42. The oscillator strengths and coefficients of absorption for transitions from $1s^2 2s^2 nl$ configurations into continuous spectrum were determined. The coefficient of absorption is given by

$$a_\nu = \frac{\pi e^2}{mc} f_{nk} \frac{k^3}{2R_y Z^2}, \qquad (3)$$

---

* Parts II and IV of this study are the only other parts located to date. No reference is made in any of these articles to parts I or III. Part II deals with the calculation of N II energy levels and is not included in this report. Part IV is entry 60.

where Z is the effective charge, and k is a parameter associated with the frequency of emission in the continuous spectrum by the relationship

$$\frac{\nu}{R_y} = \chi_n + \frac{Z^2}{k^2}, \quad R_y = 3{,}29 \cdot 10^{15}\ \text{sec}^{-1}. \tag{4}$$

where χ_n is the ionization potential of the n-th level, and f_{nk} is the oscillator strength for transitions to the state of continuous spectrum and is given by

$$f_{nk} = \frac{1}{3} \frac{\max(ll')}{2l+1} \frac{\nu}{R_y} \rho^2_{nk}, \tag{5}$$

$$\rho^2_{nk} = \left| \int_0^\infty P(nl|r) P(kl \pm 1, r) r\, dr \right|^2.$$

For practical calculations, the asymptotic expression for P^2_{nk}, which holds true for large values of k^2, are used. The formulas for P^2_{nk} for the case discussed in this paper, using wave functions derived in [60], are

$$\begin{gathered}
1. \quad \rho = \int_0^\infty P(3s|r) P(kp|r) r\, dr; \quad \rho^2 = q\left(1 + \frac{F}{k^2}\right)\frac{1}{k^3}; \\
q = N^2 \cdot 2^4 \cdot Z^3 e^{-\frac{4Z}{\lambda}} (\alpha + A\gamma\lambda^{-2} + B\lambda^{-4}\theta)^2 \lambda^{-12}; \\
F = \frac{4Z^3}{3\lambda^3} + 1 - \frac{2(3\alpha\varphi + 4Z^2 A\lambda^{-2} + 4\varphi A\gamma\lambda^{-2} + B\varkappa\lambda^{-4} + 5B\lambda^{-4}\theta\varphi}{\alpha + A\gamma\lambda^{-2} + B\lambda^{-4}\theta}; \\
\alpha = 4\lambda - 2Z; \quad \gamma = 20\lambda^2 + 4Z^2 - 20Z\lambda; \quad \varkappa = 72Z^2\lambda - 28Z^3; \\
\theta = 72Z^2\lambda + 120\lambda^3 - 180Z\lambda^2 - 8Z^3; \quad \varphi = Z^2\lambda^{-2}.
\end{gathered} \tag{6}$$

The results of calculations are given in Table 43.

The quadrupole transition probability for the $2p^2P$ - $3p^2P$ transition in N III was determined as

$$A(3p^2P - 2p^2P) = 2.6 \cdot 10^5. \tag{7}$$

The transition probability for the $sp^3\,{}^4P$ - $p^3\,{}^4S$ transition in N III was determined as

$$A({}^4P - {}^4S) = 1.4\cdot 10^9. \tag{8}$$

The corresponding oscillator strength for this transition is

$$f({}^4P - {}^4S) = 0.043. \tag{9}$$

The oscillator strengths and transition probabilities between terms of $1s^2 2s2p({}^1,{}^3p)nl$ configurations were evaluated from the following formulas:

$$\begin{gathered} f_{12} = \frac{1}{3}\frac{\nu_{LL'}}{R_y}\frac{1}{\omega_1}\frac{S_{LL'}\rho^2}{4l^2-1}, \\ A_{21} = \frac{2.68\cdot 10^9}{\omega_2} i^3 S_{21}; \quad i = \frac{\nu_{LL'}}{R_y}; \quad S_{12} = \frac{S_{LL'}\rho^2}{4l^2-1}, \end{gathered} \tag{10}$$

where ω_1 is the statistical weight of the lower level; $S_{LL'}$ is the multiplet strength, and l is the largest value of ll in the transition. Terms $\nu_{LL'}$ and $S_{LL'}$ are taken from other sources or calculated by the author. The results are given in Tables 44 and 45.

The oscillator strengths and coefficients of absorption are calculated for transitions into continuous spectrum from levels of $1s^2 2s^2 2p({}^1,{}^3p)nl$ configurations (Tables 46 and 47) and for transitions into the state of continuous spectrum from levels of $1s^2 2s2p({}^3P)nl$ ($n = 4$, $l = 0, 1, 2$) configurations (Tables 48 and 49).

52. Gruzdev, P. F. Relative oscillator strengths in the spectrum of the Co II ion. Optika i spektroskopiya, v. 13, no. 3, 1962, 302-307. QC350.068, v. 13

Intermediate coupling is discussed and a criterion developed to determine when the coupling between configurations can be neglected. Formulas for calculating line strengths in intermediate coupling with the phase taken into consideration are derived. The relative line strengths for the $3d^7(a^4F)4s$ - $3d^7(a^4F)4p$ transition in Co II were computed in LS and intermediate coupling (Table 50). According to the criteria developed earlier by the author, the relative line strengths computed in intermediate coupling should be in good agreement with the actual experimental values. The relative oscillator strengths were computed from line strengths in intermediate coupling and are included in Table 50.

53. Gruzdev, P. F. Relative oscillator strengths in the spectrum of the Ni II ion. Optika i spektroskopiya, v. 13, no. 3, 1962, 451-453. QC350.068, v. 13

The relative line strengths for the $3d^8(^3F)4s$ - $3d^8(^3F)4p$ transitions in N II were computed in LS and intermediate coupling (Table 51). According to criteria developed earlier by the author, the relative line strengths computed in intermediate coupling should be in good agreement with the actual (experimental) values. The relative oscillator strengths were computed from line strengths in intermediate coupling and are listed in Table 51.

Experimental Methods and Criteria

54. Beberman, L. M. Determination of oscillator strength by direct measurement of the spectral line width in a source of finite optical density. Optiki i spektroskopiya, v. 3, no. 4, 1957, 397-399. QC350.068, v. 3

A new method for measuring oscillator strengths is proposed. It is based on an earlier paper by the author in which it was shown that in a wide range of optical densities the width of an emission line varies linearly with optical density.

55. Ostrovskiy, Yu. I., N. P. Penkin, and L. N. Shabanova. Absolute values of oscillator strengths of Mg I, Sr I, Ca I, and Ba I resonance lines. IN: Akademiya nauk SSSR. Doklady, v. 120, no. 1, 1958, 66-68. AS262.S3663, v. 120

A method for the determination of absolute oscillator strengths of resonance lines based on the simultaneous measurement of total absorption and dispersion is proposed. The absolute oscillator strengths of resonance lines $^1P_1$ - $^1S_0$ of Mg I, Ca I, Sr I, and Ba I were determined. Better results were obtained in a later work [46] except for Mg I. Here, $f_{2852} = 1.2 \pm 0.3$.

56. Gruzdev, P. F., and G. P. Startsev. Some criteria for the applicability of theoretical intensities calculated in LS coupling to the spectra of complex atoms. Optika i spektroskopiya, v. 8, no. 6, 1960, 879-881. QC350.068, v. 8

Criteria are developed which allow an easy check to determine whether theoretical intensities calculated in LS coupling correspond to experimental values. These criteria are based on the differences between the experimental and the theoretical values of the Lande g factor, or

$$\Delta g = g_{exp} - g_{theor}.$$

Three cases are discussed:

1) $\Delta g \leq 0.010$. Good agreement should exist between the theoretical and the calculated values of intensity (excluding the level with the smallest j).
2) $\Delta g = 0.010 - 0.030$. Some deviation should occur between the theoretical and the calculated values of intensity.
3) $\Delta g > 0.030$. A large deviation should occur between the theoretical and calculated values of intensity.

57. Ostrovskiy, Yu. I., and N. P. Penkin. Measurement of the absolute value of oscillator strengths in atomic spectra. Part I. Optika i spektroskopiya, v. 11, no. 1, 1961, 1-11. QC350.068, v. 11

A method proposed by the authors in 1958 for measuring absolute values of oscillator strengths of resonance lines based on simultaneous measurements of total absorption and dispersion is described. The absolute value of the oscillator strength in the yellow doublet of Na was determined to be $f_D = 1.15 \pm 0.03$.

2. Wave Functions

58. Band, I. M., L. N. Zyryanova, and Ch'ing Ch'eng-jui. Numerical wave function values of K electrons which determine the probability of allowed and forbidden K capture. IN: Akademiya nauk SSSR. Izvestiya. Seriya fizicheskaya, v. 20, no. 12, 1956, 1387-1398. AS262.A62455, v. 20

The wave functions of K electrons were calculated for the elements given in Table 52. The results given were obtained by numerical integration of Dirac's equation for a potential which takes into account the presence of orbital electrons and the finite dimensions of the nucleus. The radius of the nucleus R was assumed to be

$$R = 1.2 \cdot 10^{-13} A^{1/3} \text{ cm.}$$

In addition, numerical data necessary for the calculation of K capture probabilities for elements with Z ranging from 5 to 98 were calculated.

59. Petrashen', M. I., I. V. Abarenko, and N. N. Kristofel'. Approximate wave functions of free ions and ions in crystals. IN: Leningrad. Leningradskiy universitet. Vestnik, no. 16. Seriya fiziki i khimii, no. 3, 1960, 7-21.

A simple method is developed for obtaining approximate one-electron wave functions of an ion in a crystal. It is based on the assumption that the electrons move in an effective crystalline field. The application of this method requires the knowledge of wave functions of free ions. A semiempirical method of obtaining such functions is outlined. The results of calculations for free Ca atom and the Tl^+ ion are given in Tables 53 and 54, respectively. The wave functions of a number of ions in some of the alkali-halide crystals were also obtained.

60. Nikitin, A. A., and E. P. Filatova. Determination of the wave functions for N III in connection with the investigation of its Raman spectrum in the envelopes of stars and nebulae. Part IV. IN: Leningrad. Leningradskiy universitet. Vestnik, no. 7. Seriya matematiki, mekhaniki i astronomii, no. 2, 1962, 147-160.

Approximate radial wave functions are found for the following N III configuration levels: $1s^2 2s^2 nl$, $nl \geqslant 3$, $l = 0,1,2,3,4$; and $1s^2 2s2p(^{1,3}P) + nl$, $n = 3,4$ and $l = 0,1,2,3$. The parameters that appear in these equations are evaluated. The only numerical data calculated for N III are given in Table 55. In deriving the expressions for the wave functions of N III, the authors used wave functions for some Ca II and B I levels derived by Soviet scientists [but which are unavailable at the Library of Congress]. These wave functions are reproduced in Tables 56 to 61.

61. Smirnova, E. V. Approximate wave functions for the gallium ion in crystals. IN: Leningrad. Leningradskiy universitet. Vestnik, no. 16. Seriya fiziki i khimii, no. 3, 1962, 66-71.

The semiempirical method is used for calculations of one-electron wave functions for the free Ga^+ ion (Table 62). These functions are used to obtain corresponding wave functions of the Ga^+ ion in KCl crystallophosphor with Ga^+ as an activating impurity.

3. Theoretical Developments

62. Bersuker, I. B. Concerning the theorem on the sum of oscillator strength for alkali metals. IN: Akademiya nauk SSSR. Doklady, v. 113, no. 5, 1957, 1017-1019.
AS262.S3663, v. 113

A formula for the oscillator strengths of induced transitions in alkali metals and alkaline-type atoms is derived taking into consideration changes in the screening potential and exchange operator due to deformation of the inner electron cloud. The formula is summed up to obtain an expression for the sum of the oscillator strengths for these systems. A special case of this formula is used to calculate the sum of oscillator strengths for experimentally observed transitions in the principal series of Na, K, and Ca.

63. Bersuker, I. B. The influence of the core on the transitions of optical electrons. Optika i spektroskopiya, v. 3, no. 2, 1957, 97-103. QC350.068, v. 3

The effect of the core on the processes associated with the change in state of optical electrons due to optical transitions is considered. In the adiabatic approximation, the effect of the inner electrons on the transitions of the optical electrons is taken into consideration by adding a perturbation due to noninertial polarization of the core by the field of the electromagnetic wave. A corresponding correction is introduced into the formulas for oscillator strength and the sum of the oscillator strengths. Calculation for Li, Na, K, Ca^{+}, and Al^{++} are in good agreement with available experimental data, according to which the sum of the oscillator strengths for the experimentally observed transitions is considerably greater than unity. Additional allowed transitions for molecules due to this perturbation are calculated. Some of these have already been observed in oxygen.

64. Veselov, M. G., and I. B. Bersuker. Adiabatic approximation in the quantum theory of atoms. IN: Leningrad. Leningradskiy universitet. Vestnik, no. 16. Seriya fiziki i khimii, no. 3, 1957, 55-56.

This is the earlier version of [66] with less mathematical detail.

65. Veselov, M. G., and I. B. Bersuker. Adiabatic approximation in the quantum theory of atoms. IN: Akademiya nauk SSSR. Izvestiya. Seriya fizicheskaya, v. 22, no. 6, 1958, 662-664. AS262.A62455, v. 22

A new method for quantum mechanical calculations of many-electron systems is presented. The many-electron quantum problem is divided into two parts. The total wave function U of the system is made up of the product of the wave function U_n of core electrons and the wave function φ of the outer electrons N-n.

The quantum problem of core electrons for different space configurations is considered first:

$$\left[H_{core} + \sum_{i=1}^{n} \sum_{k=n+1}^{N} V(r_{ik})\right] U(r_1, \ldots, r_n; r_{n+1}, \ldots, r_N) = W(r_{n+1}, \ldots, r_N)\, U(r_1, \ldots, r_n; r_{n+1}, \ldots, r_N). \quad (1)$$

H_{core} is the energy operator of the core electrons with no allowance for its interaction with outer electrons (which is expressed by the $\Sigma\Sigma V(r_{ik})$ operator). The wave function U includes the coordinates of outer electrons as parameters; the energy W of the core is a function of these parameters and is equivalent to the potential energy in the equation for outer electrons:

$$[H_0 + W(r_{n+1}, \ldots, r_N)]\, \varphi(r_{n+1}, \ldots, r_N) = E\varphi(r_{n+1}, \ldots, r_N), \quad (2)$$

Here H_0 is the energy operator of outer electrons with no allowance for their interaction with the core electrons, and E is the total energy of the system. This method is a variation of the method of incomplete separation of variables extended to include the polarizing effect of the outer electrons on the core and the reverse effect of the core on the outer electrons.

66. Yutsis, A. P., Ya. T. Vizbarayte, V. I. Kavedtskis, and I. V. Batarunas. Two-electron-state model approximation and the so-called anomaly in the spectra of carbon, nitrogen, and oxygen. IN: Akademiya nauk SSSR. Izvestiya. Seriya fizicheskaya, v. 22, no. 6, 1958, 665-667.
AS262.A62455, v. 22

The possibility of developing an approximation method on the basis of two-electron states described by more precise two-electron wave functions is considered. In this method, the wave functions of each electron pair are obtained by the method of incomplete separation of variables or the multi-configuration-approximation method. The wave function of the whole system is obtained by multiplication of the wave functions of individual electron pairs and a subsequent antisymmetry operation. Numerical calculations of energy for the $1s^2 2s, 1s^2 2P$ configuration of the lithium atom on the basis of this model are in good agreement with experimental values. Good agreement is also obtained between theoretical and experimental values for the relationship

$$\frac{^1S - {}^1D}{^1D - {}^3P}$$

for the $1s^2 2s^2 2p^q (q = 2,3,4)$ configuration of carbon and oxygen atoms, and for the relationship

$$\frac{^2P - {}^2D}{^2D - {}^4S}$$

for the same configuration of nitrogen atoms.

67. Bersuker, I. B. Optical transition probabilities in atoms and molecules with a polarizable core. IN: Akademiya nauk SSSR. Izvestiya. Seriya fizicheskaya, v. 22, no. 6, 1958, 749-752.
AS262.A62455, v. 22

The effect of the core on the transitions of optical electrons is considered. Formulas for transition probabilities and oscillator strengths in many electron systems are derived with this effect taken into consideration. The absolute f-value for the resonance transition in Na calculated by means of this formula,

$$f_{3s}^{3p} = 1.22 ,$$

is very close to experimental f-value (1.24) calculated by G. S. Kvater (USSR) in 1945.

68. Bersuker, I. B. Quantum transitions in self-consistent field approximation. Optika i spektroskopiya, v. 9, no. 6, 1960, 685-691. QC350.068, v. 9

A different and more exact method of solving nonstationary problems in self-consistent field approximation is proposed, in which the probability of quantum transitions is obtained as a solution of a system of nonstationary equations of the self-consistent field, analogous to the equations of Fock for the stationary case. It is shown that the conventional formula for the transition probabilities is an approximation of the zero order in the matrix elements of the interaction operator between the electrons. A first approximation correction is obtained for this formula. The specific case of optical dipole transitions in atoms is investigated in more detail and the expression for the correction term reduced to a form which is convenient for numerical calculations.

69. Veselov, M. G., and I. B. Bersuker. Computation of the lithium atom and the calculation of the nuclear magnetic moment. Optika i spektroskopiya, v. 13, no. 3, 1962, 297-301. QC350.068, v. 13

The results of computation of the lithium atom by adiabatic approximation are given. According to the method used [see 45], the effect of polarization of the core by the optical electron and the reverse effect of this polarization on the optical electron are automatically taken into consideration. At the same time, the wave function of the inner 1s electron is deformed and depends parametrically on the position of the optical electron. The equation for the optical electron includes the "potential of mirror forces"; i.e., a potential acting on the optical electron due to the polarization of the core by the optical electron. Wave functions are obtained for the 2s, 2p, and 3p states of the lithium atom, and it is shown that the adiabatic approximation method results in better values of the wave function near $r = 0$. This made it possible to compute the magnetic moment of the Li^7 nucleus. The value of the magnetic moment obtained is in better agreement with the experimental value than the one obtained by the Hartree-Fock method.

70. Veselov, M. G., and L. N. Labzovskiy. Exchange in the adiabatic approximation in the theory of the atom. IN: Leningrad. Leningradskiy universitet. Vestnik, no. 16. Seriya fiziki i khimii, no. 3, 1962, 30-35.

The effect of exchange in the adiabatic approximation method is considered. An approximate expression for the exchange correction to the energy of an atom in the adiabatic approximation is obtained, and the correction term is evaluated for the ground state of the lithium atom. In this example, inclusion of the exchange in the adiabatic approximation method resulted in an improvement of the same order as the one obtained by including the exchange in the Hartree method.

4. Tables for Part Two

Table 18. Oscillator Strengths for the Strongest Lines of Al I [33]

Å	Transition	f
3944.03	$3^2P_{1/2} - 4^2S_{1/2}$	99
3961.53	$3^2P_{3/2} - 4^2S_{1/2}$	100
3082.15	$3^2P_{1/2} - 3^2D_{3/2}$	149
3092.75	$3^2P_{3/2} - 3^2D_{5/2}, {}_{3/2}$	152

Table 19. Absolute f-Values for Lines of Cr [34]

Multiplet no.	λ (Å)	Transition	J	$f \cdot 10^3$
4	3578.7	$a^7S - y^7P^0$	3—4	49
	3593.5		3—3	39
	3605		3—2	28
1	4254.3	$a^7S - z^7P^0$	3—4	15
	4274.8		3—3	11
	4289.7		3—2	8.2
22	4337.6	$a^5D - z^5P^0$	1—2	4.7
	4344.5		3—0	5.3
	4359.6		2—2	2.8
	4371.3		3—3	1.5
	4385		4—4	0.8
10	4496.9	$a^5S - y^5P^0$	2—3	2.3
	4545.9		2—2	1.6
	4580.1		2—1	0.97
21	4565.5	$a^5D - y^5P^0$	2—3	0.50
	4591.4		1—2	1.2
	4600.1		3—3	1.6
	4618.8		0—1	4.6
	4616.1		2—2	2.2
	4626.2		1—1	2.7
	4646.2		4—3	3.1
	4652.2		3—2	2.5
7	5204.5	$a^5S - z^5P$	2—1	17
	5206.0		2—2	29
	5208.4		2—3	41
18	5247.6	$a^5D - z^5P$	0—1	4.7
	5264.2		1—1	3.0
	5265.7		1—2	1.3
	5296.7		2—1	1.4
	5298.3		2—2	2.1
	5300.7		2—3	0.37
	5345.8		3—2	2.7
	5348.3		3—3	1.3
	5409.8		4—3	3.5

Table 20. Absolute f-Values for Lines of Mn [34]

λ (Å)	Transition	J	$f \cdot 10^3$
5432.548	$a^6S - z^6P^0$	$^5/_2 - ^5/_2$	0.035
5394.674		$^5/_2 - ^7/_2$	0.052
4034.490	$a^6S - z^6P^0$	$^5/_2 - ^3/_2$	27
4033.073		$^5/_2 - ^5/_2$	40
4030.755		$^5/_2 - ^7/_2$	56
3224.761	$a^6S - z^4P^0$	$^5/_2 - ^5/_2$	0.53
3216.946		$^5/_2 - ^3/_2$	0.28
2801.064	$a^6S - y^6P^0$	$^5/_2 - ^3/_2$	290
2798.271		$^5/_2 - ^5/_2$	420
2794.817		$^5/_2 - ^7/_2$	570

Table 21. Relative Oscillator Strengths of Sc I Lines [35]

Multiplet no.	λ (Å)	Transition	J	I	I *	I **
1	6378.824	$a^2D-z^4F^\circ$	3/2 — 3/2	20.6	—	—
	6413.358		5/2 — 5/2	19.5	—	—
2	6210.626	$a^2D-z^2D^\circ$	3/2 — 3/2	155	55.6	64.8
	6276.310		5/2 — 3/2	11.8	6.2	7.2
	6305.671		5/2 — 5/2	194	100	100
3	6258.962	$a^2D-z^4D^\circ$	5/2 — 5/2	55.0	—	—
5	4758.152	$a^2D-z^2F^\circ$	3/2 — 5/2	89.2	97	70
	4779.349		5/2 — 7/2	62.6	100	100
6	4054.555	$a^2D-y^2P^\circ$	3/2 — 3/2, 1/2	965	65.6	66.7
	4082.396		5/2 — 3/2	1000	100	100
7	3996.607	$a^2D-y^2D^\circ$	3/2 — 5/2	89.6	11.6	7.2
	4020.399		3/2 — 3/2	528	67.1	64.8
	4023.688		5/2 — 5/2	526	100	100
	4047.792		5/2 — 3/2	41.4	7.7	7.2
8	3907.476	$a^2D-y^2F^\circ$	3/2 — 5/2	714	68.7	70
	3911.810		5/2 — 7/2	693	100	100
	3933.381		5/2 — 5/2	57.7	8.2	5
9	3255.678	$a^2D-z^2P^\circ$	3/2 — 3/2	814	11.4	11.[illegible]
	3269.904		5/2 — 1/2	3870	53.4	55.6
	3273.962		5/2 — 3/2	4840	100	100
10	3030.769	$a^2D-x^2F^\circ$	5/2 — 5/2	235	9.1	5
	3015.315		3/2 — 5/2	2670	70	70
12	5671.805	$a^4F-z^4G^\circ$	9/2 — 11/2	6900	100	100
	5686.826		7/2 — 9/2	6500	74.2	76.1
	5700.14		5/2 — 7/2	6900	59.2	57.1
	5711.754		3/2 — 5/2	7600	43.4	42.9
14	4737.642	$a^4F-y^4D^\circ$	5/2 — 3/2	6800	58.8	44.8
	4741.018		7/2 — 5/2	6700	76.9	68.6
	4743.814		9/2 — 7/2	7000	100	100
15	5514.215	$a^2F-z^2G^\circ$	5/2 — 7/2	8200	83.7	77.1
	5520.496		7/2 — 9/2	7400	100	100
16	5481.989	$a^2F-x^2F^\circ$	7/2 — 7/2	8500	100	100
	5482.618		5/2 — 5/2	9100	80.6	74.1

* Relative intensities of each multiplet line calculated from the authors' data.

** Relative intensities of each multiplet line computed from the Kronig-Hönl formula.

Table 22. Absolute Oscillator Strengths for the Five Strongest Lines of Ga I [36]

λ (Å)	Transition	J	f
4172.048	$4^2P^0 - 5^2S$	$3/2 - 1/2$	0.135
4032.975		$1/2 - 1/2$	0.129
2943.689	$4^2P^0 - 4^2D$	$3/2 - 5/2$	0.287
2874.240		$1/2 - 3/2$	0.818
2944.175		$3/2 - 3/2$	0.088

Table 23. Absolute Oscillator Strengths for the Five Stongest Lines of In I [36]

λ (Å)	Transition	J	f
4511.310	$5^2P^0 - 6^2S$	$3/2 - 1/2$	0.216
4101.764		$1/2 - 1/2$	0.201
3256.09	$5^2P^0 - 5^2D$	$3/2 - 5/2$	0.509
3039.36		$1/2 - 3/2$	0.506
3258.56		$3/2 - 3/2$	0.079

Table 24. Relative Oscillator Strengths for Lines of Ca II, Fe I, Mn II, and Mg II [37]

Element	λ, Å	Transition	f_i / f_m
CaII	3933,66	$4^2S_{1/2} - 4^2P_{3/2}$	2,05
	3968,47	$4^2S_{1/2} - 4^2P_{1/2}$	
FeI	3047,60	$a^5D_4 - y^5F^0_5$	1,34
	2994,43	$a^5D_3 - y^5D^0_2$	
MnII	2949,20	$a^8S_2 - z^7P^0_3$	7,0 : 5,1 : 3,1 ±2,8 %
	2939,30	$a^8S_2 - z^7P^0_2$	
	2933,05	$a^8S_2 - z^7P^0_1$	
MgII	2795,2	$1^2S_{1/2} - 2^2P_{3/2}$	2,09±6,8 %
	2802,7	$1^2S_{1/2} - 2^2P_{1/2}$	
MnII	2576,11	$a^7S_3 - z^7P^0_4$	9 : 6,7 : 5,2 ±3,0%
	2593,73	$a^7S_3 - z^7P^0_3$	
	2605,10	$a^7S_3 - z^7P^0_2$	

Table 25. Relative f-Values of V I Spectrum [40]

Multiplet no.	λ (A)	Transition	J	f	Intensity Theor.*	Intensity Exp.**
3	4881.554	$a^4F - z^4D^\circ$	9/2 — 7/2	1160	100	100
	4875.462		7/2 — 5/2	952	68.6	65.4
	4864.741		5/2 — 3/2	861	44.8	34.3
	4851.483		3/2 — 1/2	850	28.8	21.2
	4827.458		7/2 — 7/2	218	11.4	14.9
	4831.642		5/2 — 5/2	287	14.6	14.7
	4832.427		3/2 — 3/2	456	11.2	15.7
4	4594.103	$a^4F - z^4G^\circ$	9/2 — 11/2	1000	100	100
	4586.364		7/2 — 9/2	908	76.4	72.4
	4580.394		5/2 — 7/2	907	57.4	54.2
	4577.173		3/2 — 5/2	958	42.9	38.2
	4635.176		9/2 — 9/2	77	6.9	7.7
	4619.771		7/2 — 7/2	96	9.1	7.6
	4606.146		5/2 — 5/2	125	6.9	7.5
5	4352.872	$a^4F - z^4F^\circ$	9/2 — 9/2	776	100	100
	4341.013		7/2 — 7/2	656	66.5	67.6
	4332.823		5/2 — 5/2	605	45.0	46.7
	4330.024		3/2 — 3/2	668	34.9	34.4
	4368.042		7/2 — 5/2	123	11.7	12.6
	4309.795		7/2 — 9/2	153	9.1	16.0
	4306.214		5/2 — 7/2	214	11.7	16.5
	4307.184		3/2 — 5/2	233	8.7	12.0
7	3902.250	$a^4F - y^4F^\circ$	9/2 — 9/2	2480	100	100
	3864.862		5/2 — 5/2	2540	45.0	61.4
	3909.894		9/2 — 7/2	351	9.5	14.2
	3892.859		7/2 — 5/2	358	11.7	18.1
	3867.602		7/2 — 9/2	277	9.1	9.0
	3844.438		3/2 — 5/2	778	8.7	12.6
8	3890.184	$a^4F - z^2G^\circ$	7/2 — 7/2	643	—	—
9	3828.559	$a^4F - y^4D^\circ$	5/2 — 3/2	3180	—	—
14	3207.410	$a^4F - z^4G^\circ$	9/2 — 9/2	1670	6.9	6.9
	3202.381		7/2 — 7/2	2690	9.1	8.9
	3198.012		5/2 — 5/2	2790	6.9	6.9
15	3069.645	$a^4F - x^4D^\circ$	7/2 — 7/2	668	—	—
17	3066.575	$a^4F - w^4F^\circ$	9/2 — 9/2	13700	100	100
	3060.360		7/2 — 7/2	9180	66.5	55.2
	3056.334		5/2 — 5/2	8700	45.0	38.0
	3053.65		3/2 — 3/2	8500	34.9	24.8
	3044.936		7/2 — 9/2	973	9.1	5.7
	3043.124		5/2 — 7/2	1980	11.7	8.7
	3043.555		3/2 — 5/2	1740	8.7	5.1
21	4437.837	$a^6D - z^6P^\circ$	7/2 — 7/2	1270	28.6	28.6
	4441.683		5/2 — 5/2	1710	36.6	29.2
	4444.207		3/2 — 3/2	2170	28.0	25.5
	4419.935		5/2 — 7/2	159	4.7	6.0
	4428.515		3/2 — 5/2	1010	12.0	11.3
	4436.138		1/2 — 3/2	2940	20.0	16.5
22	4379.238	$a^6D - y^6F^\circ$	9/2 — 11/2	17600	100	100
	4389.974		5/2 — 7/2	12500	42.9	41.9
	4395.228		3/2 — 5/2	11200	24.0	25.3
	4400.575		1/2 — 3/2	6120	10.4	10.4
	4429.796		9/2 — 7/2	370	1.2	1.9

* Intensities calculated from the Kronig-Hönl formula.

** Intensities computed from the authors' f-values.

Table 25 (Cont.)

Multiplet no.	λ (Å)	Transition	J	f	Intensity Theor.*	Intensity Exp.**
22	4426.005	$e^6D - y^6F^\circ$	7/2 — 5/2	708	2.9	3.2
	4421.573		5/2 — 3/2	1320	4.0	4.5
	4416.474		3/2 — 1/2	1820	3.7	4.1
27	4111.785	$e^6D - y^6D^\circ$	9/2 — 9/2	11800	100	100
	4115.185		7/2 — 7/2	7520	43.9	51.0
	4116.470		5/2 — 5/2	3820	12.6	19.4
	4134.488		9/2 — 7/2	2950	31.6	25.0
	4132.017		7/2 — 5/2	5030	29.5	34.1
	4128.071		5/2 — 3/2	5860	29.5	29.8
	4123.566		3/2 — 1/2	5910	19.1	20.0
	4092.694		7/2 — 9/2	3450	22.7	23.4
	4099.796		5/2 — 7/2	6120	31.6	31.1
	4109.786		1/2 — 3/2	12000	19.1	20.3
28	3794.964	$e^6D - x^6D^\circ$	9/2 — 9/2	2340	100	100
	3803.471		7/2 — 7/2	1530	43.9	52.4
	3778.684		7/2 — 9/2	616	22.7	21.1
	3790.324		5/2 — 7/2	1110	31.6	28.5
	3799.912		3/2 — 5/2	1880	29.5	32.2
29	3688.069	$e^6D - y^6P^\circ$	7/2 — 7/2	3360	28.6	28.6
	3692.225		5/2 — 5/2	5130	36.6	32.7
	3695.865		3/2 — 3/2	6300	28.0	26.8
	3675.700		5/2 — 7/2	7850	4.7	5.0
	3683.126		3/2 — 5/2	2880	12.0	12.3
	3690.281		1/2 — 3/2	8590	20.0	18.3
41	4090.579	$e^4D - w^4F^\circ$	7/2 — 9/2	12400	100	100
	4095.486		5/2 — 7/2	11300	68.6	68.2
	4102.159		3/2 — 5/2	12400	44.8	47.8

Table 26. Relative f-Values of Co I [40]

Multiplet no.	λ (Å)	Transition	J	f	Intensity Tf. Ex.*	Intensity Tf. Ex.**
1	4190.712	$a^4F - z^6F^\circ$	9/2 — 9/2	54	—	—
	4229.955		5/2 — 3/2	21	—	—
3	3909.933	$a^4F - z^6G^\circ$	9/2 — 11/2	19	—	—
4	3526.847	$a^4F - z^4F^\circ$	9/2 — 9/2	984	100	100
	3575.361		7/2 — 7/2	696	66.5	56.0
	3594.870		5/2 — 5/2	636	45.0	38.8
	3602.079		3/2 — 3/2	767	34.9	31.2
	3520.075		7/2 — 5/2	250	11.7	19.5
	3550.592		5/2 — 3/2	296	8.7	18.0
	3641.590		7/2 — 9/2	67	9.1	4.9
	3652.541		5/2 — 7/2	93	11.7	5.7
	3647.658		3/2 — 5/2	130	8.7	5.3
5	3465.792	$a^4F - z^4G^\circ$	9/2 — 11/2	875	100	100
	3529.032		5/2 — 7/2	1000	57.4	70.6
	3533.556		3/2 — 5/2	1000	42.9	46.6
6	3412.633	$a^4F - z^4D^\circ$	9/2 — 7/2	710	100	100
	3451.582		7/2 — 5/2	633	68.6	71.3
	3442.918		5/2 — 3/2	617	44.8	51.1
	3455.237		3/2 — 1/2	726	28.0	40.9
	3491.316		3/2 — 3/2	405	11.2	26.2
	3584.801		5/2 — 7/2	16	0.8	1.3
9	3159.947	$a^4F - y^4D^\circ$	7/2 — 5/2	124	68.6	68.6
	3149.310		5/2 — 3/2	114	44.8	47.3
10	3082.614	$a^4F - y^4G^\circ$	9/2 — 11/2	185	100	100
	3147.060		5/2 — 7/2	364	57.4	118
	3089.596		7/2 — 7/2	163	9.1	61.8
	3098.194		5/2 — 5/2	147	6.9	44.5
	3013.592		9/2 — 7/2	66	0.2	35.9
	3012.481		7/2 — 5/2	79	0.3	34.4
11	3044.004	$a^4F - y^4F^\circ$	9/2 — 9/2	1360	100	100
	3061.822		7/2 — 7/2	918	66.5	53.9
	3086.777		3/2 — 3/2	1120	34.9	32.9
	2987.166		9/2 — 7/2	225	9.1	16.5
	3017.548		7/2 — 5/2	301	11.7	17.7
	3048.888		5/2 — 3/2	304	8.7	13.4
13	2989.590	$a^4F - y^2G^\circ$	9/2 — 9/2	219	—	—
	3064.370		7/2 — 9/2	51	—	—
16	4020.818	$b^4F - z^4F^\circ$	9/2 — 9/2	52	—	—
17	3876.881	$b^4F - z^4G^\circ$	9/2 — 9/2	39	—	—
18	3873.120	$b^4F - z^4D^\circ$	9/2 — 7/2	1080	100	100
	3875.953		7/2 — 5/2	818	68.6	60.8
	3881.869		5/2 — 3/2	686	44.8	38.2
	3894.976		3/2 — 1/2	583	28.0	21.7
19	3627.806	$b^4F - z^2G^\circ$	7/2 — 9/2	526	—	—
	3564.947		5/2 — 7/2	898	—	—
	3496.681		7/2 — 7/2	454	—	—
20	3521.567	$b^4F - z^2F^\circ$	9/2 — 7/2	947	—	—
	3605.370		7/2 — 7/2	501	—	—
21	3523.423	$b^4F - y^4D^\circ$	3/2 — 1/2	7010	28.0	28.0
	3585.154		7/2 — 7/2	782	11.4	6.3

* Intensities calculated from the Kronig-Hönl formula.

** Intensities computed from the authors' f-values.

Table 26 (Cont.)

Multiplet no.	λ (Å)	Transition	J	Intensity		
					Theo.*	Exp.**
21	3574.967	$b^4F - y^4D^\circ$	5/2 — 5/2	1420	14.6	8.5
	3560.891		3/2 — 3/2	1480	11.2	5.9
22	3453.514	$b^4F - y^4G^\circ$	9/2 — 11/2	14700	100	100
	3529.816		7/2 — 9/2	5140	76.4	27.9
	3495.682		5/2 — 5/2	6690	42.9	18.1
	3449.441		9/2 — 9/2	1310	6.9	8.9
	3443.644		7/2 — 7/2	5760	9.1	31.3
	3449.170		5/2 — 5/2	3130	6.9	12.7
23	3405.120	$b^4F - y^4F^\circ$	9/2 — 9/2	13600	100	100
	3409.177		7/2 — 7/2	3320	66.5	19.5
	3417.154		5/2 — 5/2	3000	43.0	13.2
	3433.045		3/2 — 3/2	8360	34.9	24.6
	3483.410		7/2 — 9/2	181	9.1	1.1
	3462.801		3/2 — 5/2	10900	8.7	32.0
25	3412.339	$b^4F - y^2G^\circ$	7/2 — 9/2	7000	—	—
	3395.370		5/2 — 7/2	2930	—	—
28	4121.318	$a^2F - z^2G^\circ$	7/2 — 9/2	3170	100	100
	4118.774		5/2 — 7/2	3250	77.4	76.9
29	4092.386	$a^2F - z^2F^\circ$	7/2 — 7/2	630	100	100
	4110.532		5/2 — 5/2	583	74.1	69.4
31	3995.306	$a^2F - y^4G^\circ$	7/2 — 9/2	4950	—	—
32	3935.964	$a^2F - y^4F^\circ$	7/2 — 9/2	1040	—	—
	3997.301		5/2 — 7/2	1370	—	—
33	3842.047	$a^2F - z^2D^\circ$	7/2 — 5/2	1300	—	—
34	3845.468	$a^2F - y^2G^\circ$	7/2 — 9/2	7190	100	100
	3894.073		5/2 — 7/2	9300	77.1	97.0
	3745.491		7/2 — 7/2	1050	2.9	14.6
35	3569.370	$a^2F - y^2F^\circ$	7/2 — 7/2	14200	100	100
	3587.186		5/2 — 5/2	14800	74.1	78.2
	3704.060		5/2 — 7/2	1590	3.7	8.4
36	3489.399	$a^2F - y^2D^\circ$	7/2 — 5/2	11000	100	100
	3518.340		5/2 — 3/2	11200	70	76.4

Table 27. Relative Oscillator Strengths for some Zn I Lines [41]

λ (Å)	Transition	J	f	gf exp.	gf * theor.
4810.53	$4^3P - 5^3S$	2—1	1.08	540	543
4722.16		1—1	1.06	318	308
4680.14		0—1	1.00	100	100
3345.03 •	$4^3P - 4^3D$	2—1	0.03	1.2	1.2
3345.57 •		2—2	0.51	17.9	17.9
3345.02		2—3	2.85	100	100
3302.94		1—1	0.75	15.8	17.4
3302.59		1—2	2.49	52.4	52.2
3282.33		0—1	2.96	20.8	22.9
280 .17 •	$4^3P - 5^3D$	2—1	0.009	1.2	1.2
2801.06 •		2—2	0.13	17.8	17.9
2800.87		2—3	0.74	100	100
2770.98 •		1—1	0.22	17.8	17.5
2770.87		1—2	0.66	53.5	52.5
2756.45		0—1	0.93	25.1	23.0

* Calculated on the assumption of LS coupling.

Table 28. Relative Oscillator Strengths for some Cd I Lines [41]

λ (Å)	Transition	J	f	gf exp.	gf * theor.
5085.82	$5^3P - 6^3S$	2—1	1.03	515	500
4799.92		1—1	1.07	321	316
4678.16		0—1	1.00	100	100
3614.45 •	$5^3P - 5^3L$	2—1	0.03	1.2	1.2
3612.80		2—2	0.53	19.9	17.9
3610.51		2—3	2.66	100	100
3467.68		1—1	0.90	20.3	16.3
3466.20		1—2	2.66	60.0	49.7
3403.65		0—1	3.10	23.3	21.2
2981.89 •	$5^3P - 6^3D$	2—1	0.01	1.2	1.2
2981.34 •		2—2	0.15	17.4	17.9
2980.63		2—3	0.86	100	100
2881.23 •		1—1	0.23	16.0	16.6
2880.77		1—2	0.68	47.5	49.7
2836.91		0—1	0.80	18.6	21.6

* Calculated on the assumption of LS coupling.

Table 29. Relative Oscillator Strengths of Ba I Lines [42]

No. of multiplet	Transition	$l-l'$	J	λ (A)	f	** f_{rel}	+ $f_{theor.}$	$f_{exp.}$
I	$6^1S - 6^1P^o$	0—1	0.000	7911.38	6.00	—	—	—
2	$6^1S - 6^1P^o$	0—1	0.000	5535.484	1000	—	—	—
I	$6^1S - 6p'\,^1D^o$	0—1	0.000	4132.43	6.22	—	—	—
II	$6^1S - 6p'\,^1P^o$	0—1	0.000	3889.32	6.56	—	—	—
5	$5^1D - 5d6p\,^1P^o$	3—4	1.19	7050.941	420	—	100	100.7
		2—3	1.14	7380.298	370	—	73.1	66.9
		1—2	1.12	7673.093	286	—	35.2	31.0
		3—3	1.19	7400.093	53.8	—	8.9	13.4
		2—2	1.14	7780.479	73.6	—	10.7	13.3
6	$5^1D - 5d6p\,^3D^o$	3—3	1.19	6496.750	343	—	100	92.2
		2—2	1.14	6527.312	238	—	46.3	45.8
		1—1	1.12	6546.328	205	—	37.3	34.3
		3—2	1.19	6693.812	85.5	—	13.3	23.2
		2—1	1.14	6675.271	80.6	—	12.8	17.3
		2—3	1.14	6341.092	96.5	—	11.0	19.1
		1—2	1.12	6450.854	71.8	—	11.9	8.3
7	$5^1D - 5d6p\,^1P^o$	3—3	1.19	6110.781	250	240	100	87.8
		2—1	1.14	6163.117	202	211	42.7	50.7
		1—0	1.12	6019.470	165	178	23.1	24.8
		2—2	1.14	5971.800	97.0	—	17.1	24.3
		1—1	1.12	5907.098	157	148	17.2	23.7
		1—2	1.12	5907.85	19.6	—	1.1	3.0
8	$5^1D - 6^1P^o$	3—4	1.19	3993.401	107	143	100	99.5
		2—3	1.14	3896.717	86.3	—	67.1	64.1
		1—2	1.12	3900.910	118	95.4	44.8	47.1
		3—3	1.18	3985.656	13.2	—	8.8	12.3
		2—2	1.14	3987.970	15.8	—	8.8	10.5
III	$5^1D - 6^1D^o$	1—2	1.12	7120.31	144	—	—	—
		3—2	1.19	7417.52	9.33	—	—	—
IV	$5^1D - 6^1F^o$	3—3	1.19	5905.69	12.7	—	—	—
V	$5^1D - 7p\,^3P^o$	2—3	1.14	4501.93	3.26	—	17.9	23.6
		1—0	1.12	4804.00	5.10	—	23.1	22.4
		2—1	1.14	4620.33	7.25	—	32.6	32.5
		3—2	1.19	4873.62	9.56	—	100	86.7
VI	$5^1D - 6p'\,^1P^o$	2—2	1.41	6905.71	35.2	—	—	—
VII	$5^1D - 6^1P^o$	2—3	1.41	6482.91	245	—	—	—
VIII	$5^1D - 6^1P^o$	2—1	1.41	5535.70	187	198	—	—
IX	$5^1D - 7^1P^o$	2—1	1.41	4726.45	87.6	94.8	—	—
X	$5^1D - 4^1F^o$	2—3	1.41	4203.11	156	—	—	—
9	$6^1P^o - 6^1D$	2—3	1.67	5777.622	853	856	100	95.7
		2—2	1.67	5800.229	151	—	18.0	22.1
10	$6^1P^o - 7^1S$	2—1	1.67	7905.751	223	—	100	89.6
		1—1	1.56	7302.411	257	—	52.4	61.9
		0—1	1.51	7196.335	354	—	18.0	28.5
XI	$6^1P^o - 6^1S$	0—1	1.51	4619.970	56.4	—	20.7	22.0
		1—1	1.56	4700.44	46.7	—	100	88.0
XII	$6^1P^o - 6^1D$	1—2	1.56	4402.55	214	—	—	—
		2—3	1.67	4579.67	354	—	—	—
XIII	$6^1P^o - 6p\,^3P$	1—2	1.56	4350.39	179	—	10.8	29.8
		0—1	1.51	4431.90	673	—	25.6	37.2
		1—1	1.56	4546.03	202	—	19.6	33.5
		2—2	1.67	4525.24	188	—	100	51.3
		1—0	1.56	4573.08	162	—	27.3	31.8
		2—1	1.67	4601.82	206	—	45.8	56.6
XIV	$6^1P^o - 6p\,^1S$	1—0	1.56	4500.75	66.9	—	—	—
XV	$6^1P^o - 6d'\,^1D$	1—2	1	4242.62	18.0	—	51.6	35.9
		2—3	1.	4325.18	17.4	—	100	65.1
		2—2	1.67	4400.85	18.0	—	18.6	70.4
XVI	$6^1P^o - 7^1D$	2—3	1.67	4489.97	112	—	100	90.4
		2—2	1.67	4493.63	69.3	—	17.9	61.4
		0—1	1.51	4264.39	78.5	—	21.5	13.9
		1—1	1.56	4322.91	37.3	—	16.7	14.5
		1—2	1.56	4323.09	45.0	—	40.7	28.9
XVII	$6^1P^o - 6d\,^3G$	2—3	1.67	4607.11	17.5	—	—	—
XVIII	$6^1P^o - 7^1S$	2—1	1.67	4239.57	23.9	—	—	—

* Arabic numerals represent multiplet numbers from Moore tables; Roman numerals represent multiplet numbers derived from Ba spectral lines using Moore's data for energy levels.

** Calculated by A. Kruithof.

\+ Calculated on the assumption of LS coupling.

Table 30. Absolute f-Values for the p^2-ps Transitions of Pb I [43]

λ (Å)	Transition p^2	Transition ps	Relative Intensity	f
2833	$^3P_0$	$^3P_1$	10	0,6
3639	$^3P_1$		6,55±0,7	0,28
4057	$^3P_2$		24,2±1,2	0,85
7229	$^1D_2$		1,4±0,8	0,19
17180	$^1S_0$			
3683	$^3P_1$	$^3P_0$	11,1	0,49
2022	$^3P_0$	$^1P_1$	(1)	
2401	$^3P_1$		10	0,09
2577	$^3P_2$		24,1±1,7	0,16
3572	$^1D_2$		55,5±8,3	0,98
5005	$^1S_0$		(5,5)	
2476	$^3P_1$	$^3P_2$	10	0,32
2663	$^3P_2$		26,6±1,6	0,65
3739	$^1D_2$		16,4±1,8	1,08

Table 31. Absolute f-Values for the p^2-ps Transitions of Sn I [43]

λ (Å)	Transition p^2	Transition ps	Relative Intensity	f
2863	$^3P_0$	$^3P_1$	10	1,15
3009	$^3P_1$		7,6±0,5	0,33
3175	$^3P_2$		17,9±1,1	0,56
3801	$^1D_2$		3,93±0,5	0,21
5631	$^1S_0$		0,075±0,02	0,066
3034	$^3P_1$	$^3P_0$	12	0,315
2540	$^3P_0$	$^1P_1$	10	0,27
2661	$^3P_1$		6±0,3	0,062
2790	$^3P_2$			
3262	$^1D_2$		92,5±10	1,08
4524	$^1S_0$		4,7±1,2	0,71
2706	$^3P_1$	$^3P_2$	10	0,4
2839	$^3P_2$		22,8±1,4	0,63
3330	$^1D_2$		2,13±0,32	0,006

Table 32. Relative Oscillator Strengths of Ca I Lines [45]

λ	Transition	J	f**	f+ coul	f++ V	gf**
4226.728	$4^1S-4^1P^\circ$	0—1	1000	1000	1000	—
2398.555	$4^1S-5^1P^\circ$	0—1	25.1	15.0	24.5	—
2275.471	$4^1S-6^1P^\circ$	0—1	40.4	37.6	—	—
2200.728	$4^1S-7^1P^\circ$	0—1	—	10.8	—	—
6572.781	$4^1S-4^3P^\circ$	0—1	0.0279	-	—	—
2721.65	$4^1S-4p^2\,{}^1P$	0—1	—	—	—	—
2617.66	$4^1S-4p^2\,{}^1D$	0—1	—	.	—	—
2541.40	$4^1S-4p^2\,{}^1P$	0—1	—		-	—
4454.781	$4^3P^\circ-4^3D$	2—3	177	168	181	98.8
4434.960		1—2	181	-	--	60.6
4425.441		0—1	212		—	23.7
4455.887		2—2	31.6*		—	17.7
4435.688		1—1	56.7	-	—	19.0
4456.612		2—1	2.1*	.	—	1.2
3644.410	$4P^\circ-5^3D$	2—3	54.7	41.2	51.7	92.0
3630.748		1—2	58.0	-	—	58.6
3624.111		0—1	78.7	—	—	26.5
3644.765		2—2	9.94*	—	—	16.7
3630.974		1—1	19.4*	-	—	19.5
3644.940		2—1	0.65*	--	—	1.2
3361.918	$4^3P^\circ-6^3D$	2—3	28.7	—	—	91.5
3350.209		1—2	30.0	—	—	57.3
3344.513		0—1	45.3	—	—	28.9
3362.131		2—2	5.14*	—	—	16.4
3350.361		1—1	10.0*	—	—	19.1
3362.28		2—1	0.34*	—	—	1.2
6162.172	$4^3P^\circ-5^3S$	2—1	69.8	41.0	58.2	94.2
6122.219		1—1	79.9	—	—	64.7
6102.722		0—1	78.2	—	—	21.1
3973.707	$4^3P^\circ-6^3S$	2—1	14.1	4.8	7.5	[illegible]
3957.053		1—1	13.5	—	—	[illegible]
3948.901		0—1	10.8*	—	—	19.9
4302.527	$4^3P^\circ-4p^2\,{}^3P$	2—2	197	—	—	97.6
4298.986		1—1	72.8	—	—	21.6
4318.652		2—1	64.5	—	—	31.3
4307.741		1—0	98.7	—	—	27.8
4283.010		1—2	116	—	—	34.4
4289.364		0—1	269	—	—	26.6

* Oscillator strength of the doublet was not independently measured.

** Measured by Ostrovskiy and Penkin.

\+ Calculated in the Coulomb approximation.

++ Calculated by the semiempirical method of Vaynshteyn.

Table 33. Absolute Oscillator Strengths for Resonance Lines of Ca I, Sr I, and Ba I [46]

I	λ (Å)	f
Ca I	4226.73	1.49 - 0.04
Sr I	4607	1.54 - 0.05
Ba I	5535	1.40 - 0.05

Table 34. Absolute Oscillator Strengths for Resonance Lines of Ca II, Sr II, and Ba II [46]

I	λ (Å)	f
Ca II	3933.67	0.84
Ca II	3968.47	0.43
Sr II	4077.71	0.76
Sr II	4215.52	0.39
Ba II	4554.04	0.66
Ba II	4934.09	0.33

Table 35. Absolute and Relative f-Values of the Principal Series ($ns^2 {}^1S_0 - nsmp {}^1P^0_1$)

No. *	λ (Å)	m**	$f_{rel.}$	$f_{abs.}$	λ (Å)	m**	$f_{rel.}$	$f_{abs.}$
1	4607.33	5	1000	1.54	5535.48	6	1000	1.40
2	2931.83	6	3.40	0.0052	3071.58	7	109	0.153
3	2569.47	7	7.15	0.0110	2785.28	8	6.2	0.0087
4	2428.09	8	20.9	0.032	2646.50	9	2.22	0.0031
5	2354.32	9	22.3	0.034	2543.2	10	7.4	0.010
6	2307.32	10	13.1	0.020	2500.2	11	2.7	0.0038
7	2275.29	11	8.2	0.013	2473.20	12	0.98	0.0014
8	2253.32	12	4.7	0.0073	2452.38	13	0.11	0.00015
9	2237.65	13	2.8	0.0043	2438.81	14	0.21	0.00029
10	2226.38	14	1.90	0.0030	2427.43	15	1.30	0.0018
11	2217.8	15	1.34	0.0021	2420.11	16	0.42	0.00059
12	2211.3	16	1.16	0.0017	2414.10	17	0.19	0.00027
13	2206.2	17	0.81	0.0012	2409.25	18	0.10	0.00015

* Number of the series member.

** Principal quantum number of the upper level.

Table 36. Absolute and Relative f-Values of Ba I Spectral Lines for $6s^2$ – 5dmp Transitions [47]

λ (Å)	Series	m*	$f_{rel.}$	$f_{abs.}$
5535.48	$6s^2\,{}^1S_0 - 6smp\,{}^1P^0_1$	6	1000	1.4
3889.33	$6s^2\,{}^1S_0 - 5dmp\,{}^3P^0_1$	6	6.3	0.0088
2702.63		7	5.1	0.0071
2432.54		8	1.59	0.0022
4132.43	$6s^2\,{}^1S_0 - 5dmp\,{}^3D^0_1$	6	6.22	0.0087
2739.24		7	1.94	0.0027
2444.64		8	0.97	0.0014
3501.11	$6s^2\,{}^1S_0 - 5dmp\,{}^1P^0_1$	6	102	0.14
2596.64		7	22.2	0.031
2454.07	$6s^2\,{}^1S^0 - 5dmf\,{}^1P^0_1$ (?)	4	0.096	0.0001

*Principal quantum number of the upper level.

Table 37. Relative f-Values* of Mg I Lines for $^3P^o_{0,1,2}$ - ^3S, and $^3P^o_{0,1,2}$ - $^3D_{1,2,3}$ Transitions [47]

λ (Å)	Transition	J	$f_{rel.}$	$gf_{exp.}$	$gf^{**}_{theor.}$
5183.60	$3^3P^o-4^3S$	2—1	100	100	100
5172.68		1—1	100	60	60
5167.32		0—1	100	20	20
3838.29	$3^3P^o-3^3D$	2—3	460	100	100
		2—2			
		2—1			
3832.30		1—2	450	62.8	60
		1—1			
3829.35		0—1	410	19.1	20
3096.90	$3^3P^o-4^3D$	2—3	83	91.3	100
		2—2			
		2—1			
3092.99		1—2	87	57.4	60
		1—1			
3091.08		0—1	106	23.3	20
2736.56	$3^3P^o-6^3D$	2—3	22		
2779.83*	$3^3P^o-3p^23^3P$	2—2	280	100	100
2779.83*		1—1	94	20	20
2782.97		2—1	99	35.0	33.3
2781.42		1—0	126	26.7	26.7
2776.69		1—2	160	34.6	33.3
2778.28		0—1	350	24.5	26.7

*Calculated on the assumption that the intensity rule holds true for the multiplet.

**Calculated from data of Condon and Shortley on the assumption of LS coupling.

Table 38. Absolute f-Values of Sr I Lines for Transitions From $^3P_{0,1,2}$ Levels [47]

λ (Å)	Transition	J	$f_{abs.}$	$gf_{exp.}$	gf^*_{theor}
4607.33	5^1S-5^1P	0—1	1.54		
7070.10	$5^3P^0-6^3S$	2—1	0.17	95.7	100
6878.38		1—1	0.17	54.8	56.8
6791.05		0—1	0.18	19.9	18.4
4962.26	$5^3P^0-5^3D$	2—3	0.33	98.6	100
4872.49		1—2	0.31	55.4	51.7
4967.94		2—2	0.06	17.0	17.9
4811.88	$5^3P^0-5p^{23}P$	2—2	0.35	94.0	100
4784.32		1—1	0.14	22.0	19.8
4722.28		1—2	0.20	31.8	32.1
4741.92		0—1	0.47	25.1	25.9
4438.04	$5^3P^0-7^3S$	2—1	0.029	97.7	100
4361.71		1—1	0.025	50.5	58.0
4326.44		0—1	0.034	22.9	19.0
3351.25	$5^3P^0-4d^{23}P$	2—2	0.17	90.1	100
3222.23		1—1	0.06	20.2	18.5
3366.33		2—1	0.06	32.5	33.6
3329.99		1—0	0.08	27.7	26.2
3307.53		1—2	0.14	34.5	32.4
3301.73		0—1	0.23	24.5	25.9

* Calculated from data of Condon and Shortley on the assumption of LS coupling.

Table 39. Relative Oscillator Strengths [49]

λ, см⁻¹	lg gf/λ	g
Mg I		
1		
4571,1	−0,60:	5
2		
5183,6	5,32	5
5172,7	5,12	5
3		
3838,3	5,81	3
3832,3	5,53	5
3829,4	5,20	5
8		
5711,1	4,12	3
9		
5528,4	5,77	5
10		
4730,0	3,60:	5
11		
4703,0	5,82	7
15		
4167,3	5,60	9
16		
4057,5	5,99	8
17		
3986,8	5,43	7
Mg II		
4		
4481,3	8,51	9
9		
4334,0	6,94	6
4428,0	6,63	9
10		
4390,6	7,45	6
4384,7	6,97	4
19		
4436,5	7,85	4
Si I		
1		
3856,0	6,12	4
3862,6	5,80	5
2		
6347,1	5,86	5
6371,4	5,37	5
3		
4128,0	7,02	4
4130,9	7,12	4

λ, см⁻¹	lg gf/λ	g
Ca I		
2		
4226,7	2,44	12
3		
6162,2	2,82	5
6122,2	2,61	5
6102,7	2,03	2
4		
4454,8	2,93	3
4435,0	2,70	7
4425,4	2,39	12
4455,9	2,41	7
4435,7	2,49	10
5		
4302,5	2,84	9
4318,6	2,25	6
4283,0	2,48	12
18		
6439,1	3,10:	5
6462,6	3,20	2
6493,8	2,56	5
6471,8	1,59	3
6499,6	1,55	3
20		
6166,4	1,31	3
21		
5588,8	3,04	3
5594,5	2,71	3
5601,3	2,52	5
5582,0	2,16:	5
5990,1	1,80	3
22		
5262,2	2,98	2
5260,4	0,91	3
23		
4585,9	2,46	5
4578,6	2,20	7
25		
4094,9	2,69	3
32		
6717,7	2,43	3
37		
4355,1	2,39	6
39		
4108,6	1,64	3
46		
5867,6	2,10	3
48		
5513,0	2,22	3
51		
4686,3	2,25:	5

λ, см⁻¹	lg gf/λ	g
Sc II		
7		
4246,8	2,10	15
8		
3986,1	0,33	4
14		
4374,4	1,59	12
4400,3	1,39	11
4415,6	1,16	10
4420,7	−0,46	3
4431,4	0,06	5
4354,6	0,22	7
15		
4314,1	2,05	8
4320,7	2,13	7
4325,0	1,70	8
4294,8	0,97	6
19		
6604,6	0,67	3
23		
5031,0	1,33	3
26		
5239,8	1,10	3
28		
6320,8	−0,01	3
29		
5667,2	0,77	3
5669,0	0,83	3
31		
5526,8	1,49	5
Ti I		
3		
5426,6	−2,82	3
4		
5210,4	−0,86	3
5173,7	−1,29	3
5219,7	−2,10	3
5147,5	−1,91	3
5		
5064,6	−0,99	3
5040,0	−1,26	3
6		
4656,5	−1,30	3
4715,3	−2,51	3
4693,7	−2,40	3
7		
4562,6	−2,51	3
12		
3998,6	0,20	5

Table 39 (Cont.)

λ, cm⁻¹	lg gf/λ	g	λ, cm⁻¹	lg gf/λ	g	λ, cm⁻¹	lg gf/λ	g
38			107			233		
4981,7	0,67	3	5490,2	—0,70	3	4759,3	0,73	5
5016,1	—0,55	3	109			4758,1	0,71	5
5022,9	—0,43	3	5113,5	—0,54	3	4742,8	0,45	3
5024,8	—0,61	3	110			238		
42			5071,5	—0,52	3	6091,2	0,00	3
4533,2	0,65	5	113			240		
4534,8	0,17:	5	4457,4	0,62:	3	5644,1	0,39	3
4535,6	0,11	4	4453,3	0,04	1	249		
4555,5	—0,40	4	4482,7	—0,22	1	5675,4	0,75	3
4548,8	—0,38	3	4474,8	0,05	1	250		
4512,7	—0,44	4	126			4827,6	0,18	3
4518,0	—0,26	4	4820,4	—0,10	3	252		
43			129			4261,6	0,35	1
4326,4	—0,97	3	4186,1	—0,12	1	259		
44			145			5429,1	0,06	3
4301,1	—0,19	1	4617,3	0,41	5	287		
4298,7	—0,09	2	4623,1	0,28	3	5503,9	0,42	3
4295,8	—0,48	1	4639,4	0,04	4	288		
4287,4	—0,40	5	4639,9	—0,02	1	5120,4	0,86	3
4286,0	—0,25	2	4650,0	—0,32	4	309		
4289,1	—0,39:	3	4645,2	—0,31	4	5774,0	0,99	3
4290,9	0,13	2	146			5766,3	0,88	3
4272,4	—0,96	1	4479,7	0,02	2			
48			4465,8	0,47	2	Ti II		
6743,1	—1,47	3	154			11		
49			5969,8	—0,12	3	3987,6	—1,03	4
6599,1	—1,73	3	5978,5	—0,22	3	4025,1	0,17	4
53	46		157			4056,2	—0,94	2
4840,9	—0,48	3	4885,1	0,50	3	12		
56			4913,6	0,41	3	3813,4	0,25	5
3904,8	0,80	2	170			18		
69			4449,1	0,69	3	4469,2	0,09	1
6126,3	—1,11	3	4050,9	0,47	4	4493,5	—0,92	5
72			162			19		
5866,5	—0,71	3	4263,1	0,41	1	4395,0	1,42	16
77			173			4443,8	1,21	15
4675,1	—0,76	3	5001,0	0,31	3	4450,5	0,68	14
80			4973,1	0,50	3	20		
4060,3	—0,53	4	199			4294,1	0,82	1
102			5052,9	0,13	3	4287,9	0,51	7
6556,1	—0,91	3	218			30		
6554,2	—0,96	3	4404,3	0,14	1	4506,7	—1,40	2
104			228			4545,1	—0,36	6
6258,7	—0,27	3	5739,5	0,40	3	31		
6258,1	—0,17	3	5740,1	0,54	3	4468,5	1,25	13
6261,1	—0,34	3	231			450 3	1,23	16
6312,2	—1,27	3	4870,1	0,61	3	4444,6	0,17	3
			4868,3	0,48	3			

Table 39 (Cont.)

λ, cm⁻¹	lg gf/λ	g
34		
3900,5	1,75	7
3913,5	1,58	10
3932,0	0,99	4
38		
4636,3	—1,06	3
4665,7	—0,16	1
39		
4583,4	—0,49	2
40		
4441,7	0,00	7
4470,9	0,22	7
4495,5	0,19	1
4417,7	0,85	13
4464,5	0,67	1
41		
4300,1	1,55	12
4290,2	1,24	6
4301,9	1,14	13
4312,9	1,00	9
4315,0	1,19	1
4330,7	—0,52	6
49		
4708,7	—0,49	5
50		
4534,0	1,78	4
4563,8	1,32	15
4590,0	0,34	3
51		
4400,0	0,92	9
4394,1	0,51	14
4418,3	0,33	10
4407,7	—0,03	6
59		
719,5	0,50	1
)		
544,0	—0,51:	4
4580,5	0,21	1
4524,7	0,41	1
4568,3	—0,71:	4
31		
4395,8	0,15:	12
4409,5	0,19	7
4411,9	—0,21	9
4423,3	—0,37	1
69		
5336,8	0,11	3
5381,0	—0,06	5
5418,8	—0,21	5

λ, cm⁻¹	lg gf/λ	g
70		
5154,1	0,25	3
82		
4572,0	1,79	14
4529,5	0,61	14
86		
5129,1	1,10	2
5185,9	0,57	5
87		
4028,3	1,38	16
4053,8	1,51	1
91		
6491,6	0,13	3
6559,6	—0,22	3
6607,1	—0,68	3
92		
4805,1	1,40	7
4780,0	0,59	7
93		
4374,8	1,48	1
4422,0	0,64	16
94		
4316,8	0,52	13
4337,3	1,29	4
4330,3	0,60	3
103		
5211,5	0,66	2
104		
4367,7	1,49	4
4386,9	1,44	10
105		
4163,6	2,06	7
4171,9	2,00	6
4174,1	1,35	1
106		
4064,2	0,90	1
113		
5010,2	1,12	3
114		
4911,2	1,43	3
4874,0	1,68	3
115		
4488,3	1,99	14
4411,1	1,80	7
4456,6	1,51	1
VI		
8		
3862,2	—2,69	3
19		
6243,1	—1,71	3

λ, cm⁻¹	lg gf/λ	g
6199,2	—2,41	3
6216,4	—1,74	3
20		
6150,1	—2,28	3
22		
4379,2	0,13	5
4390,0	—0,05	5
4406,6	—0,35	5
27		
4111,8	0,05	7
4128,1	—0,28	3
4099,8	—0,55	3
28		
3803,5	—1,10	3
3822,9	—0,26	3
34		
6090,2	—0,83	3
6039,7	—1,43	3
6081,4	—1,35	3
6111,6	—1,44	3
35		
5703,6	—0,93	3
5737,0	—1,37	3
87		
4452,0	—0,02	3
4469,7	—0,13	3
VII		
9		
4036,8	1,40	12
4002,9	1,73	7
10		
3951,9	2,21	5
3916,4	2,28	5
3929,7	1,63	3
24		
4234,2	0,86	3
25		
4178,4	1,22	2
32		
4005,7	2,79	7
4023,4	2,45	10
4035,6	2,40	6
4039,6	1,22	2
37		
4183,4	2,17	15
4225,2	2,77	4
56		
4564,6	2,47	2

Table 39 (Cont.)

λ, cm⁻¹	lg gf/λ	g
199		
4453,3	3,06	6
215		
4065,1	3,22	2
225		
4232,1	3,44	2
Cr I		
1		
4254,4	1,21	10
4274,8	0,96	12
4289,7	0,77:	5
7		
5208,4	1,84	2
5206,0	1,83:	5
9		
4942,5	0,15	2
10		
4546,0	0,20	8
18		
5409,8	0,93:	5
5296,7	0,34	3
5348,3	0,34	3
5300,8	—0,46	3
5247,6	—0,14	3
21		
4646,2	0,65	10
4652,2	0,58	8
4651,3	0,11	8
4600,8	0,53	1
4616,1	0,30	8
4626,2	0,19	7
4591,4	0,12	4
22		
4351,0	0,56	2
33		
4530,8	1,53	1
4540,5	1,66	2
4544,7	1,28	1
4541,1	0,74	3
35		
4126,5	1,16	5
4153,1	0,19	3
38		
3963,7	2,78	3
3991,1	1,91	3
62		
4397,1	1,19:	4
69		
3857,6	3,40	3
94		
5297,4	2,08	3
96		
4299,7	1,77	1
4319,6	0,91	3
119		
5712,8	0,90	3
5787,0	0,45	3
150		
4540,7	2,06	2
4511,9	2,14	4
169		
4729,7	1,80	1
186		
4718,4	2,19	6
4708,0	2,02:	4
4689,4	1,53	3
4628,5	0,70	3
205		
5257,1	3,15	2
225		
5304,2	1,40	3
5312,9	1,50	3
249		
4197,2	2,29	1
4198,5	2,71	1
268		
4001,4	2,35	1
282		
6661,1	1,95	3
Cr II		
16		
4456,8	1,90:	4
18		
4172,6	1,72	1
4217,0	1,53	1
19		
4054,1	2,19	1
4030,7	1,47	1
4051,9	2,04	7
4053,4	1,62	1
4075,9	1,81	1
23		
5246,7	2,03	3
5510,9	2,07	2
25		
4621,4	2,13	1
26		
4179,4	2,81	1
4072,6	2,59	1
4207,4	2,27	10
4132,4	2,35	1
30		
4848,2	2,92	2
4876,4	2,83	2
4884,6	2,25	3
4812,4	2,24	7
31		
4242,4	3,11	8
4261,9	3,02	16
4275,6	2,74	11
4284,2	2,62	9
4252,6	2,53	13
4269,3	2,63	4
37		
4318,8	1,51	1
39		
4539,6	2,32	1
4565,8	2,64	4
43		
5237,3	3,10	5
5334,9	2,75	5
5308,4	2,28	3
5310,7	1,90	3
5313,6	2,31	3
44		
4558,7	3,79	14
4588,2	3,50	16
4618,8	3,27	7
4634,1	3,14	14
4555,0	2,96	16
4592,1	2,96	16
4616,6	2,85	16
4589,9	2,69	1
50		
5503,2	3,26	3
5508,6	3,63	3
127		
4204,7	1,49	1
128		
3936,9	2,77	1
129		
3911,4	3,31	1
3930,9	2,47	1
130		
3866,5	2,86	1
3866,0	2,84	1

Table 39 (Cont.)

λ, cm⁻¹	lg gf/λ	g
142		
3945,1	3,16	1
161		
4195,4	3,47	1
162		
4145,7	3,53	5
4224,8	3,23	1
4209,0	3,18	1
163		
4135,7	2,47	1
4185,5	2,61	1
4151,0	3,37	1
165		
4082,3	3,09	1
166		
4018,0	2,83	1
167		
3865,6	4,13	1
177		
4697,6	3,23	1
178		
4715,1	3,71	1
4671,3	3,01	1
179		
4362,9	3,38	1
180		
4209,8	3,03	1
4222,0	3,01	1
181		
4127,1	3,60	1
4170,9	3,75	1
182		
4048,0	3,30	1
4056,1	3,35	1
183		
4012,5	3,88	1
4022,4	3,73	1
191		
4465,8	3,79	1
192		
4256,1	4,15	1
4268,9	3,73	1
193		
4049,1	4,41	1
4070,9	4,13	1
194		
4038,0	4,71	1
4003,3	4,13	1

λ, cm⁻¹	lg gf/λ	g
Mn I		
2		
4030,8	1,67	5
4033,1	1,40	9
4034,5	0,97	12
4		
5470,6	0,59	3
5516,8	0,53	3
5		
4041,4	2,68	9
4055,5	2,44	12
4082,9	2,89	2
16		
4823,5	2,82	4
4783,4	2,71	5
4754,0	2,48	7
21		
4762,4	2,88	5
4766,4	2,56	3
4765,9	2,14	3
4761,5	2,07	3
4709,7	1,86	3
4739,1	1,86:	4
22		
4470,1	1,72	3
4472,8	2,40	1
4436,4	2,00	3
4453,0	1,68	3
4502,2	1,82	6
4498,9	1,70	3
23		
4235,3	2,33	1
4239,7	2,02	1
4265,9	1,88	4
27		
6021,8	2,35	3
6016,6	2,30	3
6013,5	2,01	3
29		
4061,7	2,13	3
4059,4	1,86	5
42		
5377,6	2,32	3
Mn II		
5		
4755,7	6,12	2
4730,4	5,21	1
4727,9	5,30	1

λ, cm⁻¹	lg gf/λ	g
6		
4292,2	5,41	3
4283,8	5,06	3
7		
4206,4	5,66	6
4259,2	5,64	1
4253,0	5,34	1
4244,3	5,14	3
17		
4510,2	10,49	2
Fe I		
1		
5166,3	—0,38	3
5110,4	—0,04	3
2		
4375,9	0,59	10
4427,3	0,88	7
4482,2	1,56	4
4489,7	—0,39	7
4347,2	—1,73	3
4389,2	—1,11	5
3		
4216,2	0,30	9
4206,7	—0,13	7
4200,0	—0,54	2
4291,5	—0,46	5
4		
3859,9	2,36	7
3886,3	1,60	4
3899,7	1,68	7
3906,5	1,50:	5
3824,4	2,00:	5
3856,4	2,04	8
3895,7	1,46	3
3922,9	1,94	10
3930,3	2,15	13
3927,9	2,04	10
3920,3	1,89	11
15		
5269,5	2,40:	5
5371,5	1,91	3
5405,8	1,82	5
5434,5	1,41	5
5307,1	1,69	5
5429,7	1,91	5
5446,9	1,88	5
5506,8	0,90	5
5497,5	1,09:	5

Table 39 (Cont.)

λ, cm⁻¹	lg gf/λ	g
16		
5083,3	0,53	3
5123,7	0,58	2
4939,7	0,43	3
4994,1	0,50	3
5127,4	0,36	3
5150,8	0,60	3
5151,9	0,61	3
18		
4100,7	0,96	3
4152,2	1,20:	4
4139,9	0,29	5
19		
4174,9	1,08	12
20		
3820,4	3,36	5
3825,9	3,12	5
3834,2	3,17	3
3840,4	2,76	5
3850,0	2,77	3
3887,0	2,05	7
3878,0	2,76	7
3872,5	2,88	7
3885,5	2,50	3
3940,9	2,26	1
3917,2	2,08	4
22		
3813,0	2,38	3
3850,8	2,47	7
3876,0	1,23	2
36		
5171,6	1,86	3
5216,3	1,53	5
5332,9	0,85	3
5307,4	1,20	5
38		
4733,6	0,96	2
39		
4602,9	1,50	7
4531,1	1,09	4
4592,7	1,54	2
4632,9	1,21	2
4602,0	0,67	5
41		
4383,6	3,51	16
4404,5	3,37	16
4415,1	3,17	12
4337,0	1,70	12
4291,5	1,57	2
42		
4271,8	3,26	16
4325,8	3,49	12
4202,0	3,11	8
4250,8	2,96	15
4147,7	1,81	10
43		
4045,8	3,80	14
4063,7	3,55	16
4071,7	3,42	16
4005,2	3,24	10
4143,9	3,16	12
4132,1	3,25	12
44		
4132,9	1,86	4
45		
3815,8	3,69	5
3827,8	3,34	5
3841,0	3,32	5
62		
6430,8	1,58	3
6335,3	1,35	3
6297,8	0,85	3
6265,1	0,90	3
6219,3	1,09	3
6213,4	0,87	3
6151,6	0,54	3
6173,3	0,76	3
66		
5145,1	0,62	3
5250,6	1,83	3
5196,7	1,75	3
68		
4528,6	3,39	10
4494,6	2,97	16
4459,1	2,53	1
4442,3	2,75	13
4447,7	2,74	12
4430,6	2,44	9
71		
4282,4	3,16	13
4315,1	3,09	1
4352,7	2,50	9
72		
4001,7	2,32	6
3977,7	2,83	1
3949,9	2,62	8
4009,7	2,76	8
73		
3852,6	2,89	7
3807,5	3,11:	5
111		
6421,4	1,61	5
6750,2	1,07	3
6254,3	1,61	3
114		
5049,8	2,54	3
4924,8	1,96	3
5141,8	1,85	3
115		
4630,1	2,06:	5
4574,7	3,21	1
116		
4439,9	1,88	3
117		
4047,3	0,69	2
120		
4058,8	3,02	1
124		
3885,5	2,51	2
3845,2	2,75	3
152		
4280,5	3,87	16
4235,9	3,73	16
4222,2	3,10	16
4210,3	3,14	10
4187,8	3,75	13
4187,0	3,49	13
4191,4	3,50	6
4299,2	3,46	7
4271,2	3,55	15
4250,1	3,55	17
4233,6	3,36	12
153		
3980,6	0,76	3
168		
6495,0	2,59	2
6393,6	2,19	2
6318,0	2,49	2
169		
6252,6	2,00	5
6191,6	2,33	2
6136,6	2,41	3
6344,2	0,96	3
170		
5916,2	0,93	3
175		
3859,2	3,39	3
3973,8	3,39	2

Table 39 (Cont.)

λ, cm⁻¹	lg gf/λ	g
176		
3813,1	4,32	2
206		
6647,0	0,04	3
6609,1	1,18	3
6575,0	1,10	3
6475,6	1,02	3
207		
6230,7	2,43	5
6137,7	2,64	5
6065,5	2,42	5
6005,5	0,53	3
6322,7	1,32	3
6200,3	1,19	3
209		
5701,6	1,65	5
5567,4	1,22	5
5778,5	0,51	5
5833,9	0,39	5
217		
4095,0	2,57	2
218		
4049,3	1,78	5
222		
3808,8	3,02	5
3821,8	3,54	2
268		
6678,0	2,28	3
6592,9	2,32	3
6546,2	1,33	3
6703,6	0,99	3
273		
4267,0	2,35	4
276		
3998,0	3,31	2
277		
4007,3	2,69	2
278		
3997,4	3,49	1
4021,9	3,32	4
3937,3	2,74	5
280		
3932,6	3,42	1
3863,7	3,54	3
3907,9	3,02	4
282		
3884,4	2,52	4
283		
3861,3	2,84	4

λ, cm⁻¹	lg gf/λ	g
284		
3910,8	3,20	1
287		
3811,9	3,37	2
318		
4920,5	4,40	5
4891,5	4,05	5
4871,3	3,90	3
4859,8	3,42	3
4919,0	3,90	5
4890,8	3,61	5
4872,1	3,68	3
5044,2	1,58	3
4938,8	2,89	3
4903,3	3,22	3
342		
6518,4	1,33	3
6355,0	1,52	3
6270,2	1,33	3
6311,5	0,90	3
6229,2	1,04	3
350		
4466,6	3,50	13
4476,0	3,52	10
4443,2	3,40	8
4454,4	2,86	2
351		
4258,6	1,64	2
4241,1	1,41	3
352		
4207,1	2,80:	3
4245,3	3,03	10
354		
4181,8	4,13	4
4175,6	3,30	13
4143,8	3,55	1
4156,8	3,35	4
4107,5	3,07	7
4126,9	1,27	3
355		
4184,9	3,16	6
4154,5	3,50	6
4213,6	2,71	6
4204,0	3,27	5
4191,7	2,79	3
357		
4134,7	3,45	8
4132,9	3,24	8
4114,4	2,65	9
4091,6	1,80	5

λ, cm⁻¹	lg gf/λ	g
358		
4085,0	3,07	2
359		
4044,6	3,05	16
4062,4	3,20	11
4079,8	2,61	9
361		
3964,5	3,15	3
364		
3942,4	3,15	4
3926,0	3,26	4
367		
3809,0	2,55	3
383		
5232,9	3,62:	5
5266,6	3,89:	5
5281,8	3,27	5
5192,4	3,81	5
5191,5	3,78:	5
409		
4647,4	2,94	10
4691,4	2,70	3
4710,3	2,80:	5
4662,0	1,55	3
410		
4556,1	3,41	1
414		
4309,4	3,04	1
4367,6	3,71	4
415		
4365,9	1,68	3
419		
4219,4	3,61	4
422		
4141,9	2,37:	5
423		
4120,2	2,60	4
429		
3897,4	2,94	5
3871,8	3,59	4
3903,9	3,61:	4
472		
4517,5	2,29	4
476		
4387,9	2,69	9
476a		
4182,4	2,66	4
482		
4210,4	3,61:	4

Table 39 (Cont.)

λ, cm⁻¹	lg gf/λ	g	λ, cm⁻¹	lg gf/λ	g	λ, cm⁻¹	lg gf/λ	g
4220,4	3,00:	3	4073,8	3,42	4	4946,4	3,09	5
4248,2	2,88	6	4080,2	2,83	4	4882,2	2,41	3
4267,8	2,89	6	4109,1	2,64	6	4863,6	2,36	3
488			559			4875,9	2,09	3
3867,2	3,57	8	4068,0	3,78	13	5002,8	2,56	3
3956,0	2,75	2	4085,3	3,77	3	4950,1	2,60	3
515			560			4907,7	2,24	3
4480,1	2,72	2	4030,5	4,20	1	689		
518			4016,4	3,81	3	4224,2	3,76	7
4369,8	3,15	4	3986,3	3,15	7	4200,9	3,28	6
520			561			4238,0	3,27	9
4298.0	3,31	1	3947,0	3,26	7	4208,6	3,45	4
522			562			4176,6	3,60	5
4199,1	3,99	12	3941,3	3,51	4	4227,4	4,78	4
523			3955,4	3,26	4	690		
4143,4	3,89	12	597			4228,7	1,76	2
524			4285,4	3,30	3	692		
4074,8	3,32	1	599			4264,2	2,52	2
527			4167,9	2,95	4	693		
4017,2	3,17	6	603			4227,4	4,78	5
529			4006,3	3,11	5	4247,5	4,01	13
3839,3	2,65	2	606			4238,8	3,99	8
553			3916,7	3,59	8	4225,5	3,55	3
5324,2	4,24:	5	608			4217,6	3,56	1
5263,3	3,33	3	3821,2	4,36	5	4198,3	5,06	4
5253,5	2,42	3	3805,3	4,40	5	4196,2	3,60	5
5217,4	3,18	5	652			694		
5215,2	3,36	5	3948,0	3,64	5	4154,8	4,02	2
5229,9	3,44	5	655			4136,5	2,71	5
5393,2	3,30:	5	3986,2	3,24	4	4087,1	2,97	7
5339,9	3,55	5	4040,6	3,73	6	4140,4	2,61	2
5302,3	3,74	3	3976,6	3,67	4	695		
554			661			4126,2	3,03	6
4736,8	3,66	8	3923,0	3,88	1	4115,0	1,66	2
4707,3	3,46	4	3951,2	3,49	3	4150,3	3,35:	5
4668,1	3,23	5	665			4112,4	3,87	3
4637,5	2,91	10	3810,8	3,82	5	4157,8	3,80	12
4613,2	3,19	1	666			4158,8	3,46	5
4625,0	3,00	9	3802,3	3,32	3	698		
4607,7	2,77	3	686			4084,5	3,58	9
555			5615,6	4,39:	5	4065,4	2,81	9
4531,6	2,19	2	5586,8	4,18	5	4133,9	3,39	9
4504,8	1,90	5	5572,8	4,06:	5	4082,1	2,98	5
556			5569,6	3,69:	5	4072,5	3,10	5
4022,7	2,37	2	5576,1	3,36	5	702		
558			5624,6	3,51	3	3804,0	3,68	3
4076,6	3,87	2	5784,7	1,49	3	726		
4056,2	3,80	1	687			4137,0	3,65	6
4070,8	3,47	9	4966,1	3,24	5			

Table 39 (Cont.)

λ, cm⁻¹	lg gf/λ	g	λ, cm⁻¹	lg gf/λ	g	λ, cm⁻¹	lg gf/λ	g
752			830			1066		
4705,5	2,19	2	4388,4	3,60	7	4989,0	3,56	2
753			4485,7	3,23	7	1067		
4789,6	3,26	2	4433,2	3,59	7	5638,3	3,25	3
755			4469,4	3,64	1	5775,1	2,92	3
4547,8	3,51	1	883			5731,8	3,00	3
764			5027,2	3,36	2	5873,2	2,26	3
4240,4	2,74	2	889			5759,6	2,06	3
767			4709,0	3,82	2	1089		
4059,7	3,11	2	896			5162,3	4,73	2
795			4536,5	2,85	2	1092		
4587,1	2,75	2	906			5133,7	4,57	2
797			4246,1	3,55	7	5097,0	4,24	2
4432,6	2,63	2	913			1094		
800			3960,3	3,29	3	5074,8	4,39	2
4219,4	4,54	2	959			1095		
802			6003,0	2,90	3	5121,6	3,62	2
4014,5	3,62	1	5976,8	2,74	3	1103		
816			6188,0	2,66:	5	4113,0	3,84	4
6400,0	3,73	5	6096,7	2,42	1	1107		
6411,7	3,75	5	965			5763,0	3,67	3
6408,0	2,94	5	5001,9	4,35	5	5753,1	3,37	3
6246,3	3,49	2	5015,0	3,82	5	5717,8	3,12	3
6336,8	3,12	5	5022,2	3,87	3	5618,6	2,82	3
6232,7	2,84:	5	973			5655,5	3,19	3
820			4494,0	2,79	2	1110		
4596,1	5,15	3	4392,6	2,33:	5	5027,8	3,51	2
4673,2	3,32	5	974			1145		
4643,5	3,10	6	4490,8	3,40	7	5404,5	5,06	2
821			976			5400,5	4,91	2
4745,8	3,43:	4	4276,7	2,91	5	5389,5	4,17	2
4619,3	3,62:	4	4300,8	3,29	6	1146		
4705,0	2,85	2	982			5383,4	5,04	2
822			5934,7	2,83	3	5369,9	4,91	2
4638,0	3,34	6	5809,2	2,46	3	5367,5	4,71	2
823			984			5364,9	4,71	2
4560,1	3,10	2	4973,1	3,00	5	1147		
825			4896,4	2,28	3	5409,1	3,81	2
4433,8	3,38	4	993			1163		
4496,0	2,55	2	4265,3	3,09	2	5445,0	4,58	5
826			4264,7	2,67	2	5562,7	3,20	2
4525,1	3,87	1	4200,1	2,95	4	1165		
4611,3	4,05	5	1025			5410,9	4,76	2
828			5487,8	3,94	2	1175		
4484,2	3,42	6	1026			5983,7	4,92	2
4479,6	3,33	4	5424,2	4,89	2	5927,8	3,77	2
4427,3	3,84	5	1042			1178		
4446,8	3,03	2	4735,8	3,40	4	6024,1	4,57	2
4436,4	2,79	2	1062			6020,2	4,31	2
			5543,9	3,06	3			

Table 39 (Cont.)

λ, cm^{-1}	lg gf/λ	g	λ, cm^{-1}	lg gf/λ	g	λ, cm^{-1}	lg gf/λ	g
1179			28			44		
5816,4	3,77	2	4178,9	2,26	14	4663,7	1,27	1
1180			4296,6	2,11	14	46		
5862,4	4,20	3	4369,4	1,20	10	5991,4	1,23	2
5914,2	4,25	2	4122,6	1,56	7	6084,1	0,94	2
5930,2	4,16	5	4258,2	1,70	7	48		
5752,0	3,66	3	29			5362,9	2,62	2
5806,7	3,75	5	4002,1	1,31	4	5264,8	1,88	2
1183			32			5414,1	2,01	2
5554,9	4,04	5	4314,3	1,00	6	49		
5565,7	4,14	5	4278,1	0,97	1	5276,0	2,80	3
5679,0	3,60	3	4413,6	0,67	4	5234,6	2,60	5
1195			36			5197,6	2,51	5
6713,1	2,81	3	4993,4	0,47	2	5425,3	1,62	5
6752,7	3,06	3	4893,8	0,38	2	5325,6	1,76	5
6639,7	2,66	3	37			55		
6733,2	2,88	3	4629,3	2,33	6	5534,9	2,08	2
1259			4555,9	2,42	8	74		
6056,0	3,92	5	4515,3	2,24	13	6456,4	3,10	5
6078,5	3,96	5	4491,4	1,99	13	6247,6	2,91	2
6102,2	4,16	2	4520,2	2,17	14	6147,7	2,50	3
1260			4489,2	1,93	14	6416,9	2,30	5
5984,8	3,99	5	4472,9	1,48	13	6238,4	2,31	5
5987,1	3,86	3	4666,7	1,72	9	6149,2	2,20	5
6170,5	3,68	3	4582,8	1,80	8	6407,3	2,08	3
			38			6239,9	1,71	3
Fe II			4583,9	2,79	14	126		
3			4549,5	2,59	1	4032,9	2,80	1
3938,3	1,20	7	4522,6	2,68	13	127		
3914,5	0,85	1	4508,3	2,30	13	4024,5	2,94	7
17			4620,5	1,59	14	3863,9	2,80	1
4664,8	0,11	1	4576,3	1,83	14	140		
22			4541,5	1,93	11	4455,8	2,57	1
4124,8	0,79	3	4648,2	0,87	1	151		
4168,7	0,65	1	4595,7	0,87	1	4031,5	2,58	1
4035,5	0,70	1	39			152		
25			4138,4	1,40	1	3863,4	2,62	1
4670,2	1,42	1	40			3863,9	2,94	1
26			6516,0	1,35	2	153		
4580,1	1,07	1	6432,7	1,22	2	3814,1	3,72	2
27			42			170		
4233,2	2,95	7	5169,0	3,45	2	4626,8	2,19	1
4351,8	2,64	3	5018,4	3,33	5	171		
4416,8	2,16	14	4923,9	3,15	5	4526,6	2,89	1
4173,5	2,36	7	43			4474,2	2,57	1
4303,2	2,28	14	4731,4	1,84	1	172		
4385,4	2,30	14	4656,9	1,84	1	4048,8	3,20	1
4128,7	1,22	11	4601,3	1,19	1	4044,0	3,00	7
4273,3	1,69	7				173		
						3935,9	3,78	7

Table 39 (Cont.)

λ, cm⁻¹	lg gf/λ	g
186		
4635,3	3,78	9
4625,9	3,20	1
187		
4446,2	2,70	4
188		
4069,8	3,80	1
189		
4061,8	3,80	1
4007,7	2,84	1
190		
4002,5	3,00	1
3938,9	2,64	7
212		
3960,9	4,18	3
4057,4	4,46	7
213		
4354,3	4,45	3
216		
4366,1	4,03	1
219		
4631,9	4,38	1
220		
4319,7	4,30	4
4318,2	3,98	1
222		
4493,6	4,71	1
4449,7	4,40	4
4431,6	4,32	1
Ni I		
15		
3913,0	—1,19	3
31		
3837,7	1,84	3
32		
3858,3	1,58	7
33		
3807,1	1,29	5
47		
5578,7	0,13	3
51		
4520,0	—0,07	3
64		
6532,9	—0,36	3
68		
5892,9	0,70	3
69		
5592,3	0,97	2

λ, cm⁻¹	lg gf/λ	g
70		
5435,9	0,45	3
88		
4410,5	2,30	5
98		
4714,4	3,54	7
4648,7	2,80	7
4605,0	2,65	9
4756,5	2,68	5
4715,8	2,72	5
4686,2	2,48	5
4874,8	1,74	3
4814,6	1,74	3
100		
4606,2	2,34	4
111		
5017,6	3,08	5
4998,2	2,35	3
4953,2	2,51	3
4866,3	2,73	3
4873,4	2,55	3
4857,4	2,48	3
112		
4980,2	2,49	2
129		
4904,4	2,94	2
130		
5082,6	2,46	3
131		
4829,0	2,54	2
133		
4703,8	2,65	4
143		
5080,5	3,48	2
144		
5011,0	2,09	3
145		
5036,0	3,22	2
5000,3	2,66	3
161		
5099,9	2,74	3
162		
5084,1	3,21	2
5146,5	3,20	3
163		
4807,0	2,66	3
168		
4437,6	1,96	5

λ, cm⁻¹	lg gf/λ	g
177		
5115,4	2,92	5
4935,8	2,84	3
5130,4	2,08	3
194		
5081,1	3,39	2
209		
5176,7	2,63	3
210		
5155,8	2,97	5
221		
5625,3	2,52	3
228		
6176,8	2,72	3
6224,0	2,34	3
229		
6133,9	1,51	3
6186,7	2,32	3
6360,8	2,14	3
230		
6111,1	2,47	3
6366,5	2,36	3
231		
5760,8	2,46	3
235		
4735,5	2,80	3
248		
6130,1	2,37	3
249		
6598,6	2,43	3
6086,3	2,77	3
6322,2	2,17	3
5996,7	2,30	3
250		
5669,9	2,33	3
5614,8	2,69	3
264		
6635,1	2,58	3
Ni II		
9		
4362,1	2,52	5
4244,8	2,30	6
10		
4192,1	2,26	8
12		
4015,5	2,66	7
Y II		
1		
4204,7	0,07	2

Table 39 (Cont.)

λ, cm⁻¹	lg gf/λ	g
5		
4309,6	1,58	4
4398,0	0,96	6
6		
3982,6	1,43	4
3950,5	1,41	7
7		
3818,3	1,01	3
12		
4682,3	0,38	2
13		
4374,9	2,28	8
14		
4177,5	2,92	6
20		
5087,4	1,81	5
5200,4	1,56	5
22		
4883,7	2,01	5
4900,1	2,78	2
27		
5521,6	1,33	3
5546,0	1,47	3
5544,6	1,16	3
Zr II		
15		
4211,9	1,03	3
16		
3999,0	1,23	1
17		
3915,9	0,80	1
29		
4156,2	1,50	1
40		
4277,4	1,26	1
4317,3	1,43	3
4497,0	0,87	1
41		
4149,2	2,01	5
4209,0	0,95	3
42		
4161,2	2,05	2
4151,0	1,68	6
43		
4050,3	1,14	4
3934,8	1,10	1
54		
4018,4	1,28	1

λ, cm⁻¹	lg gf/λ	g
67		
4613,9	0,84	6
79		
4440,5	2,08	5
88		
4379,8	1,71	1
95		
5112,3	0,96	3
97		
4210,6	2,17	1
99		
4171,8	2,45	2
130		
4553,9	1,93	1
139		
4574,5	2,05	1
140		
4388,5	2,06	1
Ba II		
1		
4554,0	2,16	5
4934,1	2,28	5
2		
6141,7	1,73:	5
6496,9	1,76:	5
5853,7	1,31	3
4		
4166,0	2,46	1
La II		
4		
5805,8	−2,53	3
8		
4662,5	−2,80	6
10		
4432,9	−1,70:	4
22		
4728,4	−2,14	1
23		
4574,9	−2,83	1
4691,2	−2,70	1
24		
4333,8	−1,60	9
25		
4322,5	−2,46:	5
27		
3929,2	−1,62	1
3995,7	−2,38	1

λ, cm⁻¹	lg gf/λ	g
36		
5114,6	−2,17	3
37		
4804,0	−2,44	3
38		
4429,9	−2,51	1
39		
4609,6	−1,49	1
40		
3988,5	−1,28	7
4152,0	−2,29	1
41		
4123,2	−1,66	3
4238,4	−1,63	6
53		
4559,3	−2,42	1
Ce		
4748,7	−2,01	5
75		
4286,9	−0,32	4
76		
4619,9	−1,28	2
81		
4540,7	−1,44	1
84		
4263,6	−0,01	2
92		
4688,6	−1,11	1
141		
3964,5	−1,72:	2
149		
4539,9	−0,25	1

Table 40. Factors for Conversion of Relative Oscillator Strengths (in Table 39) to Absolute Values [49]

Element	Exp.* (log λ)	Stellar** (log λ)	Theor.+
Mg I	−1,32		
Mg II			−3,88
Si II			−3,09
Ca I	+1,30		+1,01
Sc II			+1,78
Ti I	+3,82		+3,35
Ti II		+1,96±0,10	+1,85
V I			+3,95
V II		+0,75±0,14	
Cr I	+2,54		+2,68
Cr II		+0,44±0,09	
Mn I	+1,64		+1,60
Mn II		−2,44±0,24	
Fe I	+0,43		
Fe II		−0,37±0,16	+0,32
Ni I	+0,56		+1,66
Ni II		−0,66±0,34	
Ba II			+1,54

* λ is calculated from the experimentally determined absolute f-values.

** λ is calculated from the known absolute f-values for atoms using stellar spectra containing lines of both neutral and ionized atoms.

\+ λ is calculated from theoretically determined absolute f-values.

Table 41. Line Strengths for the p^2-ps Transitions of C I, Si I, Ge I, Sn I, and Pb I [50]

Transition	LS	C I	Si I	Ge I	Sn I	Pb I	J
$ps\,^3P_0 - p^2\,^3P_1$	20	20	20	20	20	20	20
$^1P_1 - {}^1S_0$	20	19.999	19.82	18.32	17.83	19.47	20
$^1P_1 - {}^3P_0$	0	0.001	0.18	1.68	2.17	0.52	0
$^1P_1 - {}^3P_1$	0	0.045	0.165	1.975	3.675	4.21	5
$^1P_1 - {}^3P_2$	0	0.175	0.122	0.61	0.044	12.48	25
$^1P_1 - {}^1D_2$	100	99.99	99.04	89.51	81.58	67.28	50
$^3P_1 - {}^1S_0$	0	0.001	0.18	1.68	2.17	0.52	0
$^3P_1 - {}^3P_0$	20	19.999	19.82	18.32	17.83	19.47	20
$^3P_1 - {}^3P_1$	15	14.955	14.82	13.023	11.325	11.79	10
$^3P_1 - {}^3P_2$	25	25.01	25.075	25.30	31.52	44.30	50
$^3P_1 - {}^1D_2$	0	0.004	0.925	9.56	11.84	1.77	0
$^3P_2 - {}^3P_1$	25	25	25	25	25	25	25
$^3P_2 - {}^3P_2$	75	74.98	74.975	74.1	68.43	44	25
$^3P_2 - {}^1D_2$	0	0.002	0.025	0.9	6.57	31	56

Table 42. Oscillator Strengths and Transition Probabilities Between Energy Levels of $1s^2 2s^2 nl$ Configurations of N III [51]

№	Transition	$\frac{\nu_{nn'}}{R_y}$	$\varphi^2_{nn'}$	$f_{nn'}$	$S_{LL'}$	S	$\omega_{n'}$	$A_{n'n} \cdot 10^{-8}$
1	$2p^2P - 3s^2S$	2,02	0,18	0,04	6	0,36	2	39
2	$2p^2P - 3d^2D$	2,44	0,96	0,25	60	1,84	10	70
3	$3s^2S - 3p^2P$	0,22	12,90	0,95	6	25,8	6	1,2
4	$3p^2P - 3d^2D$	0,20	12,60	0,56	60	50,4	10	1,1
5	$3p^2P - 4s^2S$	0,51	2,18	0,13	6	4,36	2	7,7
6	$2p^2P - 4s^2S$	2,75	0,004	0,001	6	0,008	2	2,2
7	$4s^2S - 4p^2P$	0,09	51,12	1,53	6	102,24	6	0,32
8	$3s^2S - 4p^2P$	0,82	0,23	0,070	6	0,48	6	1,2
9	$3d^2D - 4p^2P$	0,40	0,80	0,044	60	3,20	6	0,88
10	$4p^2P - 4d^2D$	0,06	48,73	0,65	60	194,9	10	0,11
11	$3p^2P - 4d^2D$	0,66	2,82	0,41	60	11,28	10	8,8
12	$2p^2P - 4d^2D$	2,90	0,15	0,10	60	0,60	10	39
13	$4d^2D - 4f^2F$	0,023	29,33	0,12	210	176,0	14	$2,7 \cdot 10^{-3}$
14	$3d^2D - 4f^2F$	0,48	11,61	1,16	210	69,7	14	15
15	$2p^2P - 5s^2S$	3,04	$3 \cdot 10^{-5}$	$1 \cdot 10^{-5}$	6	$6 \cdot 10^{-5}$	2	0,23
16	$3p^2P - 5s^2S$	0,80	0,10	0,009	6	0,20	2	1,4
17	$4p^2P - 5s^2S$	0,20	0,10	0,003	6	0,20	2	$2,1 \cdot 10^{-2}$
18	$3s^2S - 5p^2P$	1,04	0,23	0,080	6	1,39	2	21
19	$4s^2S - 5p^2P$	0,31	2,25	0,24	6	4,50	2	1,8
20	$5s^2S - 5p^2P$	0,02	96,45	0,64	6	192,1	6	$2,1 \cdot 10^{-2}$
21	$3d^2D - 5p^2P$	0,62	0,21	0,010	60	0,84	6	1,2
22	$4d^2D - 5p^2P$	0,16	4,29	0,002	60	17,16	6	0,31
23	$2p^2P - 5d^2D$	3,12	0,04	0,017	60	0,16	10	16
24	$3p^2P - 5d^2D$	0,88	0,28	0,056	60	1,12	10	2,0
25	$4p^2P - 5d^2D$	0,28	3,42	0,21	60	13,7	10	0,60
26	$5p^2P - 5d^2D$	0,06	124,03	1,65	60	248,1	10	0,17
27	$4f^2F - 5d^2D$	0,20	11,32	0,32	210	67,9	10	1,5
28	$3d^2D - 5f^2F$	0,69	1,46	0,14	210	8,76	14	5,4
29	$4d^2D - 5f^2F$	0,23	20,46	0,67	210	122,8	14	2,9
30	$5d^2D - 5f^2F$	0,01	132,89	0,19	210	797,3	14	$1,5 \cdot 10^{-3}$
31	$5f^2F - 5g^2G$	0,04	57,58	0,44	504	460,6	18	$4,1 \cdot 10^{-2}$
32	$4f^2F - 5g^2G$	0,21	38,53	1,54	504	307,6	18	4,3

Table 43. Oscillator Strengths and Absorption Coefficients for Transitions from Levels of $1s^2 2s^2 nl$ Configurations to the State of Continuous Spectrum [51]

№	Transition	Z	γ_n	q	$-F$	$\rho^2_{nk} \cdot k^3$	$f_{nk} \cdot k^3$	$10^{18}\sigma_\nu(nk)$
1	$3s^2S - kp^2P$	3,26	1,470	4,7	12,6	$4,7 \cdot \left(\frac{\nu_0}{\nu}\right)^2$	$1,9 \cdot \frac{\nu_0}{\nu}$	$0,72 \cdot \frac{\nu_0}{\nu}$
2	$3p^2P - kd^2D$	3,07	1,248	20,8	26,3	$20,8 \cdot \left(\frac{\nu_0}{\nu}\right)^4$	$5,8 \cdot \left(\frac{\nu_0}{\nu}\right)^3$	$2,5 \cdot \left(\frac{\nu_0}{\nu}\right)^2$
3	$3d^2D - kf^2F$	3,02	1,051	12,5	38,4	$12,6 \cdot \left(\frac{\nu_0}{\nu}\right)^4$	$2,6 \cdot \left(\frac{\nu_0}{\nu}\right)^3$	$1,1 \cdot \left(\frac{\nu_0}{\nu}\right)^3$
4	$4s^2S - kp^2P$	3,26	0,743	18,1	41,4	$18,1 \cdot \left(\frac{\nu_0}{\nu}\right)^3$	$4,5 \cdot \left(\frac{\nu_0}{\nu}\right)^2$	$1,7 \cdot \left(\frac{\nu_0}{\nu}\right)^2$
5	$4p^2P - kd^2D$	3,07	0,646	60,8	46,1	$60,8 \cdot \left(\frac{\nu_0}{\nu}\right)^3$	$8,8 \cdot \left(\frac{\nu_0}{\nu}\right)^2$	$3,2 \cdot \left(\frac{\nu_0}{\nu}\right)^2$
6	$4d^2D - kf^2F$	3,02	0,591	87,9	58,1	$87,9 \cdot \left(\frac{\nu_0}{\nu}\right)^3$	$9,4 \cdot \left(\frac{\nu_0}{\nu}\right)^2$	$3,2 \cdot \left(\frac{\nu_0}{\nu}\right)^2$
7	$4f^2F - kg^2G$	3,00	0,569	48,9	76,7	$48,9 \cdot \left(\frac{\nu_0}{\nu}\right)^4$	$5,3 \cdot \left(\frac{\nu_0}{\nu}\right)^3$	$2,4 \cdot \left(\frac{\nu_0}{\nu}\right)^3$
8	$5s^2S - kp^2P$	3,26	0,446	1,07	76,8	$1,07 \cdot \left(\frac{\nu_0}{\nu}\right)^3$	$0,16 \cdot \left(\frac{\nu_0}{\nu}\right)^2$	$0,06 \cdot \left(\frac{\nu_0}{\nu}\right)^2$
9	$5p^2P - kd^2D$	3,07	0,434	170,0	221,8	$170 \cdot \left(\frac{\nu_0}{\nu}\right)^{10}$	$16,4 \cdot \left(\frac{\nu_0}{\nu}\right)^9$	$7,05 \left(\frac{\nu_0}{\nu}\right)^9$
10	$5d^2D - kf^2F$	3,02	0,371	116,4	86,8	$116,4 \cdot \left(\frac{\nu_0}{\nu}\right)^4$	$8,6 \cdot \left(\frac{\nu_0}{\nu}\right)^3$	$3,8 \cdot \left(\frac{\nu_0}{\nu}\right)^3$
11	$5f^2F - kg^2G$	3,00	0,364	159,8	103,3	$177,3 \cdot \left(\frac{\nu_0}{\nu}\right)^4$	$12,1 \cdot \left(\frac{\nu_0}{\nu}\right)^4$	$5,4 \cdot \left(\frac{\nu_0}{\nu}\right)^3$
12	$5g^2G - kh^2H$	3,00	0,360	31,6	128,3	$31,6 \cdot \left(\frac{\nu_0}{\nu}\right)^5$	$2,1 \cdot \left(\frac{\nu_0}{\nu}\right)^4$	$1,6 \cdot \left(\frac{\nu_0}{\nu}\right)^4$

Table 44. Oscillator Strengths and Transition Probabilities Between Levels of $1s^2 2s2p(^1,{}^3P)\,nl$ Configurations [51]

№	Transition	$\frac{\nu_{LL'}}{R_y}$	ω_1	$S_{LL'}$	ρ^2	$f_{nn'}$	ω_2	$\frac{S_{12}}{\omega_2}$	$A_{nn'}\cdot 10^{-8}$
1	$3s\,^4P - 3p\,^4D\,(^3P)$	0,20	12	20	15,8	0,58	20	5,26	1,13
2	$^4P - {}^4S$	0,24	12	4	15,2	0,14	4	5,07	1,87
3	$^4P - {}^4P$	0,27	12	12	14,8	0,44	12	4,92	2,59
4	$^2P - {}^2P$	0,11	6	6	14,0	0,17	6	4,68	0,16
5	$^2P - {}^2D$	0,22	6	10	13,2	0,54	10	4,39	1,25
6	$^2P - {}^2S$	0,26	6	2	12,6	0,12	2	4,20	1,98
7	$3s\,^2P - 3p\,^2S\,(^1P)$	0,27	6	2	16,3	0,16	2	5,43	2,86
8	$^2P - {}^2P$	0,27	6	6	16,3	0,49	6	5,43	2,86
9	$^2P - {}^2D$	0,23	6	10	16,1	0,68	10	5,36	1,75
10	$3p\,^2P - 3d\,^2D\,(^3P)$	0,23	6	45	12,4	0,47	10	3,71	1,21
11	$^4D - {}^4F$	0,19	20	168	11,9	0,42	28	4,76	0,87
12	$^4D - {}^4D$	0,21	20	30	12,4	0,09	20	1,24	0,31
13	$^4D - {}^4P$	0,24	20	2	12,3	0,007	12	0,14	0,051
14	$^4S - {}^4P$	0,20	4	40	12,1	0,54	12	2,68	0,57
15	$^4P - {}^4P$	0,17	12	30	12,4	0,12	12	2,06	0,27
16	$^4P - {}^4D$	0,14	12	90	12,4	0,29	20	3,72	0,27
17	$3p\,^2D - 3d\,^2D\,(^3P)$	0,10	10	15	12,8	0,04	10	1,28	0,03
18	$^2D - {}^2F$	0,17	10	84	13,1	0,42	14	5,23	0,69
19	$^2D - {}^2P$	0,19	10	1	13,6	0,006	6	0,15	0,03
20	$^2S - {}^2P$	0,15	2	20	8,7	0,29	6	1,93	0,18
21	$^2P - {}^2P$	0,30	6	15	14,0	0,23	6	2,33	1,68
22	$2s2p^2\,^4P - 3s\,^4P\,(^3P)$	2,10	12	24	0,002	0,001	12	0,001	0,32
23	$^2D - {}^2P$	1,79	10	15	0,002	$6\cdot 10^{-4}$	6	0,002	0,26
24	$^2S - {}^2P$	1,52	2	3	0,001	$3\cdot 10^{-4}$	6	$2\cdot 10^{-4}$	0,02
25	$^2P - {}^2P$	1,38	6	3	0,004	$3\cdot 10^{-4}$	6	$7\cdot 10^{-4}$	0,05
26	$^2P - {}^2P\,(^1P)$	1,26	6	9	0,004	$8\cdot 10^{-4}$	6	0,002	0,11
27	$^2S - {}^2P$	1,97	2	1	0,001	10^{-4}	6	$5\cdot 10^{-5}$	0,01
28	$^2D - {}^2P$	2,25	10	5	0,002	$3\cdot 10^{-4}$	6	$6\cdot 10^{-4}$	0,18
29	$2s2p^2\,^2P - 3d\,^4D\,(^3P)$	2,51	12	180	0,56	0,47	20	0,34	$1,42\cdot 10^2$
30	$^4P - {}^4P$	2,54	12	60	0,54	0,15	12	0,18	79,0
31	$^2D - {}^2D$	2,13	10	$^{45}/_2$	0,58	0,06	10	0,09	22,6
32	$^2D - {}^2P$	2,20	10	$^{5}/_2$	0,53	0,004	6	0,009	2,51
33	$^2D - {}^2F$	2,18	10	$^{252}/_2$	0,53	0,33	14	0,32	88,2
34	$^2S - {}^2P$	2,50	2	30	0,51	0,43	6	0,17	71,1
35	$2s2p^2\,^2P - 3d\,^2D\,(^3P)$	1,72	6	$^{45}/_2$	0,62	0,09	10	0,09	12,7
36	$^2P - {}^2P$	1,79	6	$^{15}/_2$	0,56	0,03	6	0,05	7,2
37	$2s^22p^2P - 2s2p3p\,^2D\,(^3P)$	2,93	6	15	0,15	0,12	10	0,08	50,5
38	$^2P - {}^2P$	2,82	6	9	0,13	0,06	6	0,07	39,0
39	$^2P - {}^2S$	2,87	6	3	0,13	0,02	2	0,07	41,1
40	$^2P - 2s2p^3p\,^2D\,(^1P)$	3,40	6	5	0,15	0,05	10	0,03	26,3
41	$^2P - {}^2P$	3,44	6	3	0,15	0,03	6	0,03	27,2
42	$^2P - {}^2S$	3,44	6	1	0,15	0,01	2	0,03	27,2
43	$2s^23p\,^2P - 2s2p\,(^1P)\,3p\,^2P$	1,20	6	12	0,94	0,25	6	0,63	29,0
44	$^2P - {}^2D$	1,16	6	20	0,94	0,40	10	0,63	26,2
45	$^2P - {}^2S$	1,20	6	4	0,94	0,08	2	0,63	29,0

Table 45. Oscillator Strengths and Transition Probabilities Between Levels of $1s^2 2s2p(^4,{}^3P)nl$ Configurations [51]

№	Transition	$\frac{\nu_{LL'}}{R_y}$	ω_1	$S_{LL'}$	ρ^2	$f_{nn'}$	ω_p	$\frac{S_{12}}{\omega_2}$	$A_{nn'}\cdot 10^{-8}$
1	$2s2p^2\ {}^4P - 4s^4P\ ({}^3P)$	2,84	12	24	0,02	0,01	12	0,01	8,17
2	${}^2D - {}^2P$	2,45	10	15	0,03	0,01	6	0,03	9,84
3	${}^2S - {}^2P$	2,18	2	3	0,02	0,007	6	0,003	0,92
4	${}^2P - {}^2P$	2,04	6	3	0,03	0,003	6	0,005	1,14
5	$3p^4P - 4s^4P$	0,47	12	12	1,45	0,08	12	0,48	1,34
6	${}^4S - {}^4P$	0,50	4	4	1,17	0,07	12	0,13	0,44
7	${}^4D - {}^4P$	0,54	20	20	0,94	0,06	12	0,52	2,20
8	${}^2P - {}^2P$	0,55	6	6	0,47	0,03	6	0,16	0,70
9	${}^2D - {}^2P$	0,44	10	10	0,96	0,05	6	0,53	1,22
10	${}^2S - {}^2P$	0,40	2	2	1,21	0,05	6	0,13	0,23
11	$4s^2P - 4p^2P$	0,05	6	6	48,6	0,27	6	16,2	0,05
12	$3s^2D - {}^2P$	0,37	10	45	1,21	0,04	6	0,61	0,82
13	$3s^2P - {}^2P$	0,71	6	6	1,78	0,14	6	0,59	5,68
14	$2s^22p^2P - 4p^2P$	2,00	6	9	0,04	0,01	6	0,02	4,89
15	$4s^4P - 4p^4D$	0,07	12	20	51,9	0,67	20	17,3	0,16
16	$3d^4P - 4p^4D$	0,37	12	2	1,43	0,002	20	0,01	0,01
17	${}^4D - {}^4D$	0,40	20	30	1,32	0,02	20	0,13	0,23
18	${}^4F - {}^4D$	0,42	28	168	1,15	0,06	20	0,64	1,28
19	$3s^4P - 4p^4D$	0,81	12	20	1,33	0,20	20	0,44	6,31
20	$4s^2P - 4p^2D$	0,07	6	10	66,10	0,56	10	22,0	0,20
21	$3s^2P - 4p^2D$	0,32	6	1	1,08	0,001	10	0,097	0,006
22	${}^2F - {}^2D$	0,34	14	84	0,93	0,04	10	0,52	0,55
23	$3s^2P - 4p^2D$	0,73	6	10	0,97	0,13	10	0,32	3,36
24	$2s^22p^2P - {}^2D$	2,11	6	15	0,04	0,02	10	0,02	5,03
25	$4s^4P - 4p^4S$	0,09	12	4	44,81	0,15	4	14,9	0,29
26	$3d^4P - {}^4S$	0,39	12	40	0,11	0,01	4	0,27	0,43
27	$3s^4P - {}^4S$	0,83	12	4	0,33	0,01	4	0,11	1,68
28	$4s^4P - 4p^4P$	0,10	12	12	48,29	0,54	12	16,1	0,43
29	$3d^4P - {}^4P$	0,40	12	30	0,77	0,02	12	0,13	0,22
30	${}^4D - {}^4P$	0,43	20	90	0,66	0,03	12	0,33	0,70
31	$3s^4P - {}^4P$	0,84	12	12	0,62	0,06	12	0,21	3,28
32	$4s^2P - 4p^2S$	0,11	6	2	19,56	0,08	2	6,52	0,23
33	$3d^2P - {}^2S$	0,36	6	20	1,81	0,05	2	1,21	1,50
34	$3s^2P - 4p^2S$	0,77	6	2	1,61	0,05	2	0,54	0,54
35	$2s^22p^2P - {}^2S$	3,48	6	3	0,03	0,006	2	0,02	16,9
36	$4p^4D - 4d^4F$	0,07	20	168	55,4	0,71	28	22,1	0,20
37	$3p^4D - {}^4F$	0,68	20	168	2,12	0,27	28	0,85	7,14
38	$4p^2D - 4d^2D$	0,07	10	15	50,3	0,12	10	5,0	0,05
39	${}^2P - {}^2D$	0,09	6	45	51,9	0,78	10	15,6	0,30
40	$3p^2D - {}^2D$	0,58	10	15	3,15	0,05	10	0,32	1,35
41	${}^2P - {}^2D$	0,69	6	45	2,12	0,24	10	0,04	7,59
42	$2s2p^2\ {}^2P - 4d^2D$	2,18	6	45	0,17	0,03	10	0,03	7,07
43	${}^2D - {}^2D$	3,17	10	45	0,17	0,03	10	0,03	21,7
44	$4p^4P - 4d^4D$	0,05	12	90	50,3	0,42	20	15,1	0,05
45	${}^4D - {}^4D$	0,08	20	30	55,4	0,15	20	5,5	0,08
46	$3p^4P - {}^4D$	0,62	12	90	2,87	0,30	20	0,85	5,49
47	${}^4D - {}^4D$	0,69	20	30	2,17	0,05	20	0,22	1,91
48	$2s2p^2\ {}^4P - {}^4D$	2,39	12	180	0,16	0,16	20	0,10	68,7
49	$4p^4P - 4d^4P$	0,05	12	30	45,3	0,15	12	7,5	0,04
50	${}^4S - {}^4P$	0,57	4	40	41,8	0,05	12	9,3	0,09
51	$4p^4D - 4d^4P$	0,09	20	2	47,7	0,01	12	0,53	0,01
52	$3p^4P - {}^4P$	0,63	12	30	1,79	0,06	12	0,30	0,02
53	${}^4S - {}^4P$	0,66	4	40	1,49	0,22	12	0,33	2,54
54	${}^4D - {}^4P$	0,70	20	2	1,24	0,002	12	0,01	0,12
55	$2s2p^2\ {}^4P - 4d^4P$	3,00	12	60	0,17	0,06	12	0,06	13,7
56	$4p^2D - {}^2F$	0,09	10	84	50,0	0,84	14	20,0	0,39
57	$3p^2D - {}^2F$	0,40	10	[illegible]	2,20	0,16	14	0,88	1,51
58	$2s2p^2\ {}^2D - {}^2F$	3,19	10	[illegible]	0,17	0,15	14	0,10	86,6
59	$4p^2S - 4d^2P$	0,06	2	20	62,2	0,83	6	[illegible]	0,08

Table 45 (Cont.)

№	Transition	$\frac{\varepsilon_{LL'}}{R_y}$	ω_1	$S_{LL'}$	φ^2	$f_{nn'}$	ω_2	$\frac{S_{12}}{\omega_2}$	$A_{nn'}\cdot 10^{-8}$
60	$^2P - {}^2P$	0,12	6	15	85,3	0,57	6	14,2	0,65
61	$^2D - {}^2P$	0,10	10	1	51,8	0,01	6	0,58	0,02
62	$3p^2S - {}^2P$	0,47	2	20	2,64	0,28	6	0,59	1,63
63	$^2p - {}^2P$	0,72	6	15	1,44	0,06	6	0,24	2,40
64	$^2D - {}^2P$	0,61	10	1	2,28	0,003	6	0,03	0,15
65	$2s2p^2\,{}^2D - {}^2P$	3,20	10	$^3/_2$	0,16	0,002	6	0,003	2,37
66	$^2P - {}^2P$	2,21	6	$^{15}/_2$	0,16	0,01	6	0,01	3,84
67	$^2S - {}^2P$	2,35	2	30	0,15	0,12	6	0,05	17,4
11a	$3d^2P - 4p^2P$	0,29	6	15	1,84	0,03	6	0,31	0,2
21a	$^2D - {}^2D$	0,39	10	15	0,63	0,008	10	0,06	0,1

Table 46. Values of $\rho^2_{nk} \cdot k^3$ for Transitions From Levels of $1s^2 2s2p(^1, {}^3p)nl$ Configurations to the State of Continuous Spectrum [51]

№	Transition	γ_n	Z	ω_i	$S_{LL'}$	q	$-F$	$\rho^2_{nk} \cdot k^3$
1	$3s^4P - kp^4D$	1,48	3,33	12	20	6,62	−7,70	$6{,}62 \cdot \frac{\nu}{\nu_0}$
2	$3s^2P - kp^2D$	1,39	3,24	6	10	6,81	−13,08	$6{,}81 \left(\frac{\nu}{\nu_0}\right)^2$
3	$3p^2P - kd^2D$	1,28	3,08	6	45	19,89	24,00	$19{,}89 \left(\frac{\nu_0}{\nu}\right)^3$
4	$3p^4D - kd^4F$	1,28	3,10	20	168	19,27	24,20	$19{,}27 \left(\frac{\nu_0}{\nu}\right)^3$
5	$3p^4S - kd^4P$	1,24	3,05	4	40	12,55	19,48	$12{,}55 \left(\frac{\nu_0}{\nu}\right)^3$
6	$3p^4P - kd^4D$	1,21	3,08	12	90	20,21	25,79	$20{,}21 \left(\frac{\nu_0}{\nu}\right)^3$
7	$3p^2D - kd^2F$	1,17	3,00	10	84	19,99	25,15	$19{,}99 \left(\frac{\nu_0}{\nu}\right)^3$
8	$3p^2S - kd^2P$	1,13	3,00	2	20	19,43	26,63	$19{,}43 \left(\frac{\nu_0}{\nu}\right)^3$
9	$3d^4F - kf^4G^*$	1,09	3,00	28	540	14,50	37,21	$14{,}50 \left(\frac{\nu_0}{\nu}\right)^4$
10	$3d^4D - kf^4F^*$	1,07	3,02	20	$\frac{1120}{3}$	12,55	38,36	$12{,}55 \left(\frac{\nu_0}{\nu}\right)^4$
11	$3d^2D - kf^2F$	1,05	3,02	10	$\frac{500}{3}$	12,55	38,36	$12{,}55 \left(\frac{\nu_0}{\nu}\right)^4$
12	$3d^4P - kf^4D$	1,04	3,00	12	252	12,94	38,58	$12{,}94 \left(\frac{\nu_0}{\nu}\right)^4$
13	$3d^2F - kf^2G$	1,00	3,00	14	270	10,75	40,00	$10{,}75 \left(\frac{\nu_0}{\nu}\right)^4$
14	$3d^2P - kf^2D$	0,98	3,00	6	126	8,31	40,73	$8{,}31 \left(\frac{\nu_0}{\nu}\right)^4$

Table 47. Oscillator Strengths and Absorption Coefficients for Transitions Given in Table [illegible] [51]

№	Transition	$f_{nk} \cdot k^3$	$\sigma_\nu(nk)$ 10^{-18}	№	Transition	$f_{nk} \cdot k^3$	$\sigma_\nu(nk)$ 10^{-18}
1	$3s^4P - kp^4D$	$1.8\left(\frac{\nu}{\nu_0}\right)^2$	$0{,}65\left(\frac{\nu}{\nu_0}\right)^2$	8	$3p^3S - kd^2P$	$4{,}9\left(\frac{\nu_0}{\nu}\right)^3$	$2{,}2\left(\frac{\nu_0}{\nu}\right)^3$
2	$3s^2P - kp^2D$	$1{,}8\left(\frac{\nu}{\nu_0}\right)^3$	$0{,}09\left(\frac{\nu}{\nu_0}\right)^5$	9	$3d^4F - kf^4G$	$2{,}9\left(\frac{\nu_0}{\nu}\right)^3$	$1{,}3\left(\frac{\nu_0}{\nu}\right)^3$
3	$3p^2P - kd^2D$	$4{,}2\left(\frac{\nu_0}{\nu}\right)^2$	$1{,}8\left(\frac{\nu_0}{\nu}\right)^2$	10	$3d^4D - kf^4F$	$2{,}1\left(\frac{\nu_0}{\nu}\right)^3$	$1{,}1\left(\frac{\nu_0}{\nu}\right)$
4	$3p^4D - kd^4F$	$4{,}6\left(\frac{\nu_0}{\nu}\right)^2$	$1{,}9\left(\frac{\nu_0}{\nu}\right)^2$	11	$3d^2D - kf^2F$	$2{,}4\left(\frac{\nu_0}{\nu}\right)^3$	$1{,}1\left(\frac{\nu_0}{\nu}\right)^3$
5	$3p^4S - kd^4P$	$3{,}5\left(\frac{\nu_0}{\nu}\right)^2$	$1{,}5\left(\frac{\nu_0}{\nu}\right)^2$	12	$3d^4P - kf^4D$	$2{,}7\left(\frac{\nu_0}{\nu}\right)^3$	$1{,}2\left(\frac{\nu_0}{\nu}\right)^3$
6	$3p^4P - kd^4D$	$4{,}1\left(\frac{\nu_0}{\nu}\right)^2$	$1{,}8\left(\frac{\nu_0}{\nu}\right)^2$	13	$3d^2F - kf^2G$	$2{,}0\left(\frac{\nu_0}{\nu}\right)^3$	$0{,}9\left(\frac{\nu}{\nu}\right)$
7	$3p^2D - kd^2F$	$4{,}4\left(\frac{\nu_0}{\nu}\right)^2$	$2{,}0\left(\frac{\nu_0}{\nu}\right)^2$	14	$3d^2P - kf^2D$	$1{,}6\left(\frac{\nu_0}{\nu}\right)$	$0{,}71\left(\frac{\nu_0}{\nu}\right)^3$

Table 48. Values of $\rho^2_{nk} \cdot k^3$ for Transitions for Levels of $1s^2 2s2p(^3P)nl$ ($n = 4$, $l = 0, 1, 2$) Configurations to the State of Continuous Spectrum [51]

№	Transition	χ_n	Z	ω_1	$S_{LL'}$	q	$-F$	$\rho^2_{nk} \cdot k^3$
1	$4s^4P - kp^4D$	0,74	3,33	12	20	19,98	50,23	$19,98 \left(\frac{\nu_0}{\nu}\right)^3$
2	$4s^2P - kp^2D$	0,73	3,24	6	10	17,29	51,23	$17,29 \left(\frac{\nu_0}{\nu}\right)^3$
3	$4p^4D - kd^4F$	0,67	3,10	20	168	54,06	44,04	$54,06 \left(\frac{\nu_0}{\nu}\right)^3$
4	$4p^4S - kd^4P$	0,65	3,05	4	40	48,06	41,64	$48,06 \left(\frac{\nu_0}{\nu}\right)^3$
5	$4p^4P - kd^4D$	0,64	3,08	12	90	52,58	44,43	$52,58 \left(\frac{\nu_0}{\nu}\right)^3$
6	$4p^2P - kd^2D$	0,68	3,08	6	45	52,00	40,74	$52,00 \left(\frac{\nu_0}{\nu}\right)^3$
7	$4p^2D - kd^2F$	0,66	3,00	10	84	44,74	37,68	$44,74 \left(\frac{\nu_0}{\nu}\right)^3$
8	$4p^2S - kd^2P$	0,62	3,00	2	20	44,56	41,60	$44,56 \left(\frac{\nu_0}{\nu}\right)^3$
9	$4d^2D - kf^2F$	0,59	3,02	10	$\frac{560}{3}$	87,87	58,11	$87,87 \left(\frac{\nu_0}{\nu}\right)^4$
10	$4d^4F - kf^4G$	0,60	3,00	28	540	92,54	57,23	$92,54 \left(\frac{\nu_0}{\nu}\right)^4$
11	$4d^4D - kf^4F$	0,59	3,02	20	$\frac{1120}{3}$	87,87	58,11	$87,87 \left(\frac{\nu_0}{\nu}\right)^4$
12	$4d^4P - kf^4D$	0,58	3,00	12	252	80,28	58,95	$80,28 \left(\frac{\nu_0}{\nu}\right)^4$
13	$4d^2F - kf^2G$	0,57	3,00	14	270	94,25	63,58	$94,25 \left(\frac{\nu_0}{\nu}\right)^4$
14	$4d^2P - kf^2D$	0,56	3,00	6	126	70,36	62,37	$70,36 \left(\frac{\nu_0}{\nu}\right)^4$

Table 49. Oscillator Strengths and Absorption Coefficients for Transitions Given in Table 48 [51]

№	Transition	$f_{nk} \cdot k^3$	$\alpha_\nu(nk)$ 10^{-18}	№	Transition	$f_{nk} \cdot k^3$	$\alpha_\nu(nk)$ 10^{18}
1	$4s^4P - kp^4D$	$2{,}7 \left(\frac{\nu_0}{\nu}\right)^2$	$0{,}98 \left(\frac{\nu_0}{\nu}\right)^2$	8	$4p^2S - kd^2P$	$6{,}1 \left(\frac{\nu_0}{\nu}\right)^2$	$2{,}7 \left(\frac{\nu_0}{\nu}\right)^2$
2	$4s^2P - kp^2D$	$2{,}3 \left(\frac{\nu_0}{\nu}\right)^2$	$0{,}88 \left(\frac{\nu_0}{\nu}\right)^2$	9	$4d^2D - kf^2F$	$9{,}2 \left(\frac{\nu_0}{\nu}\right)^3$	$4{,}1 \left(\frac{\nu_0}{\nu}\right)^3$
3	$4p^4D - kd^4F$	$6{,}8 \left(\frac{\nu_0}{\nu}\right)^2$	$2{,}8 \left(\frac{\nu_0}{\nu}\right)^2$	10	$4d^4F - kf^4G$	$10{,}2 \left(\frac{\nu_0}{\nu}\right)^3$	$4{,}6 \left(\frac{\nu_0}{\nu}\right)^3$
4	$4p^4S - kd^4P$	$6{,}9 \left(\frac{\nu_0}{\nu}\right)^2$	$3{,}0 \left(\frac{\nu_0}{\nu}\right)^2$	11	$4d^4D - kf^4F$	$9{,}2 \left(\frac{\nu_0}{\nu}\right)^3$	$4{,}1 \left(\frac{\nu_0}{\nu}\right)^3$
5	$4p^4P - kd^4D$	$5{,}6 \left(\frac{\nu_0}{\nu}\right)^2$	$2{,}4 \left(\frac{\nu_0}{\nu}\right)^2$	12	$4d^4P - kf^4D$	$9{,}3 \left(\frac{\nu_0}{\nu}\right)^3$	$4{,}2 \left(\frac{\nu_0}{\nu}\right)^3$
6	$4p^2P - kd^2D$	$5{,}9 \left(\frac{\nu_0}{\nu}\right)^2$	$2{,}5 \left(\frac{\nu_0}{\nu}\right)^2$	13	$4d^2F - kf^2G$	$9{,}9 \left(\frac{\nu_0}{\nu}\right)^3$	$4{,}4 \left(\frac{\nu_0}{\nu}\right)^3$
7	$4p^2D - kd^2F$	$5{,}5 \left(\frac{\nu_0}{\nu}\right)^2$	$2{,}5 \left(\frac{\nu_0}{\nu}\right)^2$	14	$4d^2P - kf^2D$	$7{,}9 \left(\frac{\nu_0}{\nu}\right)^3$	$3{,}5 \left(\frac{\nu_0}{\nu}\right)^3$

Table 50. Relative Line Strengths and Relative Oscillator Strengths for the $3d^7(a^4F)4s$-$3d^7(a^4F)4p$ Transitions in Co II [52]

Multiplet no.	λ(Å)	Transition	S_{LS}	$S_{inter.}$	log gf **
1	2	3	4	5	6
7	2388.930	$a^5F_5 - z^5F_5$	761	811 *	2.53 *
	2417.686	$a^5F_4 - z^5F_4$	487	173	1.85
	2414.069	$a^5F_3 - z^5F_3$	303	138	1.76
	2408.770	$a^5F_2 - z^5F_2$	192	112	1.67
	2404.187	$a^5F_1 - z^5F_1$	154	112	1.67
	2378.636	$a^5F_5 - z^5F_4$	84	493	2.32
	2383.479	$a^5F_4 - z^5F_3$	120	367	2.19
	2386.376	$a^5F_3 - z^5F_2$	116	249	2.02
	2389.565	$a^5F_2 - z^5F_1$	77	123	1.71
	2428.310	$a^5F_4 - z^5F_5$	84	34 *	1.15 *
	2449.180	$a^5F_3 - z^5F_4$	120	25	1.01
	2436.991	$a^5F_2 - z^5F_3$	116	32	1.12
	2423.645	$a^5F_1 - z^5F_2$	77	33	1.13
8	2326.493	$a^5F_5 - z^5D_4$	604	198	1.93
	2324.317	$a^5F_4 - z^5D_3$	412	170	1.86
	2326.150	$a^5F_3 - z^5D_2$	263	136	1.77
	2330.37	$a^5F_2 - z^5D_1$	154	108	1.67
	2336.246	$a^5F_1 - z^5D_0$	77	77	1.52
	2363.836	$a^5F_4 - z^5D_4$	82	457	2.29
	2353.446	$a^5F_3 - z^5D_3$	115	325	2.14
	2347.406	$a^5F_2 - z^5D_2$	110	217	1.96
	2344.293	$a^5F_1 - z^5D_1$	77	128	1.74
	2393.925	$a^5F_3 - z^5D_4$	5	34	1.15
	2375.201	$a^5F_2 - z^5D_3$	11	44	1.27
	2361.536	$a^5F_1 - z^5D_2$	11	34	1.15
9	2286.165	$a^5F_5 - z^5G_6$	1000	1000 *	2.64 *
	2307.84	$a^5F_4 - z^5G_5$	762	764 *	2.52 *

* Due to interaction between configurations neglected in the calculations, these values may not be in good agreement with experimental values.

** Log of the product of statistical weight g and oscillator strength f.

Table 50 (Cont.)

1	2	3	4	5	6
9	2311.602	$a^5F_3 - z^5G_4$	567	613	2.42
	2314.036	$a^5F_2 - z^5G_3$	412	461	2.30
	2314.97	$a^5F_1 - z^5G_2$	297	320	2.14
	2272.26	$a^5F_5 - z^5G_5$	81	31 •	1.13 •
	2283.534	$a^5F_4 - z^5G_4$	122	55	1.38
	2293.415	$a^5F_3 - z^5G_3$	120	74	1.51
	2301.419	$a^5F_2 - z^5G_2$	82	62	1.43
	. . .	$a^5F_5 - z^5G_4$	3.0	1.0	1.64
	. . .	$a^5F_4 - z^5G_3$	6.0	1.0	1.64
	. . .	$a^5F_3 - z^5G_2$	5.0	2.0	1.64
10	2211.411	$a^5F_5 - z^3G_5$	0	4.0 •	0.26 •
	2205.886	$a^5F_4 - z^3G_4$	0	4.0	0.26
	2198.279	$a^5F_3 - z^3G_3$	0	0.7	1.50
	2173.324	$a^5F_5 - z^3G_4$	0	0.2	2.96
	2245.11	$a^5F_4 - z^3G_5$	0	58 •	1.41 •
	2232.05	$a^5F_3 - z^3G_4$	0	13.2	0.77
	. . .	$a^5F_4 - z^3G_3$	0	0.03	2.13
	. . .	$a^5F_2 - z^3G_3$	0	5.0	0.26
11	2156.955	$a^5F_5 - z^3F_4$	0	0.5	1.36
	2156.701	$a^5F_4 - z^3F_3$	0	0.01	3.66
		$a^5F_3 - z^3F_2$	0	0.01	3.66
	2188.999	$a^5F_4 - z^3F_4$	0	0.2	2.96
	2181.729	$a^5F_3 - z^3F_3$	0	0.01	3.66
	2214.764	$a^5F_3 - z^3F_4$	0	7.3	0.52
	2200.412	$a^5F_2 - z^3F_3$	0	1.5	1.83
	2187.044	$a^5F_1 - z^3F_2$	0	0.13	2.77
	. . .	$a^5F_2 - z^3F_2$	0	0.01	3.66
13	2663.548	$b^3F_4 - z^5G_5$	0	52 •	1.29 •
	2694.701	$b^3F_3 - z^5G_4$	0	22	0.91
	2714.470	$b^3F_2 - z^5G_3$	0	6.7	0.39
	. . .	$b^3F_4 - z^5G_4$	0	2.0	1.87
	. . .	$b^3F_4 - z^5G_3$	0	0.1	2.57
	. . .	$b^3F_3 - z^5G_4$	0	0.3	1.95
	. . .	$b^3F_3 - z^5G_3$	0	0.01	3.57
	. . .	$b^3F_2 - z^5G_3$	0	0.1	2.57
14	2580.372	$b^3F_4 - z^3G_5$	846	783 •	2.48 •
	2587.225	$b^3F_3 - z^3G_4$	649	285	2.04
	2582.247	$b^3F_2 - z^3G_3$	494	317	2.09
	2528.654	$b^3F_4 - z^3G_4$	43	389	2.19
	2541.977	$b^3F_3 - z^3G_3$	43	204	1.90
	2485.380	$b^3F_4 - z^3G_3$	1.0	11.3	0.66
15	2506.474	$b^3F_4 - z^3F_4$	649	299	2.08
	2519.829	$b^3F_3 - z^3F_3$	452	238	1.97
	2525.015	$b^3F_2 - z^3F_2$	341	302	2.08
	2464.210	$b^3F_4 - z^3F_3$	43	99	1.10
	2486.455	$b^3F_3 - z^3F_2$	43	82	1.52
	2564.050	$b^3F_3 - z^3F_4$	43	385	2.18
	2559.418	$b^3F_2 - z^3F_3$	43	200	1.89
16	2397.423	$b^3F_4 - z^3D_3$	494	426	2.25
	2407.680	$b^3F_3 - z^3D_2$	341	302	2.10
	2416.922	$b^3F_2 - z^3D_1$	231	228	1.97
	2450.022	$b^3F_3 - z^3D_3$	43	95	1.59
	2443.804	$b^3F_2 - z^3D_2$	43	81	1.52
	. . .	$b^3F_2 - z^3D_1$	1	14	0.78
	. . .	$a^5F_4 - z^3D_3$	0	0.37	. .
	. . .	$a^5F_3 - z^3D_2$	0	0.17	. .
	. . .	$a^5F_3 - z^3D_3$	0	0.20	. .
	. . .	$a^5F_2 - z^3D_3$	0	0.23	. .
	. . .	$a^5F_2 - z^3D_2$	0	0.15	. .
	. . .	$a^5F_2 - z^3D_1$	0	1.04	. .
	. . .	$a^5F_1 - z^3D_2$	0	0.07	. .
	. . .	$b^3F_4 - z^5D_4$	0	0.18	. .
	. . .	$b^3F_4 - z^5D_3$	0	0.37	. .
	. . .	$b^3F_3 - z^5D_4$	0	0.02	. .
	. . .	$b^3F_3 - z^5D_3$	0	0.02	. .
	. . .	$b^3F_3 - z^5D_2$	0	0	. .
	. . .	$b^3F_2 - z^5D_3$	0	0.04	. .
	. . .	$b^3F_2 - z^5D_2$	0	0.03	. .
	. . .	$b^3F_2 - z^5D_1$	0	0.01	. .

Table [illegible] Wave Line and Oscillator Strengths for the $3d^8(^3F)4s$-$3d^8(^3F)4p$ Transitions in Ni II [55]

Multiplet no.	λ(Å)	s_{LS}	Sinten	$\log_{10}$**	Multiplet no.	λ(Å)	s_{LS}	Sinten	$\log_{10}$**
1	2	3	4	5	1	2	3	4	5
11	2316.034	595	640	2.11	15	2058.30	0	5	0.39
	2302.98	408	433	2.71		2083.42	0	1.5	−0.13
	2297.140	267	298	2.11		2093.55	0	20.3	0.09
	2297.486	167	167	1.86		2006.41	0	2.3	−0.05
	2307.395	68	22.5	0.08		2128.57	0	44.2	1.32
	2345.44	87	48.6	1.32		2090.14	0	8.4	0.60
	2326.44	67	33.7	1.16	16	2076.76	0	2	−0.02
	2412.25	4	1.7	−0.15		2057.38	0	1.3	−0.20
12	2216.479	1000	1000*	2.65*		2080.84	0	3.5	0.23
	2270.209	764	395	2.24	17	2630.268	0	2.5	−0.02
	2264.456	574	310	2.14		2648.713	0	0.5	−0.72
	2253.856	428	205	2.12		2551.04	0	18.4	0.86
	2222.948	69	176	1.90		2587.25	0	2.5	−0.01
	2224.88	91	279	2.10	18	2510.871	0	262	2.02
	2226.34	69	184	1.92		2545.903	0	68.5	1.43
	2179.46	2	5.3	0.37		2455.51	0	4	0.21
	2188.05	3	20.4	0.97		2497.80	0	1.7	−0.17
13	2165.55	764	566*	2.42*		2410.74	0	0.2	−1.08
	2169.10	508	340	2.10	19	2437.892	0	263*	2.03*
	2175.16	344	266	2.09		2473.13	0	55.3	1.35
	2184.61	267	297	2.13		2387.77	0	28.3	1.07
	2125.89	69	14.3	0.83		2433.57	0	12.4	0.71
	2138.60	89	28.3	1.12		2350.84	0	0.5	−0.67
	2158.73	66	34.9	1.21		2413.04	0	0.4	−0.78
	2210.38	69	5*	0.35*	20	2394.518	^{8}33	319*	2.13*
	2206.71	89	229	2.02		2416.134	^{6}42	444	2.26
	2201.41	66	193	1.94		2334.590	24	135	1.76
14	2131.27	0	88*	1.62*	21	2296.553	643	499	2.34
	2125.12	0	5	0.37		2298.269	476	446	2.29
	2083.65	0	0.2	−1.02		2224.351	24	41.5	1.27
	2174.67	0	427*	2.29*		2375.426	24	98.5	1.62
	2161.21	0	83	1.58	22	2278.771	476	440	2.28
						2287.082	333	331	2.16
						2356.41	24	39.5	1.22

* Due to interaction between configurations neglected in the calculations, these values may not be in good agreement with experimental values.

** Log of the product of statistical weight g and oscillator strength f.

Table 52. Values of K Electron Wave Functions at the Boundary of the Nucleus [58]

Z	$U_0 = \sqrt{2R}$	E_K *	G_K *	F_K *
25	0,1540	0,98723	0,0019973	—0,00014624
33	0,16050	0,97671	0,0035224	—0,00023658
41	0,16677	0,96271	0,0057705	—0,00069685
49	0,17378	0,94502	0,0088587	—0,0013835
57	0,17940	0,92335	0,013126	—0,0022225
61	0,18110	0,91091	0,015671	—0,0028470
65	0,18353	0,89733	0,018771	—0,0036441
69	0,18544	0,88256	0,022306	—0,0046106
73	0,18747	0,86651	0,026476	—0,0058081
77	0,18963	0,84911	0,031377	—0,0072850
81	0,19132	0,83025	0,037058	—0,0090834
84	0,19280	0,81509	0,042007	—0,010708
88	0,19457	0,79350	[illegible]	0,013292
92	0,19623	0,76993	0,058485	—0,016432
95	0,19746	0,75103	0,066053	—0,019258
98	0,19865	0,73092	0,074714	—0,022547

* Values G_K and F_K are the large and small components of the wave function in the s state; E_K is the theoretical binding-energy value for K electrons.

Table 53. The Cu Atom [59]

r	State $(4s)^2\,{}^1S$ I $P_{4s}(r)$	State $(4s)^2\,{}^1S$ II $P_{4s}(r)$	State $(4s4p)^1P$* I $P_{4s}(r)$	State $(4s4p)^1P$* I $P_{4p}(r)$	r	State $(4s)^2\,{}^1S$ I $P_{4s}(r)$	State $(4s)^2\,{}^1S$ II $P_{4s}(r)$	State $(4s4p)^1P$* I $P_{4s}(r)$	State $(4s4p)^1P$* I $P_{4p}(r)$
0,00	0,000	0,000	0,000	0,000	1,4	0,170	0,105	0,011	—0,035
0,02	—0,053	—0,039	—0,059	0,036	1,6	0,278	0,214	0,144	0,025
0,04	—0,033	—0,046	—0,062	0,060	1,8	0,368	0,307	0,271	0,083
0,06	0,010	—0,008	—0,023	0,072	2,0	0,437	0,383	0,377	0,139
0,08	0,051	0,032	0,002	0,080	2,2	0,489	0,443	0,465	0,190
0,10	0,085	0,067	0,048	0,086	2,4	0,526	0,488	0,535	0,236
0,12	0,110	0,095	0,088	0,089	2,6	0,548	0,520	0,588	0,278
0,14	0,124	0,115	0,121	0,089	2,8	0,560	0,539	0,624	0,314
0,16	0,130	0,126	0,144	0,086	3,0	0,562	0,549	0,647	0,344
0,18	0,128	0,129	0,160	0,080	3,2	0,556	0,550	0,657	0,370
0,20	0,119	0,126	0,166	0,073	3,4	0,544	0,545	0,658	0,392
0,22	0,105	0,117	0,166	0,063	3,6	0,528	0,535	0,649	0,409
0,24	0,087	0,104	0,160	0,053	3,8	0,508	0,520	0,634	0,422
0,26	0,066	0,088	0,148	0,041	4,0	0,486	0,501	0,614	0,432
0,28	0,043	0,069	0,132	0,029					
0,30	0,020	0,048	0,112	0,016	4,5	0,425	0,447	0,547	0,443
					5,0	0,362	0,388	0,464	0,438
0,35	—0,041	—0,008	0,053	—0,017	5,5	0,303	0,329	0,396	0,423
0,40	—0,097	—0,063	—0,012	—0,048	6,0	0,249	0,275	0,326	0,400
0,45	—0,144	—0,112	—0,076	—0,077	6,5	0,202	0,226	0,265	0,373
0,50	—0,181	—0,159	—0,135	—0,102	7,0	0,163	0,184	0,204	0,342
0,55	—0,207	—0,186	—0,185	—0,122					
0,60	—0,222	—0,208	—0,226	—0,138	8,0	0,103	0,119	0,132	0,280
					9,0	0,063	0,075	0,080	0,221
0,7	—0,224	—0,225	—0,277	—0,158	10,0	0,038	0,046	0,048	0,170
0,8	—0,194	—0,212	—0,290	—0,162	11,0	0,023	0,028	0,028	0,128
0,9	—0,146	—0,177	—0,274	—0,155	12,0	0,013	0,017	0,016	0,095
1,0	—0,087	—0,129	—0,237	—0,139	13,0	0,008	0,010	0,010	0,069
1,1	—0,072	—0,073	—0,184	—0,118	14,0	0,004	0,006	0,006	0,050
1,2	0,044	—0,013	—0,123	—0,092					

* Wave functions without exchange.

Table 54. The Tl^+ Ion [59]

r	State $(6s)^2\ ^1S$	State $(6s6p)\ ^1P$ *		r	State $(6s)^2\ ^1S$	State $(6s6p)\ ^1P$ *	
	$P_{6s}(r)$	$P_{6s}(r)$	$P_{6p}(r)$		$P_{6s}(r)$	$P_{6s}(r)$	$P_{6p}(r)$
0,000	0,000	0,000	0,000	0,65	−0,354	−0,370	−0,186
0,005	−0,036	−0,036	0,004	0,70	−0,339	−0,359	−0,212
0,010	−0,036	−0,034	0,015	0,75	−0,301	−0,322	−0,226
0,015	0,005	0,001	0,033	0,8	−0,245	−0,266	−0,228
0,020	0,044	0,043	0,056				
0,025	0,077	0,077	0,066	0,9	−0,100	−0,118	−0,204
0,030	0,098	0,101	0,069	1,0	−0,060	0,049	−0,153
0,035	0,109	0,114	0,068	1,1	0,215	0,211	−0,087
0,040	0,109	0,116	0,064	1,2	0,352	0,356	−0,014
				1,3	0,467	0,478	0,060
0,05	0,085	0,093	0,046	1,4	0,560	0,576	0,131
0,06	0,040	0,047	0,021	1,5	0,631	0,651	0,198
0,07	−0,014	−0,008	−0,007	1,6	0,682	0,705	0,260
0,08	−0,065	−0,063	−0,035				
0,09	−0,108	−0,109	−0,059	1,8	0,738	0,761	0,364
0,10	−0,139	−0,143	−0,078	2,0	0,764	0,766	0,446
0,11	−0,156	−0,162	−0,090	2,2	0,724	0,737	0,506
0,12	−0,160	−0,168	−0,097	2,4	0,682	0,687	0,547
0,13	−0,152	−0,162	−0,097	2,6	0,628	0,626	0,572
0,14	−0,133	−0,144	−0,092	2,8	0,570	0,560	0,584
0,15	−0,107	−0,117	−0,082	3,0	0,510	0,494	0,586
0,16	−0,074	−0,084	−0,069	3,2	0,452	0,431	0,578
				3,4	0,397	0,372	0,564
0,18	0,000	−0,008	−0,034	3,6	0,346	0,319	0,545
0,20	0,075	0,070	0,005	3,8	0,299	0,272	0,522
0,22	0,139	0,139	0,044	4,0	0,258	0,231	0,496
0,24	0,188	0,192	0,079				
0,26	0,218	0,225	0,107	4,4	0,189	0,163	0,302
0,28	0,229	0,240	0,126	4,8	0,136	0,114	0,380
0,30	0,223	0,236	0,138	5,2	0,097	0,078	0,324
0,32	0,202	0,216	0,142	5,6	0,068	0,053	0,271
0,34	0,169	0,184	0,138	6,0	0,048	0,036	0,224
0,36	0,127	0,141	0,128	6,4	0,033	0,024	0,184
0,38	0,079	0,093	0,112	6,8	0,022	0,016	0,149
0,40	0,028	0,040	0,093	7,2	0,015	0,010	0,120
				7,6	0,010	0,007	0,095
0,45	−0,100	−0,094	0,033	8,0	0,007	0,004	0,076
0,50	−0,212	−0,212	−0,032				
0,55	−0,293	−0,299	−0,094				
0,60	−0,340	−0,352	−0,146				

* Wave functions without exchange.

Table 55. Radial Wave Functions For The $1s^2 2s^2 nl (n \geqslant 4)$ States of N III [60]

r	$P(4p\|r)$	$P(4d\|r)$	$P(5p\|r)$	$P(5d\|r)$
0,01	0,0015	0,0000 (02)	0,0010	0,0000 (006)
0,02	0,0059	0,0000 (1)	0,0034	0,0000 (1)
0,03	0,0120	0,0000 (7)	0,0072	0,0000 (3)
0,04	0,0198	0,0001	0,0119	0,0000 (7)
0,06	0,0383	0,0003	0,0230	0,0002
0,08	0,0592	0,0007	0,0356	0,0005
0,10	0,0809	0,0013	0,0490	0,0009
0,12	0,1028	0,0021	0,0624	0,0014
0,14	0,1237	0,0030	0,0757	0,0021
0,16	0,1435	0,0044	0,0883	0,0029
0,18	0,1618	0,0058	0,0999	0,0039
0,20	0,1781	0,0073	0,1108	0,0050
0,25	0,2110	0,0124	0,1333	0,0086
0,30	0,2324	0,0189	0,1492	0,0131
0,35	0,2436	0,0266	0,1584	0,0182
0,40	0,2460	0,0354	0,1622	0,0244
0,45	0,2409	0,0455	0,1614	0,0313
0,50	0,2298	0,0564	0,1564	0,0390
0,55	0,2137	0,0685	0,1479	0,0474
0,60	0,1952	0,0816	0,1365	0,0564
0,7	0,1427	0,1099	0,1071	0,0758
0,8	0,0828	0,1405	0,0708	0,0967
0,9	0,0187	0,1718	0,0304	0,1186
1,0	−0,0506	0,2029	−0,0110	0,1394
1,1	−0,1091	0,2324	−0,0521	0,1593
1,2	−0,1682	0,2595	−0,0911	0,1777
1,4	−0,2639	0,3038	−0,1569	0,2058
1,6	−0,3246	0,3307	−0,2012	0,2209
1,8	−0,3477	0,3380	−0,2206	0,2238
2,0	−0,3350	0,3260	−0,2157	0,2103
2,2	−0,2953	0,2941	−0,1892	0,1836
2,4	−0,2263	0,2506	−0,1451	0,1452
2,6	−0,1453	0,1934	−0,0898	0,0986
2,8	−0,0509	0,1452	−0,0308	0,0469
3,0	0,0395	0,0857	0,0361	−0,0073
3,5	0,2579	−0,1256	0,1815	−0,1372
4,0	0,4190	−0,2846	0,2672	−20,2294
4,5	0,5089	−0,4007	0,2975	−0,2749
5,0	0,5349	−0,4681	0,2389	−0,2653
5,5	0,5138	−0,4925	0,1990	−0,2112
6,0	0,4637	−0,4829	0,0319	−0,1253
6,5	0,3988	−0,4495	−0,0882	−0,0232
7,0	0,3319	−0,4000	−0,1984	0,0816
7,5	0,2653	−0,3479	−0,2894	0,1788
8	0,2098	−0,2934	−0,3570	0,2615
9	0,1231	−0,1958	−0,4214	0,3472
10	0,0696	−0,1400	−0,4109	0,4062
11	0,0400	−0,0748	−0,3556	0,3864
12	0,0227	−0,0444	−0,2830	0,3331
13	0,0121	−0,0268	−0,2139	0,2697
14	0,0071	−0,0163	−0,1546	0,2078
15	0,0031	−0,0098	−0,1086	0,1534
16	0,0021	−0,0058	−0,0763	0,1097
17	0,0013	−0,0034	−0,0534	0,0767
18	0,0007	−0,0021	−0,0373	0,0527
20	0,0002	−0,0008	−0,0185	0,0260
22	0,0001	−0,0003	−0,0091	0,0120
24		−0,000 (1)	−0,0044	0,0057
26			−0,0022	0,0026
28			−0,0009	0,0013
30			−0,0005	0,0006
32			−0,0002	0,0003

Table 56. 3s Radial Wave Functions for the $1s^2 2s^2 3s$ Configuration of Ca II [60]

r	P(3s/r)	r	P(3s/r)	r	P(3s/r)
0,01	0,0081	0,40	−0,0060	2,00	−0,0205
0,02	0,0154	0,50	−0,0362	4,00	0,3351
0,03	0,0218	0,70	−0,0864	6,00	0,4317
0,10	0,0464	0,85	−0,1105	7,00	0,4019
0,14	0,0495	1,00	−0,1227	8,00	0,3486
0,20	0,0418	1,2	−0,1233	9,00	0,2870
0,32	0,0178	1,5	−0,0994	10,00	0,2270
10,5	0,1993	12,0	0,1291	13,5	0,0793
11,0	0,1736	12,5	0,1102	14,0	0,0670
11,5	0,1502	13,0	0,0936	14,5	0,0572

Table 57. 3p Radial Wave Functions for the $1s^2 2s^2 3p$ Configuration of Ca II [60]

r	P(3p/r)	r	P(3p/r)	r	P(3p/r)
0,02	0,0010	0,50	0,2037	1,40	0,2210
0,04	0,0038	0,70	0,2622	1,80	0,1011
0,10	0,0204	0,90	0,2867	3,00	−0,2889
0,20	0,0634	1,00	0,2838	5,00	−0,4862
0,40	0,1614	1,10	0,2761	9,00	−0,1619

Table 58. 3d Radial Wave Functions for the $1s^2 2s^2 3d$ Configuration of Ca II [60]

r	P(3d/r)	r	P(3d/r)	r	P(3d/r)
0,10	0,0002	0,60	0,0222	2,0	0,2343
0,12	0,0003	0,80	0,0423	3,0	0,3849
0,16	0,0007	1,00	0,0677	4,0	0,4573
0,20	0,0014	1,10	0,0819	5,0	0,4517
0,30	0,0040	1,40	0,1294	6,0	0,3964
0,40	0,0083	1,60	0,1638	7,0	0,3204
0,50	0,0144	1,80	0,1900	9,0	0,1778
11,00	0,0852	12,00	0,0565	14,0	0,0240

Table 59. 3s Radial Wave Functions for the $1s^2 2s^2 3s$ Configuration of B I [60]

r	P(3s/r)	r	P(3s/r)	r	P(3s/r)
0,02	0,0070	1,80	−0,0813	18,00	0,0388
0,08	0,0208	3,00	0,0668	20,00	0,0221
0,16	0,0280	4,00	0,2208	24,00	0,0072
0,25	0,[illegible]67	7,00	0,4077	26,00	0,0042
0,70	−0,0823	10,00	0,2915	28,00	0,0023
1,10	−0,0794	12,00	0,1930	11,00	0,2403
1,40	−0,0923	14,00	0,1176	15,00	0,0899

Table 60. 3p Radial Wave Functions for the $1s^2 2s^2 3p$ Configuration of B I [60]

r	P(3p/r)	r	P(3p/r)	r	P(3p/r)
0,10	0,0077	1,20	0,1934	5,00	−0,1404
0,16	0,0174	1,40	0,2077	6,00	−0,2305
0,20	0,0251	1,60	0,2160	8,00	−0,3516
0,30	0,0470	1,80	0,2069	12,00	−0,2853
0,50	0,0937	2,00	0,1981	15,00	−0,1812
0,80	0,1531	3,00	0,1086	22,00	−0,0401
1,00	0,1806	4,00	−0,0173	30,00	−0,0069

Table 61. 3d Radial Wave Functions for the $1s^2 2s^2 3d$ Configuration of B I [60]

r	P(3d/r)	r	P(3d/r)	r	P(3d/r)
1,0	0,0004	3,0	0,0952	14,0	0,2303
1,1	0,0117	3,5	0,1257	16,0	0,1761
1,4	0,0200	4,0	0,1571	18,0	0,1284
1,6	0,0266	5,0	0,2170	22,0	0,0616
2,0	0,0426	7,0	0,3019	24,0	0,0411
2,4	0,0618	9,0	0,3273	26,0	0,0269
2,8	0,0835	11,0	0,3054	28,0	0,0174

Table 62. The Ga^+ Ion [61]

r	State				
	$(4s)^2\,{}^1S_0$	$(4s4p)\,{}^1P_1$		$(4s4p)\,{}^3P_1$	
	$P_{4s}(r)$	$P_{4s}(r)$	$P_{4p}(r)$	$P_{4s}(r)$	$P_{4p}(r)$
0,000	0,000	0,000	0,000	0,000	0,000
0,005	−0,049	−0,060	0,026	−0,055	0,020
0,010	−0,085	−0,093	0,046	−0,088	0,037
0,015	−0,101	−0,110	0,062	−0,105	0,057
0,020	−0,105	−0,117	0,074	−0,110	0,074
0,025	−0,098	−0,115	0,085	−0,101	0,087
0,030	−0,086	−0,107	0,094	−0,088	0,100
0,035	−0,069	−0,094	0,101	−0,070	0,113
0,040	−0,050	−0,078	0,106	−0,050	0,126
0,05	−0,008	−0,039	0,116	−0,006	0,143
0,06	0,036	0,005	0,123	0,039	0,150
0,07	0,076	0,048	0,127	0,081	0,153
0,08	0,112	0,087	0,128	0,118	0,153
0,09	0,141	0,122	0,126	0,148	0,148
0,10	0,163	0,151	0,121	0,170	0,140
0,12	0,187	0,191	0,103	0,195	0,114
0,14	0,187	0,206	0,077	0,193	0,079
0,16	0,166	0,201	0,046	0,171	0,040
0,18	0,131	0,177	0,014	0,134	0,003
0,20	0,087	0,141	−0,020	0,087	−0,044
0,22	0,036	0,096	−0,052	0,035	−0,082
0,24	0,016	0,045	−0,083	−0,020	−0,118
0,26	−0,068	−0,007	−0,110	−0,074	−0,150
0,28	−0,117	−0,060	−0,135	−0,124	−0,177
0,30	−0,161	−0,110	−0,155	−0,170	−0,200
0,35	−0,247	−0,217	−0,191	−0,259	−0,235
0,40	−0,295	−0,290	−0,205	−0,307	−0,242
0,45	−0,307	−0,328	−0,201	−0,318	−0,227
0,50	−0,290	−0,334	−0,182	−0,299	−0,196
0,55	−0,251	−0,315	−0,151	−0,257	−0,153
0,60	−0,197	−0,276	−0,119	−0,200	−0,104
0,7	−0,063	−0,160	−0,038	−0,059	0,004
0,8	0,080	−0,022	0,046	0,090	0,112
0,9	0,216	0,119	0,128	0,232	0,212
1,0	0,338	0,252	0,203	0,368	0,302
1,1	0,441	0,370	0,270	0,464	0,381
1,2	0,526	0,471	0,331	0,550	0,447
1,3	0,593	0,555	0,383	0,618	0,503
1,4	0,644	0,623	0,428	0,669	0,549
1,5	0,680	0,675	0,467	0,705	0,585
1,6	0,705	0,713	0,500	0,727	0,613
1,8	0,722	0,753	0,548	0,740	0,648
2,0	0,708	0,755	0,579	0,722	0,659
2,2	0,675	0,731	0,594	0,683	0,653
2,4	0,651	0,6[illegible]0	0,598	0,635	0,634
2,6	0,601	0,599	0,592	0,581	0,606
2,8	0,546	0,537	0,578	0,524	0,571
3,0	0,490	0,475	0,559	0,467	0,533
3,2	0,435	0,416	0,535	0,413	0,492
3,4	0,382	0,362	0,508	0,362	0,451
3,6	0,334	0,313	0,480	0,314	0,411
3,8	0,289	0,268	0,450	0,272	0,372
4,0	0,250	0,229	0,419	0,234	0,335
4,5	0,169	0,151	0,342	0,157	0,253
5,0	0,111	0,097	0,271	0,103	0,186
5,5	0,072	0,062	0,211	0,066	0,134
6,0	0,046	0,038	0,161	0,042	0,095
6,5	0,029	0,024	0,121	0,026	0,067
7,0	0,018	0,014	0,090	0,016	0,046
7,5	0,011	0,009	0,066	0,010	0,032
8,0	0,007	0,005	0,048	0,006	0,022
9,0	0,003	0,002	0,024	0,002	0,009
10,0	0,001	0,001	0,012	0,001	0,004
11,0			0,006		0,002
12,0			0,003		0,001
13,0			0,001		

APPENDIX

Areas of Intensive Soviet Activity in X-Ray Research not Included in the Bibliography

1) X-ray structural analysis (x-ray diffraction)

2) X-ray spectroscopy of compounds, alloys, and solid solutions

3) Fine structure of x-ray spectra absorption (resonance structure, true edges)

4) Scattering, reflection, and refraction of x-rays

5) Photoelectric effect of x-rays

6) Instrumentation

7) X-ray data recorded by Soviet satellites

8) Methods of correcting x-ray spectra for various types of distortion

9) Effect of chemical binding on x-ray spectra

10) Nuclear x-ray spectroscopy (the Auger effect, internal conversion)

11) Translations of Western articles on x-ray spectra and earlier reviews on the subject based exclusively on Western sources